Exohedral functionalization vs. core expansion of siliconoids with Group 9 metals: catalytic activity in alkene isomerization

Nadine Poitiers, Luisa Giarrana, Volker Huch, Michael Zimmer and David Scheschkewitz*

Krupp-Chair of General and Inorganic Chemistry, Saarland University, 66123 Saarbrücken, Germany

Supporting Information

Table of Contents

1. General

All manipulations were carried out under a protective atmosphere of argon, by using a glovebox or standard Schlenk techniques. Ethereal solvents were dried by heating to reflux over Na/benzophenone and distilled and stored under an atmosphere of argon. Hydrocarbons were dried over sodium or potassium. Solution NMR spectra were recorded on a Bruker Avance IV 400 NMR spectrometer (^{1}H = 400.13 MHz, ^{13}C = 100.6 MHz, ^{29}Si = 79.49 MHz, ^{119}Sn = 149.21 MHz) and solid state NMR spectra on a Bruker Avance III 400 WB spectrometer (^{29}Si = 79.53 MHz, ^{119}Sn = 149.27 MHz). UV/Vis spectra were recorded on a Shimadzu UV-2600 spectrometer in quartz cells with a path length of 0.1 cm. Infrared spectra were measured with a Shimadzu IR Affinity-1S in a platinum ATR diamond cell. Elemental analyses were performed on an elemental analyzer Leco CHN-900 and/or an elementar vario Micro Cube. Compounds **1a-c** were prepared according to our published procedures.[1]

2. Preparation, data and spectra (NMR, UV-vis, IR)

Procedure for the synthesis of tetrylene-functionalized iridium siliconoid complexes 2a-c

The respective compounds **2a-c** are prepared by treating 1 equivalent of the *ligato*-tetrylene-functionalized siliconoids **1a-c** with the corresponding amount of chloro(1,5-cyclooctadiene)iridium(I) dimer $[(cod)IrCl]_2$ in benzene. The suspension is heated to 40°C for 5 minutes and then stirred at room temperature overnight. After removing all volatiles in vacuum, the crude product is filtered from the indicated amount of hexane and crystallized from hexane at −26°C overnight. Concentration of the mother liquor typically affords a second batch of crystalline **2a-c**.

(5-(Chlorobis(2,4,6-triisopropylphenyl)silyl)-2-(1,3-di-*tert*-butyl-4-phenyl-1,3,2λ^{3}-diazasilet-1-ium-2(3*H*)-yl)-3,3,4-tris(2,4,6-triisopropylphenyl)tricyclo[2.1.0.0$^{2.5}$] pentasilane-1-yl-iridium (2a)

Quantities: Si_6NHSi **1a**, 700 mg (0.485 mmol), $[(cod)IrCl]_2$ 162.76 mg (0.243 mmol), benzene 10 mL, filtration four times from hexane 15 mL each, crystallization from hexane. Yield: 568 mg (0.328 mmol ; 68 %) violet crystals (mp. > 147 °C, dec.).

^{1}H-NMR (400.13 MHz, C_6D_6, 300 K) δ = 7.391 (bs, 1H, Ar-H), 7.193 – 7.189 (m, 2H, Ar-H), 7.142 – 7.138 (m, 1H, Ar-H), 7.052 – 7.047 (m, 1H, Ar-H), 7.002 – 6.917 (m, 6H, Ar-H), 6.838 – 6.802 (m, 3H, Ar-H), 6.773 (bs, 1H, Ar-H), 5.831 (sept, 1H, $^{3}J_{HH}$ = 6.16 Hz, Tip-*i*Pr-CH_2), 5.185 (sept, 1H, $^{3}J_{HH}$ = 6.80 Hz, Tip-*i*Pr-CH_2), 4.913 (sept, 1H, $^{3}J_{HH}$ = 6.44 Hz, Tip-*i*Pr-CH_2), 4.583 – 4.433 (m, 4H, Tip-*i*Pr-CH_2), 3.819 (sept, 1H, $^{3}J_{HH}$ = 6.98 Hz, Tip-*i*Pr-CH_2), 3.668 (sept, 1H, $^{3}J_{HH}$ = 6.39 Hz, Tip-*i*Pr-CH_2), 3.161 (sept, 1H, $^{3}J_{HH}$ = 6.07 Hz, Tip-*i*Pr-CH_2), 2.854 – 2.569 (m, 7H, Tip-*i*Pr-CH_2), 2.363 (bs, 2H, Tip-*i*Pr-CH_2), 2.101 – 2.021 (m, 14H, Tip-*i*Pr-CH_3), 1.929 (d, 3H, $^{3}J_{HH}$ = 6.47 Hz, Tip-*i*Pr-CH_3), 1.836 (d, 3H, $^{3}J_{HH}$ = 6.56 Hz, Tip-*i*Pr-CH_3), 1.804 – 1.775 (m, 6H, Tip-*i*Pr-CH_3), 1.578 (d, 3H, $^{3}J_{HH}$ = 6.35 Hz, Tip-*i*Pr-CH_3), 1.513 (d, 6H, $^{3}J_{HH}$ = 6.35 Hz, Tip-*i*Pr-CH_3), 1.465 (d, 3H, $^{3}J_{HH}$ = 6.70 Hz, Tip-*i*Pr-CH_3), 1.384 – 1.360 (m, 6H, Tip-*i*Pr-CH_3), 1.278 – 1.134 (m, 36H, Tip-*i*Pr-CH_3), 1.077 – 1.058 (m, 7H, Tip-*i*Pr-CH_3), 0.890 (t, 6H, $^{3}J_{HH}$ = 7.18 Hz, Tip-*i*Pr-CH_3), 0.830 (s, 9H, $C(CH_3)_3$), 0.723 (d, together 6H, Tip-*i*Pr-CH_3), 0.683 (m, 12 H, Tip-*i*Pr-CH_3 overlapping with $C(CH_3)_3$), 0.460 – 0.438 (m, 6H, Tip-*i*Pr-CH_3), 0.281 (d, 3H, $^{3}J_{HH}$ = 6.49 Hz, Tip-*i*Pr-CH_3), 0.167 (d, 3H, $^{3}J_{HH}$ = 6.49 Hz, Tip-*i*Pr-CH_3) ppm.

^{13}C-NMR (100.61 MHz, C_6D_6, 300 K) δ = 169.70 (s, 1C, C-Ph), 156.15, 155.41 (s, each 1C, Ar-C), 154.42, 154.37 (s, each 1C, Ar-C), 154.14, 153.76, 153.22, 153.14, 152.90 (s, each 1C, Ar-C), 150.20, 149.91, 148.77, 147.98 (s, each 1C, Ar-C), 143.56 (s, 1C, Ar-C), 141.46 (s, 1C, Ar-C), 137.92, 137.13, 135.43, 132.13, 131.19 (s, each 1C, Ar-C), 130.03, 129.69 (s, each 1C, Ar-CH), 128.12, 127.88 (s, each 1C, Ar-CH overlapping with C_6D_6), 127.43, 127.40 (s, each 1C, Ar-CH), 123.62, 123.54, 123.51, 123.08, 122.88, 122.74, 122.57, 122.49, 122.08, 120.62 (s,

each 1C, Ar-CH), 53.81 (s, 1C, $C(CH_3)_3$), 53.67 (s, 1C, $C(CH_3)_3$), 38.12 (s, 1C, Tip-*i*Pr-CH), 35.72, 35.69 (s, each 1C, (s, 1C, Tip-*i*Pr-CH), 35.33, 34.79, 34.70, 34.59, 34.44, 34.31, 33.85, 33.57 (s, each 1C, (s, 1C, Tip-*i*Pr-CH), 32.98 (s, 1C, (s, 1C, Tip-*i*Pr-CH), 32.17 (s, 1C, (s, 1C, Tip-*i*Pr-CH), 31.92 (s, 1C, Tip-*i*Pr-CH), 31.79 (s, 1C, Tip-*i*Pr-CH), 31.18 (s, 1C, (s, 1C, Tip-*i*Pr-CH), 30.6 (s, 1C, Tip-*i*Pr-CH), 30.04, 29.09, 29.02 (s, each 1C, Tip-*i*Pr-CH_3), 28.41 (s, 1C, Tip-*i*Pr-CH_3), 27.28 (s, 1C, Tip-*i*Pr-CH_3), 26.15, 25.91, 25.69, 25.15 (s, each 1C, Tip-*i*Pr-CH_3), 24.76, 24.68, 24.61, 24.49, 24.46, 24.37, 24.26, 24.21, 24.18, 24.15, 24.13, 24.03, 23.96, 23.84, 23.74 (s, each 1C, Tip-*i*Pr-CH_3), 23.11, 23.01, 22.73, 22.40, (s, each 1C, Tip-*i*Pr-CH_3), 14.32 (s, 1C, Tip-*i*Pr-CH_3) ppm.

^{29}Si-NMR (79.49 MHz, C_6D_6, 300 K) δ = 56.7 (s, $SiTip_2$), 33.4 (s, NHSi), 13.3 (s, $SiTip_2Cl$), −38.4 (s, SiTip), −88.9 (s, Si-NHSi), −125.4 (s, unsubstituted Si), −128.7 (s, Si-Ir) ppm.

CP-MAS ^{29}Si-NMR (79.53 MHz, 13KHz, 300K) δ = 55.3 (s, $SiTip_2$), 32.9 (s, NHSi), 11.5 (s, $SiTip_2Cl$), −41.6 (s, SiTip), −88.6 (s, Si-NHSi), −126.8 (s, unsubstituted Si), −128.2 (s, unsubstituted Si) ppm.

Elemental analysis: calculated for $C_{97}H_{146}ClIrN_2Si_7$: C, 66.03 % ; H, 8.34 % ; N, 1.59 %. Found: C, 65.55, % ; H, 8.03 % ; N: 1.73 %.

UV/VIS (hexane): λ_{max} (ε) = 576 nm (1200 M^{-1} cm^{-1}).

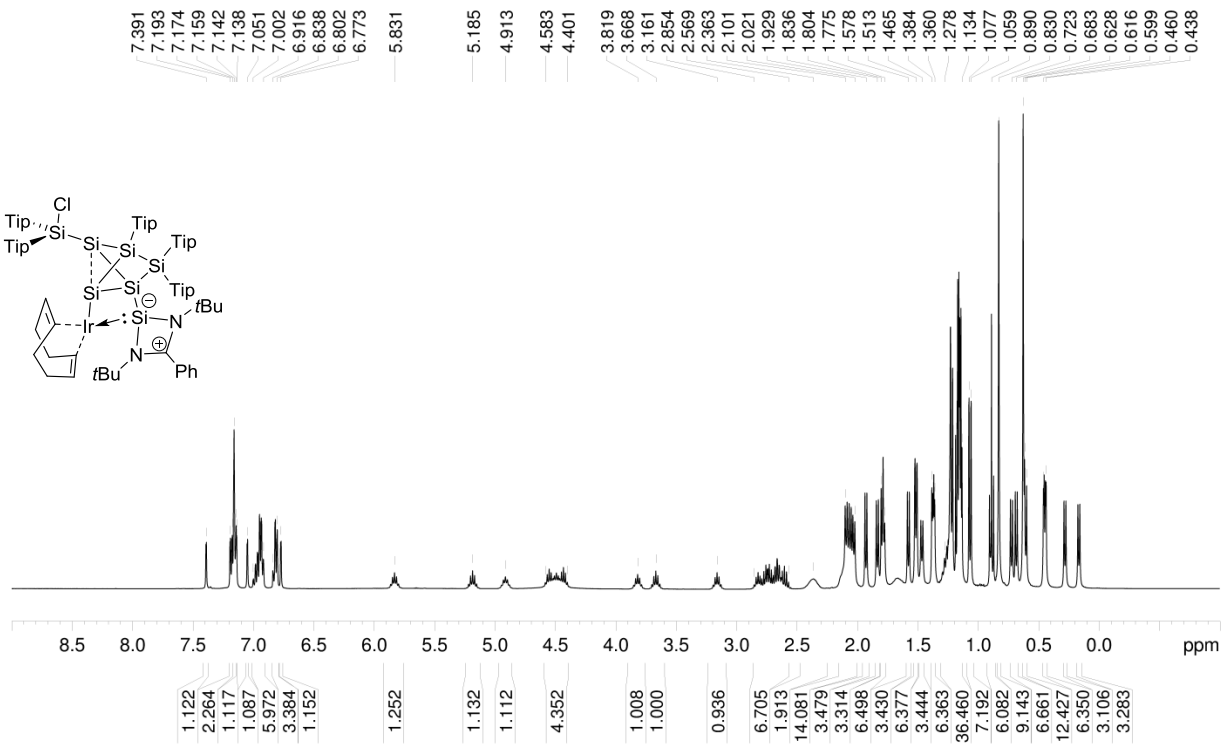

Supplementary Figure 1: ^{1}H NMR spectrum of **2a** in C_6D_6 (400.13 MHz, 300 K).

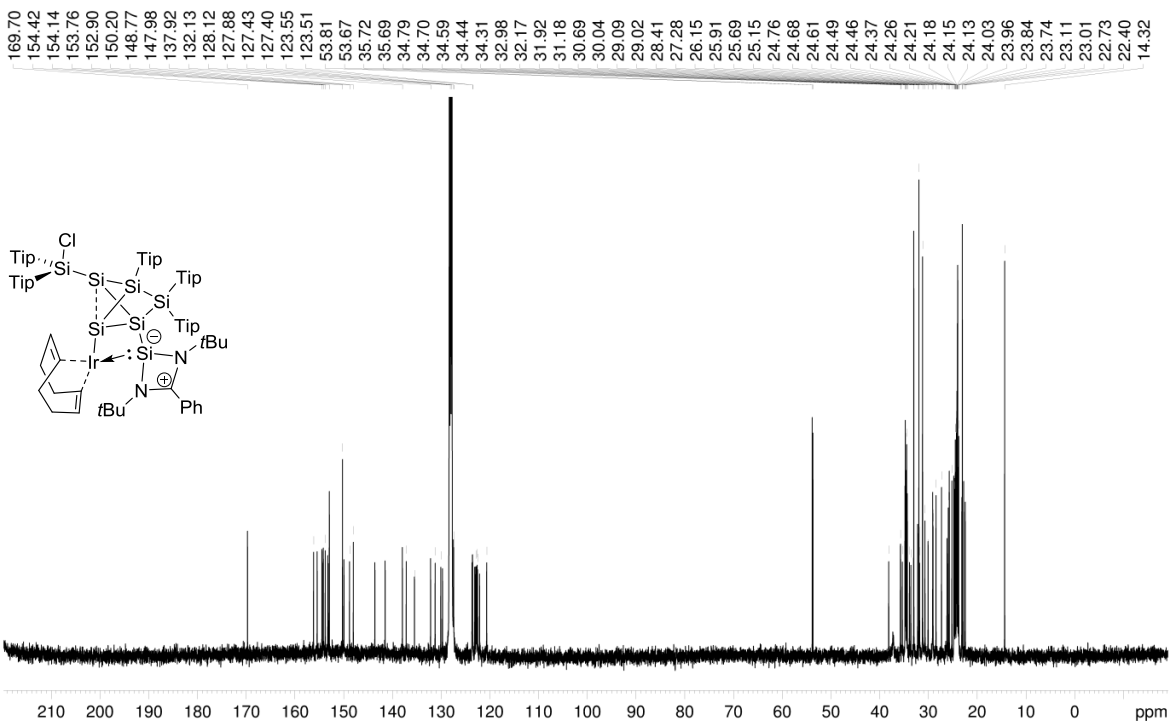

Supplementary Figure 2: ^{13}C NMR spectrum of **2a** in C_6D_6 (100.61 MHz, 300 K).

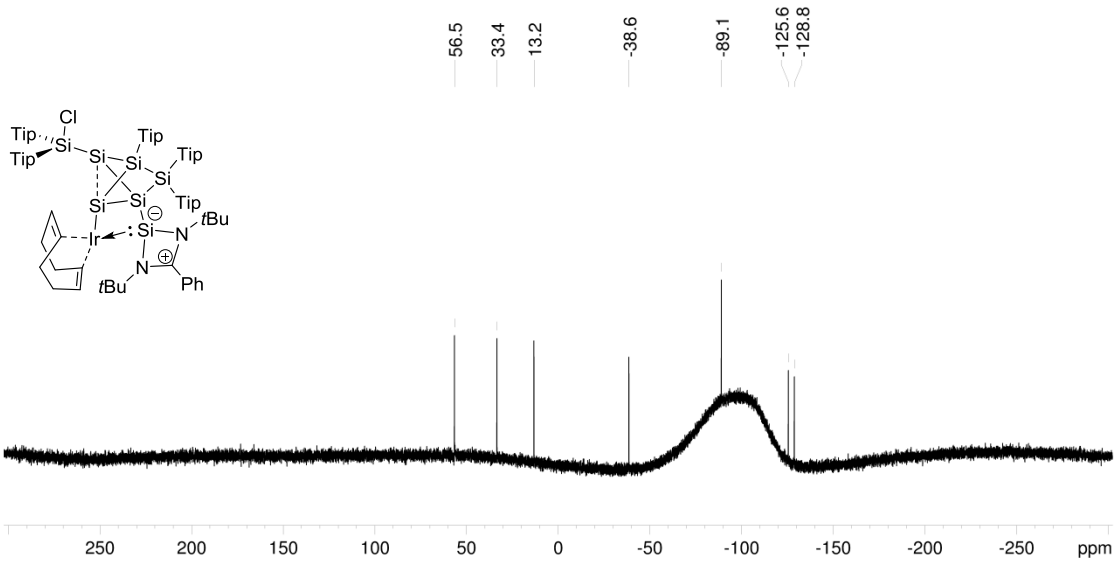

Supplementary Figure 3: ^{29}Si NMR spectrum of **2a** in C_6D_6 (79.49 MHz, 300 K).

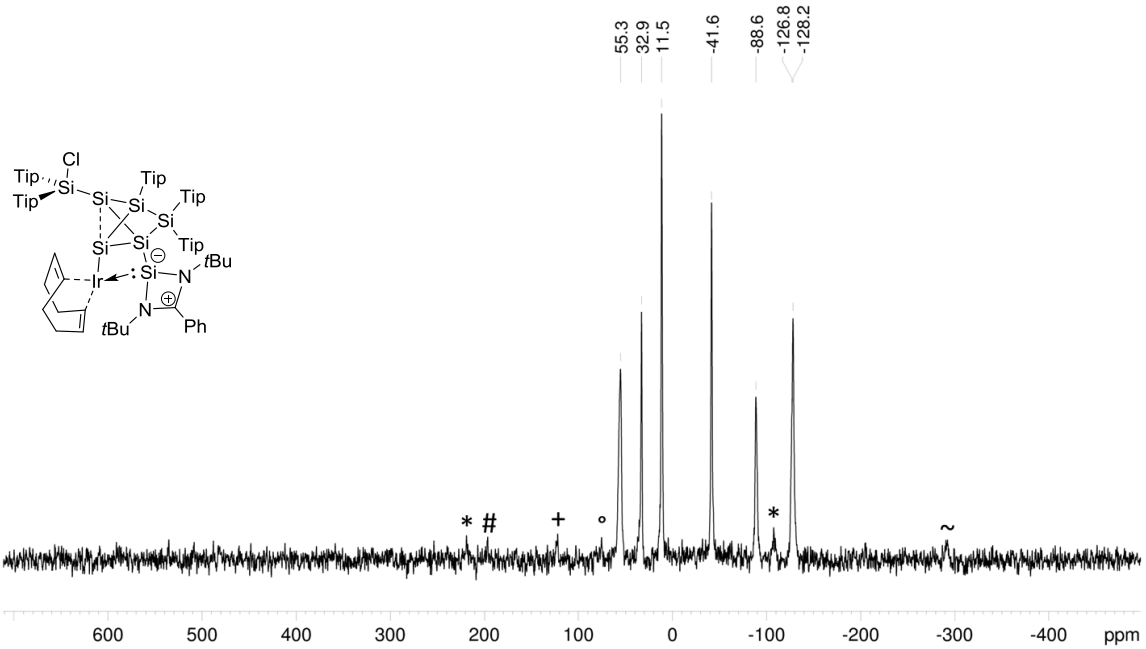

Supplementary Figure 4: CP MAS ^{29}Si NMR spectrum of **2a** (79.53 MHz, 13 KHz, 300 K), side spinning bands of: * $SiTip_2$ (55.3 ppm), # NHSi (32.9 ppm), + SiTip (−41.6 ppm), ° unsubstituted Si (−88.6 ppm), ~ unsubstituted Si (−126.8 ppm, −128.2 ppm).

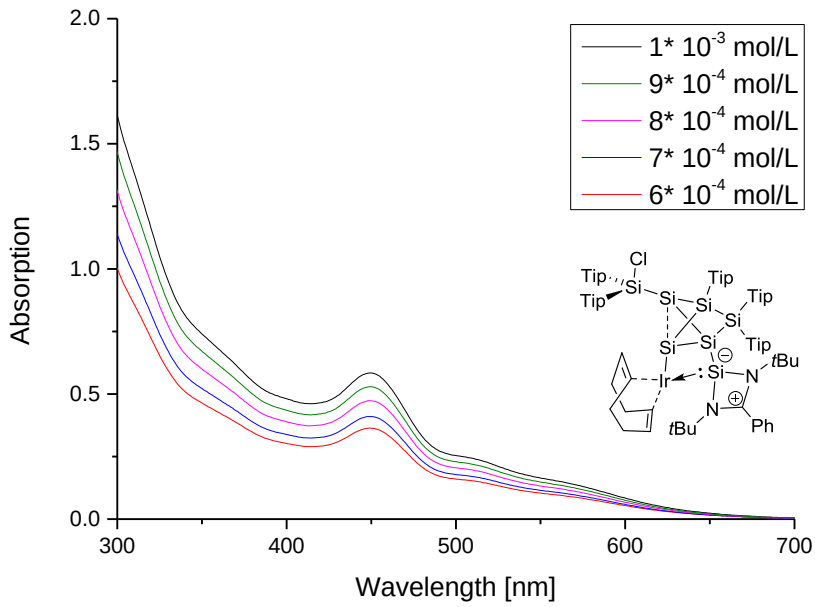

Supplementary Figure 5: UV-Vis spectrum of **2a** in hexane at different concentrations.

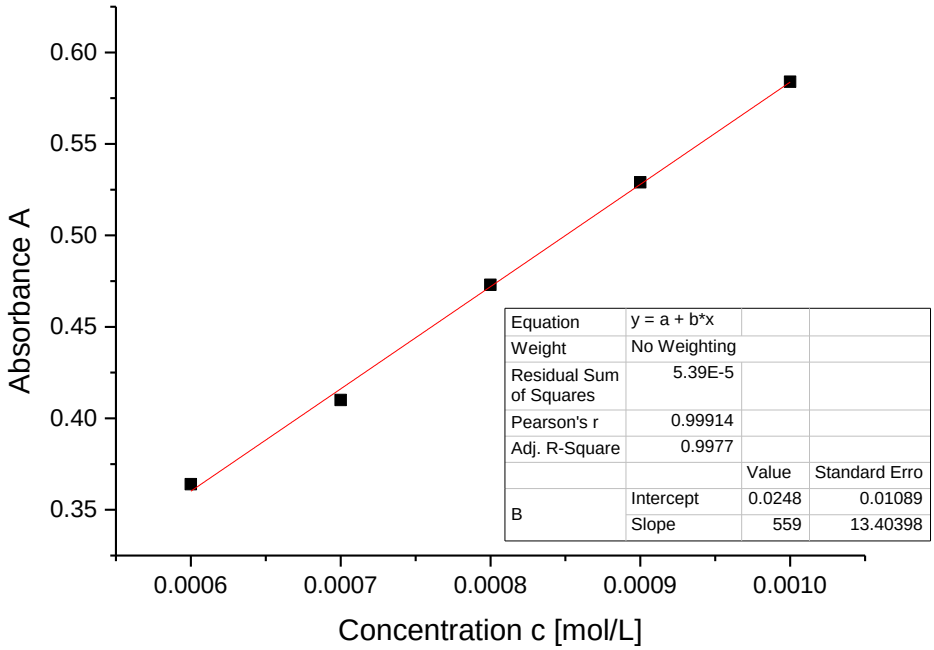

Supplementary Figure 6: Determination of ε (5590 M^{-1} cm^{-1}) by linear regression of absorptions (λ = 449 nm) of **2a** against concentration.

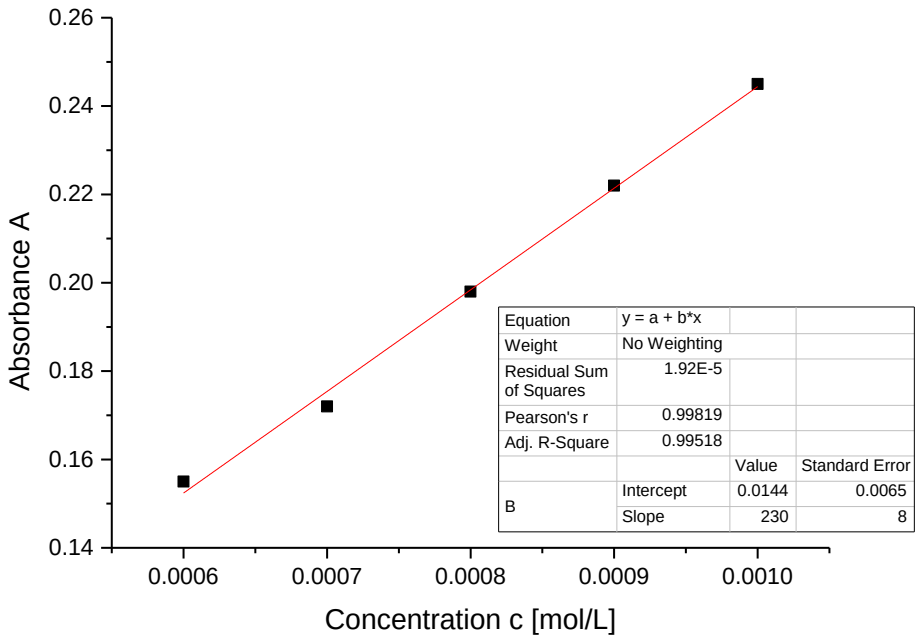

Supplementary Figure 7: Determination of ε (2300 M^{-1} cm^{-1}) by linear regression of absorptions (λ = 508 nm) of **2a** against concentration.

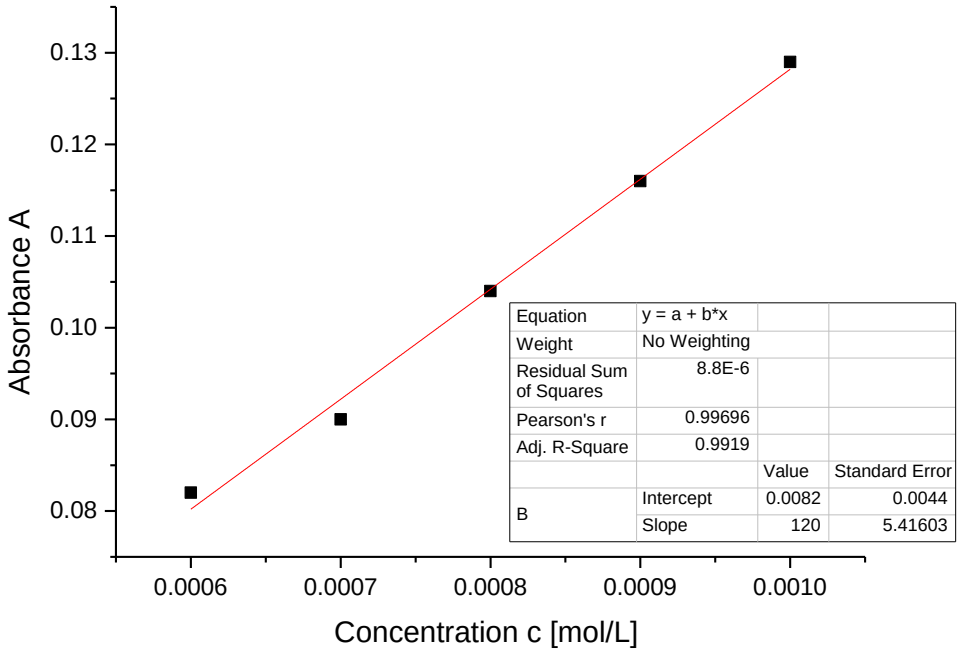

Supplementary Figure 8: Determination of ε (1200 M^{-1} cm^{-1}) by linear regression of absorptions (λ = 576 nm) of **2a** against concentration.

(5-(Chlorobis(2,4,6-triisopropylphenyl)silyl)-2-(1,3-di-*tert*-butyl-4-phenyl-1,3,2λ^3-diazagermet-1-ium-2(3*H*)-yl)-3,3,4-tris(2,4,6-triisopropylphenyl)tricyclo [2.1.0.0$^{2.5}$]pentasilane-1-yl-iridium (2b)

Quantities: Si_6NHGe **1b**, 500 mg (0.327 mmol), $[(cod)IrCl]_2$ 140.92 mg (0.21 mmol), benzene 10 mL, filtration two times from hexane 8 mL each, crystallization from hexane at −26 °C. Yield: 362 mg (0.198 mmol; 61 %) violet-brown crystals (mp. 154 °C, dec.).

^{1}H-NMR (400.13 MHz, C_6D_6, 300 K) δ = 7.375 (bs, 1H, Ar-H), 7.164 – 7.141 (m, 7H, Ar-H overlapping with C_6D_6), 7.047 – 6.907 (m, 7H, Ar-H), 6.871 – 6.814 (m, 3H, Ar-H), 6.753 (bs, 1H, Ar-H), 5.829 (sept, 1H, $^3J_{HH}$ = 6.36 Hz, Tip-*i*Pr-CH_2), 5.156 (sept, 1H, $^3J_{HH}$ = 6.89 Hz, Tip-*i*Pr-CH_2), 4.918 (sept, 1H, $^3J_{HH}$ = 6.97 Hz, Tip-*i*Pr-CH_2), 4.641 (bs, 1H, Tip-*i*Pr-CH_2), 4.468 (m, 3H, Tip-*i*Pr-CH_2), 3.867 (sept, 1H, $^3J_{HH}$ = 6.42 Hz, Tip-*i*Pr-CH_2), 3.575 (sept, 1H, $^3J_{HH}$ = 6.42 Hz, Tip-*i*Pr-CH_2), 3.192 (sept, 1H, $^3J_{HH}$ = 6.42 Hz, Tip-*i*Pr-CH_2), 2.849 – 2.576 (m, 7H, Tip-*i*Pr-CH_2), 2.329 (bs, 2H, Tip-*i*Pr-CH_2), 2.103, 2.051, 2.001 (each d, together 12H, each $^3J_{HH}$ = 6.34 Hz, Tip-*i*Pr-CH_3), 1.927 (d, 4H, $^3J_{HH}$ = 6.67 Hz, Tip-*i*Pr-CH_3), 1.840 (d, $^3J_{HH}$ = 6.67 Hz, Tip-*i*Pr-CH_3), 1.793, 1.755 (each d, together 6H, each $^3J_{HH}$ = 6.67 Hz, Tip-*i*Pr-CH_3), 1.605 – 1.506 (m, 16H, Tip-*i*Pr-CH_3), 1.390 (d, 3H, $^3J_{HH}$ = 6.61 Hz, Tip-*i*Pr-CH_3),) 1.352 (d, 3H, $^3J_{HH}$ = 6.61 Hz, Tip-*i*Pr-CH_3), 1.299 – 1.136 (m, 37H, Tip-*i*Pr-CH_3), 1.087 – 1.066 (m, 6H, Tip-*i*Pr-CH_3), 0.889 (dd, 6H, $^3J_{HH}$ = 6.55 Hz, Tip-*i*Pr-CH_3), 0.783 (s, 9H, $C(CH_3)_3$), 0.710 (d, 3H, $^3J_{HH}$ = 6.59 Hz, Tip-*i*Pr-CH_3), 0.674 (d, 3H, $^3J_{HH}$ = 6.59 Hz, Tip-*i*Pr-CH_3), 0.581 – 0.567 (m, 12H, Tip-*i*Pr-CH_3 overlapping with $C(CH_3)_3$), 0.484 (d, 3H, $^3J_{HH}$ = 6.59 Hz, Tip-*i*Pr-CH_3), 0.441 (d, 3H, $^3J_{HH}$ = 6.59 Hz, Tip-*i*Pr-CH_3), 0.301 (d, 3H, $^3J_{HH}$ = 6.27 Hz, Tip-*i*Pr-CH_3), 0.176 (d, 3H, $^3J_{HH}$ = 6.27 Hz, Tip-*i*Pr-CH_3) ppm.

^{13}C-NMR (100.61 MHz, C_6D_6, 300 K) δ = 169.08 (s, 1C, C-Ph), 156.22, 155.45, 154.58, 154.41, 154.13, 153.71, 153.60, 153.29, 152.83 (s, each 1C, Ar-C), 150.35, 150.22, 150.02, 148.94, 148.04 (s, each 1C, Ar-C), 142.89 (s, 1C, Ar-C), 140.71 (s, 1C, Ar-C), 137.58, 135.81, 134.98, 134.06 (s, each 1C, Ar-C), 130.99 (s, 1C, Ar-C), 129.79,

129.5 (s, each 1C, Ar-CH), 128.14, 127.89 (s, each 1C, Ar-CH overlapping with C_6D_6), 127.34, 127.24 (s, each 1C, Ar-CH), 123.66, 123.53, 123.43, 123.16, 122.94, 122.70, 122.40, 121.94 (s, each 1C, Ar-CH), 120.67 (s, 1C, Ar-CH), 54.06 (s, 1C, $C(CH_3)_3$), 53.63 (s, 1C, $C(CH_3)_3$), 38.47 (s, 1C, Tip-*i*Pr-CH), 36.38 (bs, 1C, Tip-*i*Pr-CH), 35.93, 35.75, 35.65 (s, each 1C, Tip-*i*Pr-CH), 34.79, 34.75, 34.71 (bs, each 1C, Tip-*i*Pr-CH), 34.60, 34.39, 34.34 (s, each 1C, Tip-*i*Pr-CH), 33.94, 33.76 (s, each 1C, Tip-*i*Pr-CH), 32.57 (s, 1C, Tip-*i*Pr-CH), 31.97 (s, 1C, Tip-*i*Pr-CH), 31.92 (s, 1C, Tip-*i*Pr-CH), 31.75 (s, 1C, Tip-*i*Pr-CH), 31.21 (s, 1C, Tip-*i*Pr-CH), 30.37, 29.89 (s, each 1C, Tip-*i*Pr-CH_3), 29.68 (bs, 1C, Tip-*i*Pr-CH_3), 29.25, 28.51, 27.43 (s, each 1C, Tip-*i*Pr-CH_3), 26.00, 25.89, 25.65 (s, each 1C, Tip-*i*Pr-CH_3), 25.11, 24.83 (s, each 1C, Tip-*i*Pr-CH_3), 24.72, 24.55, 24.48, 24.43, 24.36, 24.30 (s, each 1C, Tip-*i*Pr-CH_3), 24.19, 24.17 (bs, each 1C, Tip-*i*Pr-CH_3), 24.07, 24.03, 23.97, 23.92 (bs, each 1C, Tip-*i*Pr-CH_3), 23.77, 23.74 (s, each 1C, Tip-*i*Pr-CH_3), 23.20, (s, 1C, Tip-*i*Pr-CH_3), 23.01 (s, 1C, Tip-*i*Pr-CH_3), 22.51, 22.48 (bs, each 1C, Tip-*i*Pr-CH_3), 14.32 (s, 1C, Tip-*i*Pr-CH_3) ppm.

^{29}Si-NMR (79.49 MHz, C_6D_6, 300 K) δ = 54.6 (s, $SiTip_2$), 12.8 (s, $SiTip_2Cl$), −41.6 (s, SiTip), −90.5 (s, Si1), −91.3 (s, Si-NHGe), −121.6 (s, Si-Ir) ppm.

CP-MAS ^{29}Si-NMR (79.53 MHz, 14KHz, 300K) δ = 52.6 (s, $SiTip_2$), 12.3 (s, $SiTip_2Cl$), −41.5 (d, SiTip), −90.0 (s, Si-NHGe), −90.8 (s, unsubstituted Si), −121.7 (s, unsubstituted Si) ppm.

Elemental analysis: calculated for $C_{97}H_{146}ClGeIrN_2Si_6$: C: 64.40 % ; H: 8.14 % ; N: 1.55 %. Found: C: 64.68 % ; H: 8.18 % ; N: 1.35 %.

UV/VIS (hexane): λ_{max} (ε) = 580 nm (2500 M^{-1} cm^{-1}).

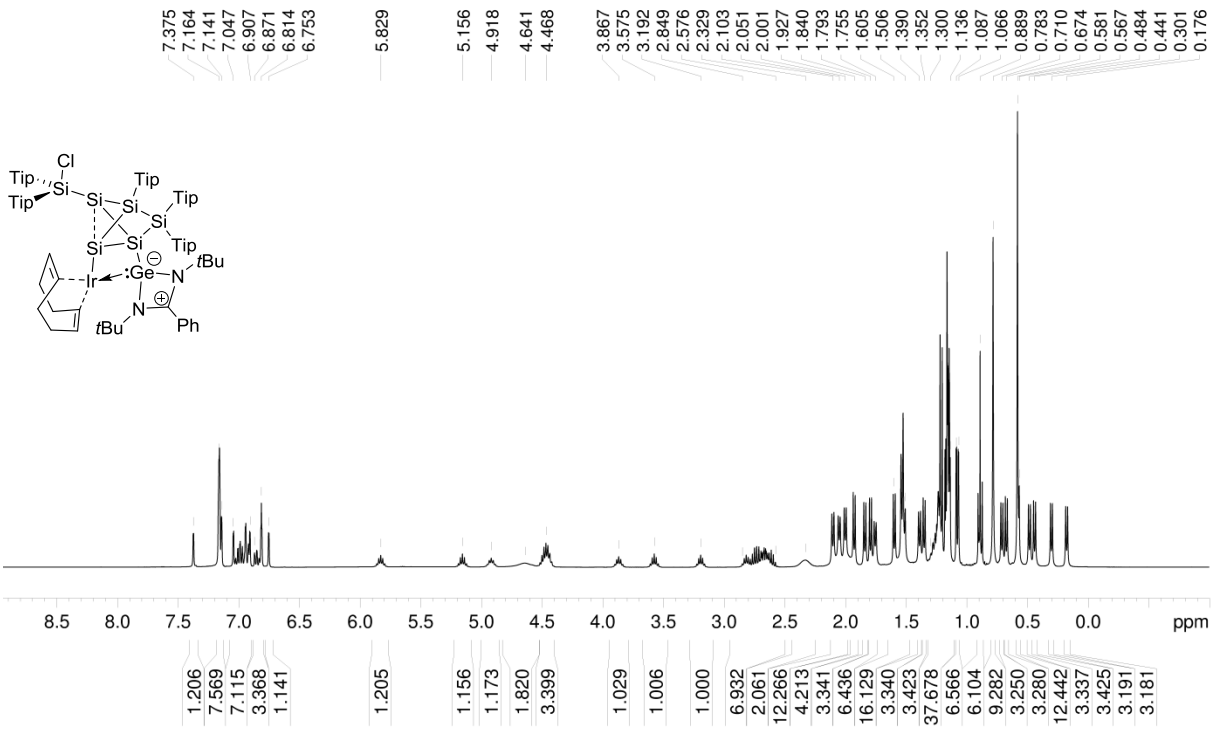

Supplementary Figure 9: ^{1}H NMR spectrum of **2b** in C_6D_6 (400.13 MHz, 300 K).

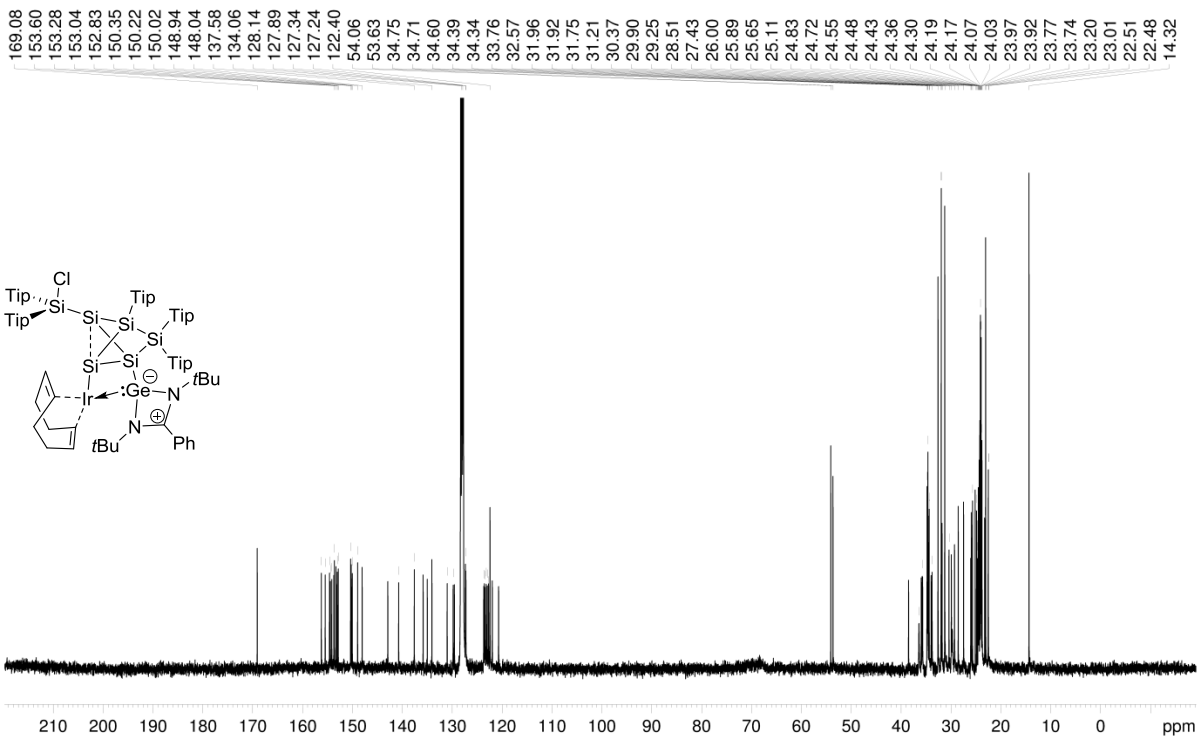

Supplementary Figure 10: ^{13}C NMR spectrum of **2b** in C_6D_6 at (100.61 MHz, 300 K).

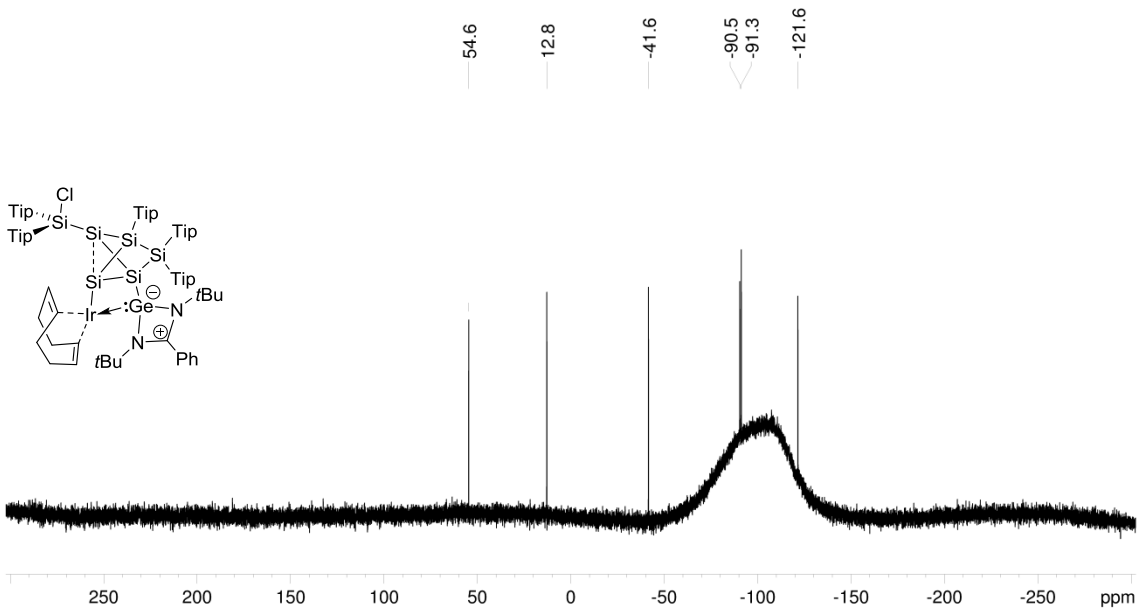

Supplementary Figure 11: ^{29}Si NMR spectrum of **2b** in C_6D_6 (79.49 MHz, 300 K).

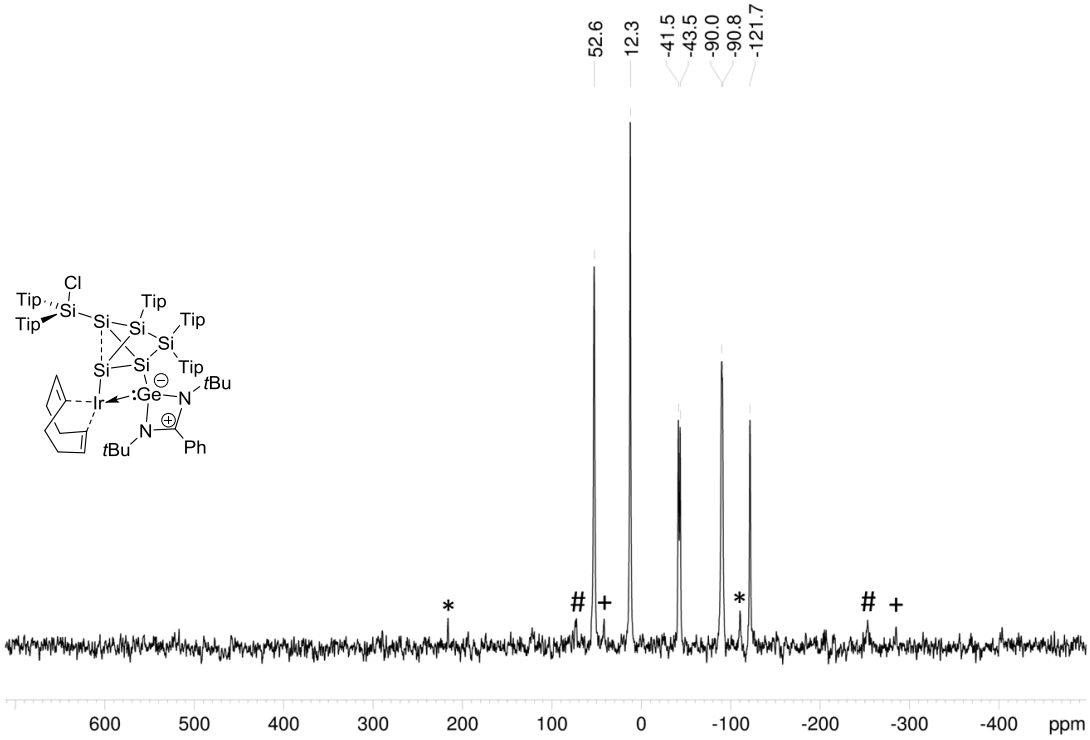

Supplementary Figure 12: CP MAS ^{29}Si NMR spectrum of **2b** (79.53 MHz, 13 KHz, 300 K), side spinning bands of: * $SiTip_2$ (52.6 ppm), # unsubstituted Si, Si-NHGe (−90.0 ppm, −90.8 ppm), + unsubstituted Si (−121.7 ppm).

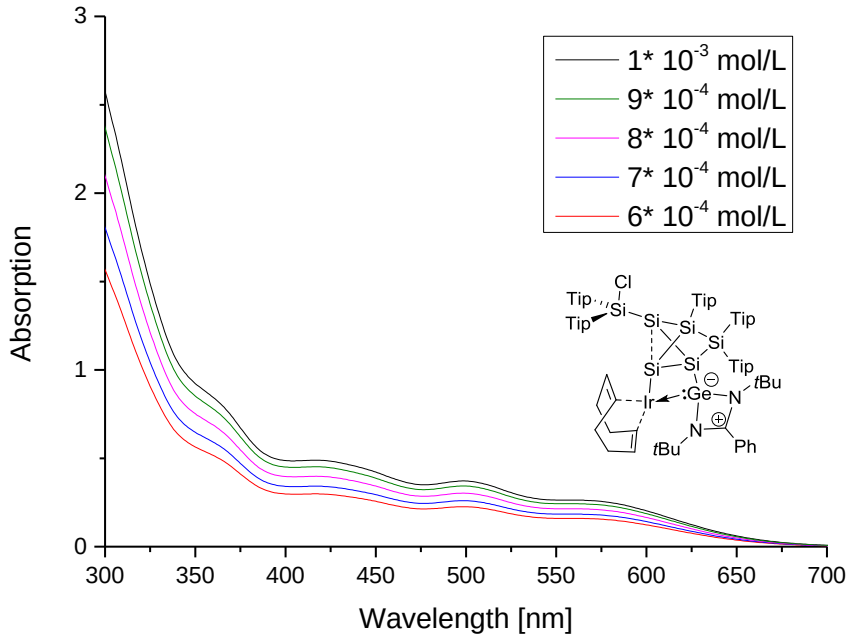

Supplementary Figure 13: UV-Vis spectrum of **2b** in hexane at different concentrations.

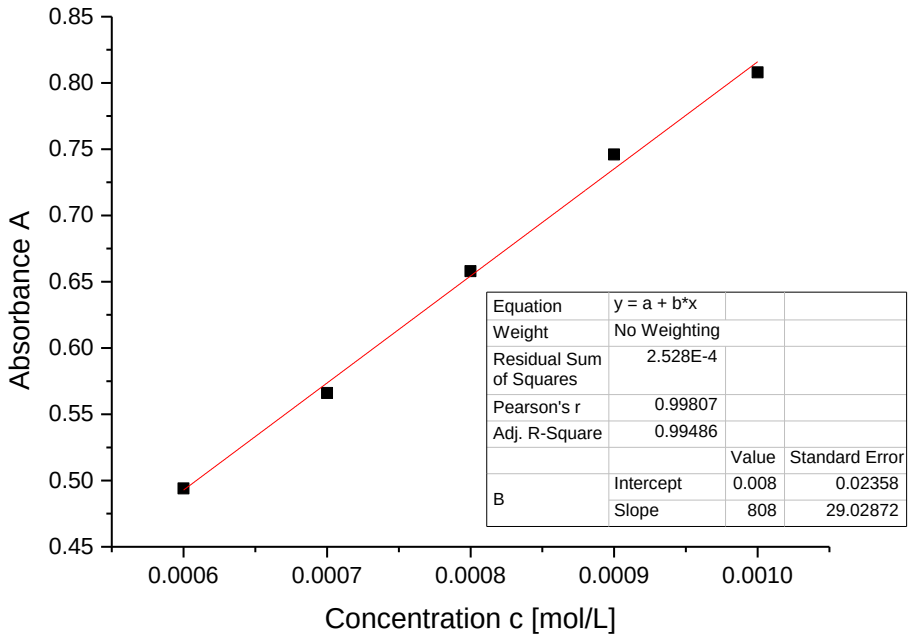

Supplementary Figure 14: Determination of ε (8080 M^{-1} cm^{-1}) by linear regression of absorptions (λ = 364 nm) of **2b** against concentration.

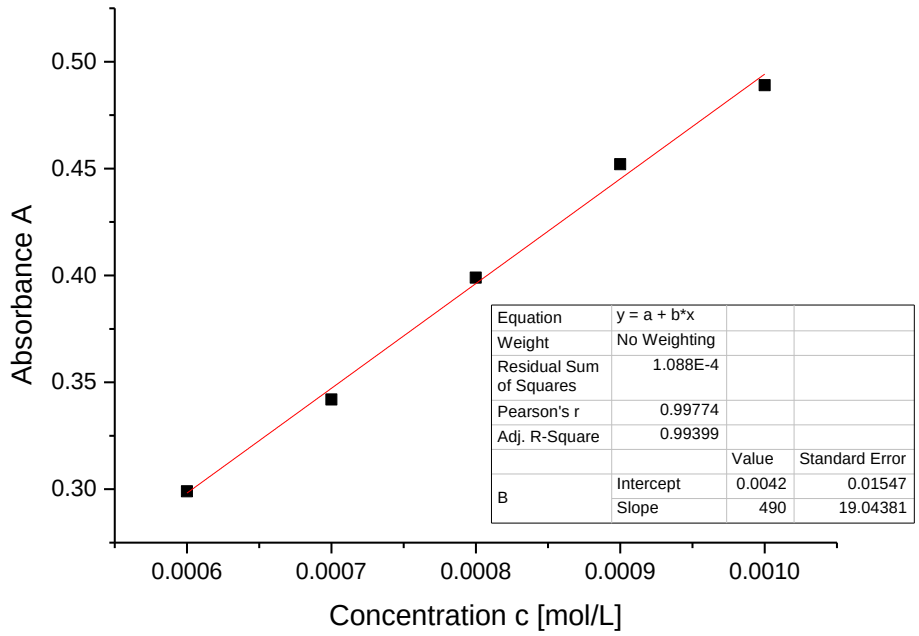

Supplementary Figure 15: Determination of ε (4900 M^{-1} cm^{-1}) by linear regression of absorptions (λ = 417 nm) of **2b** against concentration.

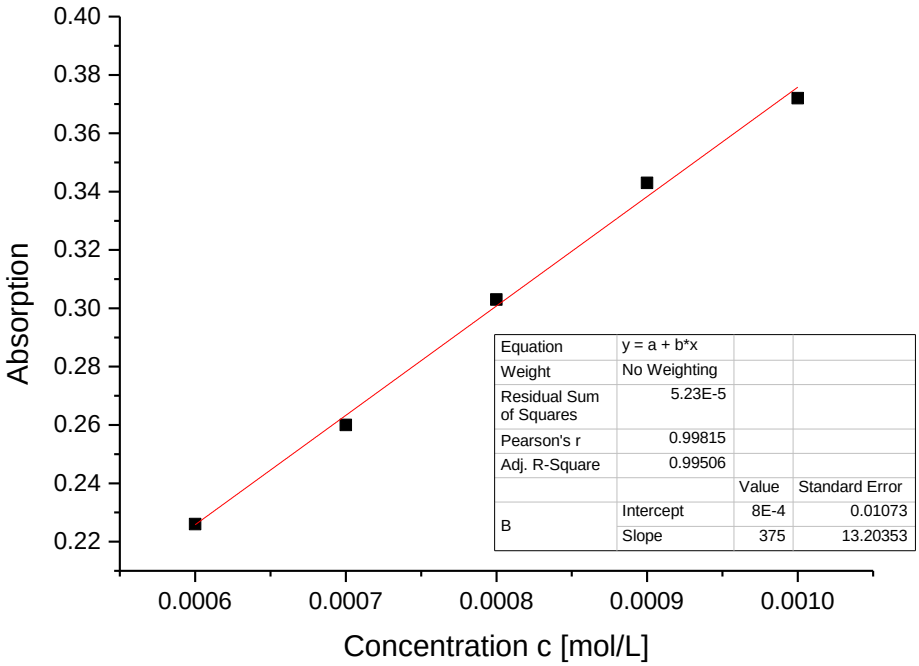

Supplementary Figure 16: Determination of ε (3750 M^{-1} cm^{-1}) by linear regression of absorptions (λ = 499 nm) of **2b** against concentration.

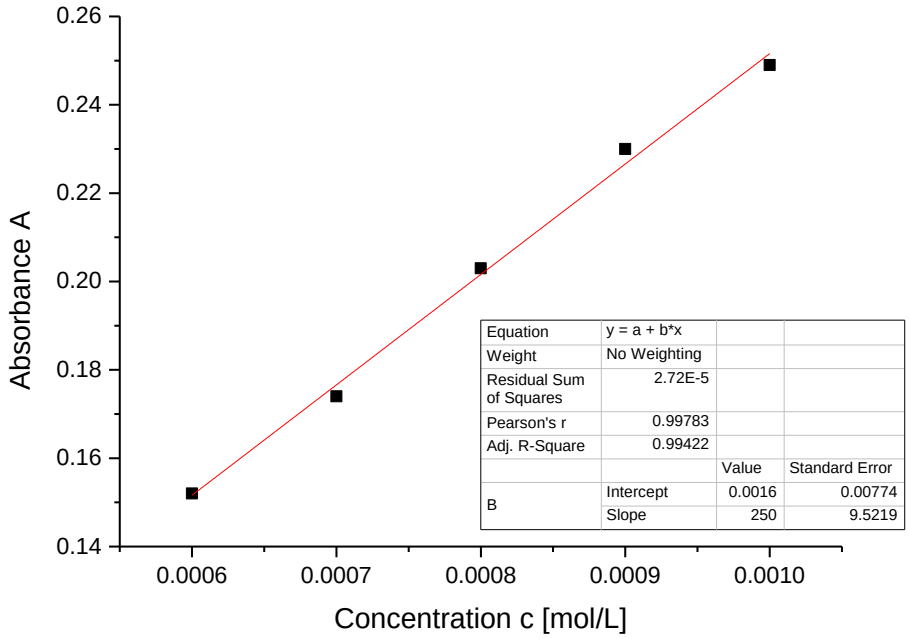

Supplementary Figure 17: Determination of ε (2500 M^{-1} cm^{-1}) by linear regression of absorptions (λ = 580nm) of **2b** against concentration.

(5-(Chlorobis(2,4,6-triisopropylphenyl)silyl)-2-(1,3-di-*tert*-butyl-4-phenyl-1,3,2λ^3-diazastannet-1-ium-2(3*H*)-yl)-3,3,4-tris(2,4,6-triisopropylphenyl)tricyclo [2.1.0.0$^{2.5}$]pentasilane-1-yl)iridium (2c)

Quantities: Si_6NHSn **1c**, 400 mg (0.24 mmol), $[(cod)IrCl]_2$ 113.07 mg (0.168 mmol), benzene 10 mL, filtration from hexane 10 mL, crystallization from hexane. Yield: 284 mg (0.152 mmol ; 63 %) violet crystals (mp. 182 °C, dec.).

^{1}H-NMR (400.13 MHz, C_6D_6, 300 K) δ = 7.637 – 7.613 ($C_{10}H_8$), 7.364 – 7.237 (m, 1H, Ar-H), 7.261 – 7.237 ($C_{10}H_8$), 7.157 – 7.7126 (m, 8H, Ar-H overlapping with C_6D_6), 7.050 – 78.863 (m, 9H, Ar-H), 6.809 (bs, 2H, Ar-H), 6.709 – 6.705 (m, 1H, Ar-H), 5.841 (sept, 1H, $^3J_{HH}$ = 6.41 Hz, Tip-*i*Pr-CH_2), 5.122 (sept, 1H, $^3J_{HH}$ = 6.52 Hz, Tip-*i*Pr-CH_2), 4.947 – 4.862 (m, 3H, Tip-*i*Pr-CH_2), 4,681 (sept, 1H, $^3J_{HH}$ = 6.41 Hz, Tip-*i*Pr-CH_2), 4.467 – 4.359 (m, 2H, Tip-*i*Pr-CH_2), 3.908 (sept, 1H, $^3J_{HH}$ = 6.74 Hz, Tip-*i*Pr-CH_2), 3.449 (sept, 1H, $^3J_{HH}$ = 6.81 Hz, Tip-*i*Pr-CH_2), 3.148 (sept, 1H, $^3J_{HH}$ = 6.43 Hz, Tip-*i*Pr-CH_2), 2.826 – 2.592 (m, 7H, Tip-*i*Pr-CH_2), 2.133 (d, 3H, $^3J_{HH}$ = 6.58 Hz, Tip-*i*Pr-CH_3), 2.070 (d, 3H, $^3J_{HH}$ = 6.32 Hz, Tip-*i*Pr-CH_3), 1.931 (t, 7 H, $^3J_{HH}$ = 6.58 Hz, Tip-*i*Pr-CH_3), 1.856 (d, 3H, $^3J_{HH}$ = 6.58 Hz, Tip-*i*Pr-CH_3), 1.814 (d, 3H, $^3J_{HH}$ = 6.58 Hz, Tip-*i*Pr-CH_3), 1.728 (d, 3H, $^3J_{HH}$ = 6.58 Hz, Tip-*i*Pr-CH_3), 1.609 (d, 4H, $^3J_{HH}$ = 6.54 Hz, Tip-*i*Pr-CH_3), 1.550 – 1.526 (m, 7H, Tip-*i*Pr-CH_3), 1.475 (d, 4H, $^3J_{HH}$ = 6.54 Hz, Tip-*i*Pr-CH_3), 1.376 (d, 4H, $^3J_{HH}$ = 6.54 Hz, Tip-*i*Pr-CH_3), 1.332 (d, 4H, $^3J_{HH}$ = 6.54 Hz, Tip-*i*Pr-CH_3), 1.277 – 1.083 (m, 44 H, Tip-*i*Pr-CH_3), 0.888 (t, hexane), 0.735 – 0.688 (m, 16H, Tip-*i*Pr-CH_3) overlapping with $C(CH_3)_3$), 0.580 – 0.567 (m, 12H, Tip-*i*Pr-CH_3) overlapping with $C(CH_3)_3$), 0.524 (d, 3H, $^3J_{HH}$ = 6.51 Hz, Tip-*i*Pr-CH_3), 0.456 (d, 3H, $^3J_{HH}$ = 6.51 Hz, Tip-*i*Pr-CH_3), 0.310 (d, 3H, $^3J_{HH}$ = 6.51 Hz, Tip-*i*Pr-CH_3), 0.179 (d, 3H, $^3J_{HH}$ = 6.51 Hz, Tip-*i*Pr-CH_3) ppm.

^{13}C-NMR (100.61 MHz, C_6D_6, 300 K) δ = 170.51 (s, 1C, C-Ph), 156.34, 155.42, 154.84, 154.60, 154.25, 154.06, 153.66, 153.42, 152.67 (s, each 1C, Ar-C), 150.47, 150.14, 150.06, 149.04, 148.01 (s, each 1C, Ar-C), 141.45, 139.90, 136.96, 136.21, 135.42, 134.38 (s, each 1C, Ar-C), 130.41, 129.87, 129.10 (s, each 1C, Ar-CH), 128.11, 127.87 (s, each 1C, overlapping with C_6D_6, Ar-CH), 127.29, 127.13 (bs, each 1C, Ar-CH), 126.00 (s, 1C, Ar-CH), 123.76, 123.49, 123.14, 122.98, 122.38, 122-29, 122.18, 121.81, 120.42 (s, each 1C, Ar-CH), 53.35 (s, 1C, $C(CH_3)_3$), 52.82 (s, 1C, $C(CH_3)_3$), 38.54 (s, 1C, Tip-*i*Pr-CH), 36.11, 35.95 (s, each 1C, Tip-*i*Pr-CH), 35.17 (s, 1C, Tip-*i*Pr-CH), 34.80, 34.71, 34.62, 34.58, 34.38, 34.29, 34.15, 34.07 (bs, each 1C, Tip-*i*Pr-CH), 32.34 (s, 1C, Tip-*i*Pr-CH), 31.91, 31.89 (bs, overlapping, together 2C, Tip-*i*Pr-CH), 31.16 (s, 1C, Tip-*i*Pr-CH), 29.97, 29.77 (s, each 1C, Tip-*i*Pr-CH_3), 28.16, 27.76 (s, each 1C, Tip-*i*Pr-CH_3), 26.21, 25.89, 25.73, 25.60, 25.24, 25.06, 24.87 (s, each 1C, Tip-*i*Pr-CH_3), 24.52, 254.40, 24,30, 24.15, 23.99, 23.88, 23.80, 23.77 (bs, each 1C, Tip-*i*Pr-CH_3), 23.50 (s, 1C, Tip-*i*Pr-CH_3), 23.19 (s, 1C, Tip-*i*Pr-CH_3), 23.00 (s, 1C, Tip-*i*Pr-CH_3), 22.71, 22.21 (s, 1C, Tip-*i*Pr-CH_3), 14.3 (s, 1C, Tip-*i*Pr-CH_3) ppm.

^{29}Si-NMR (79.49 MHz, C_6D_6, 300 K) δ = 50.2 (s, $SiTip_2$), 12.2 (s, $SiTip_2Cl$), −42.1 (s, SiTip), −80.4 (s, Si1), −95.6 (s, Si-NHSn), −116.0 (s, Si-Ir) ppm.

^{119}Sn-NMR (149.21 MHz, C_6D_6, 300 K) δ = 180.3 (s) ppm.

CP-MAS ^{29}Si-NMR (79.53 MHz, 14KHz, 300K) δ = 50.6 (s, $SiTip_2$), 42.4 (s, $SiTip_2$), 10.3 (s, SiTip), −42.2 (s, $SiTip_2$), −43.5 (s, $SiTip_2$), −68.1 (bs, Si-NHSn), −77.0 (bs, Si-NHSn), −94.6 (bs, unsubsituted-Si), −103.8 (s, unsusbtituted-Si), −120.2 (s, unsubstituted-Si) ppm.

CP-MAS ^{119}Sn-NMR (149.27 MHz, 13KHz, 300K) δ = 204.2 (s), 181.7 (s) ppm.

CP-MAS ^{119}Sn-NMR (149.27 MHz, 11KHz, 300K) δ = 204.9 (s), 182.6 (s) ppm.

Elemental analysis: calculated for $C_{97}H_{146}ClIrN_2Si_6Sn$: C: 62.80 % ; H: 7.93 % ; N: 1.51 %. Found: C: 62.59 % ; H: 8.02 % ; N: 1.42 %.

UV/VIS (hexane): λ_{max} (ε) = 592 nm (2660 M^{-1} cm^{-1}).

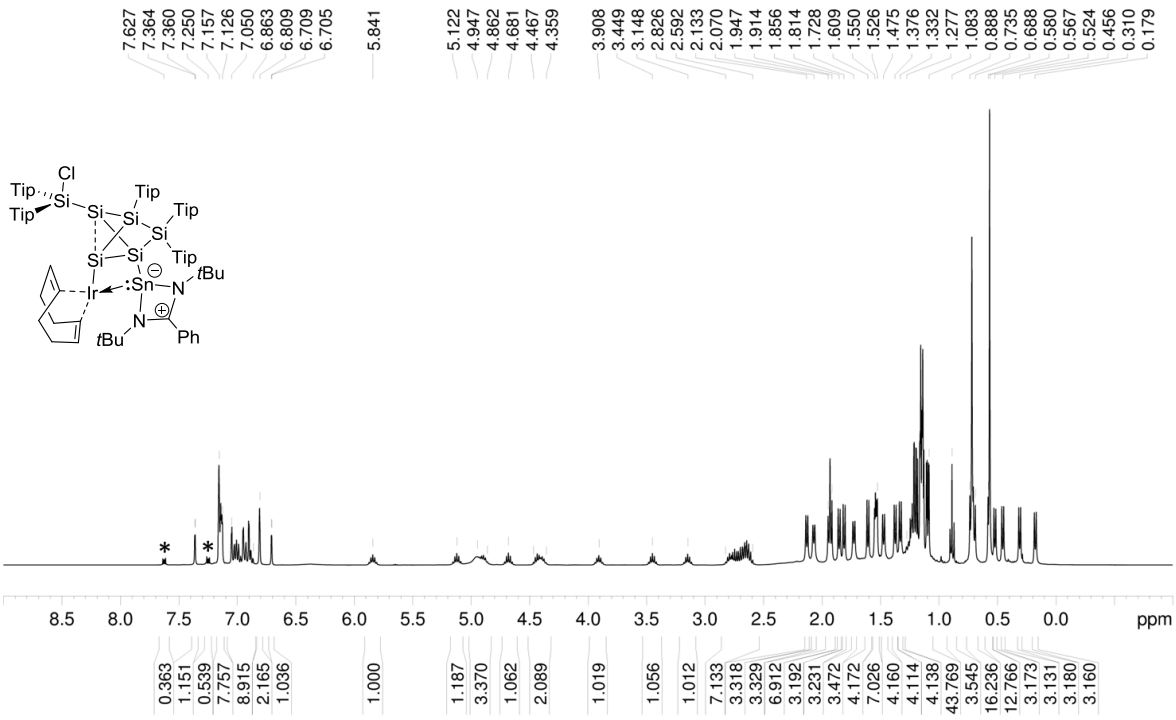

Supplementary Figure 18: ^{1}H NMR spectrum of **2c** in C_6D_6 (400.13 MHz, 300 K). Residual naphthalene ($C_{10}H_8$) marked with asterisk (*).

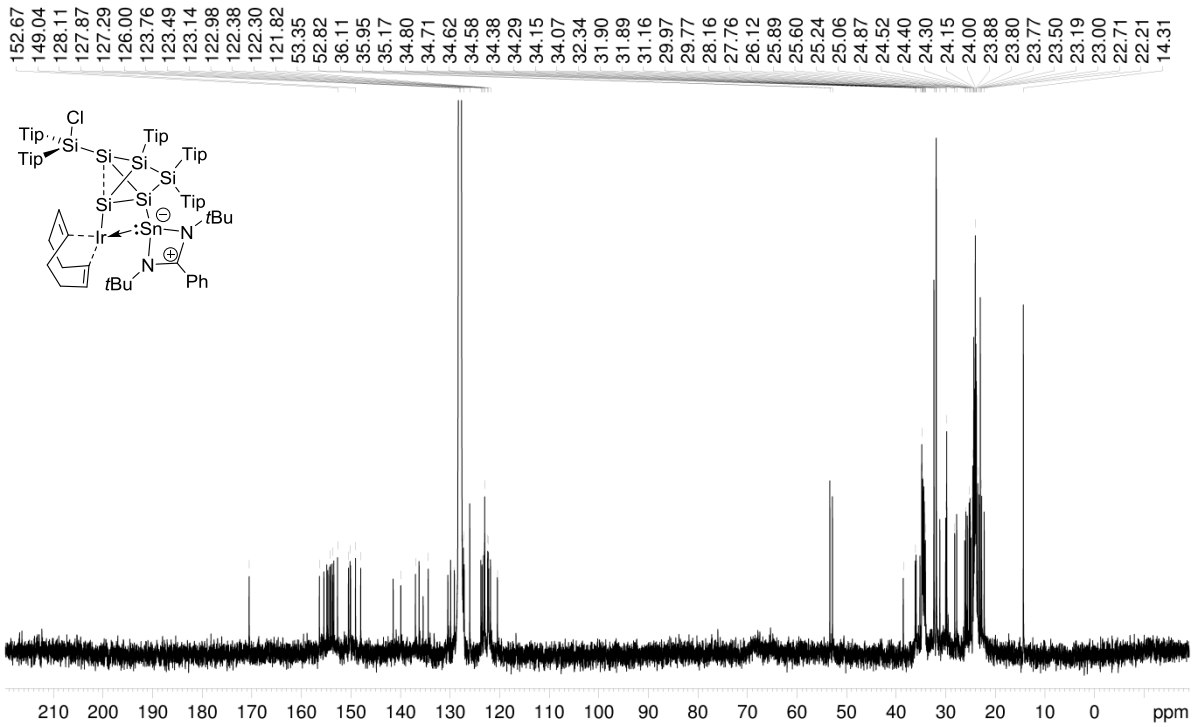

Supplementary Figure 19: ^{13}C NMR spectrum of **2c** in C_6D_6 (100.61 MHz, 300 K).

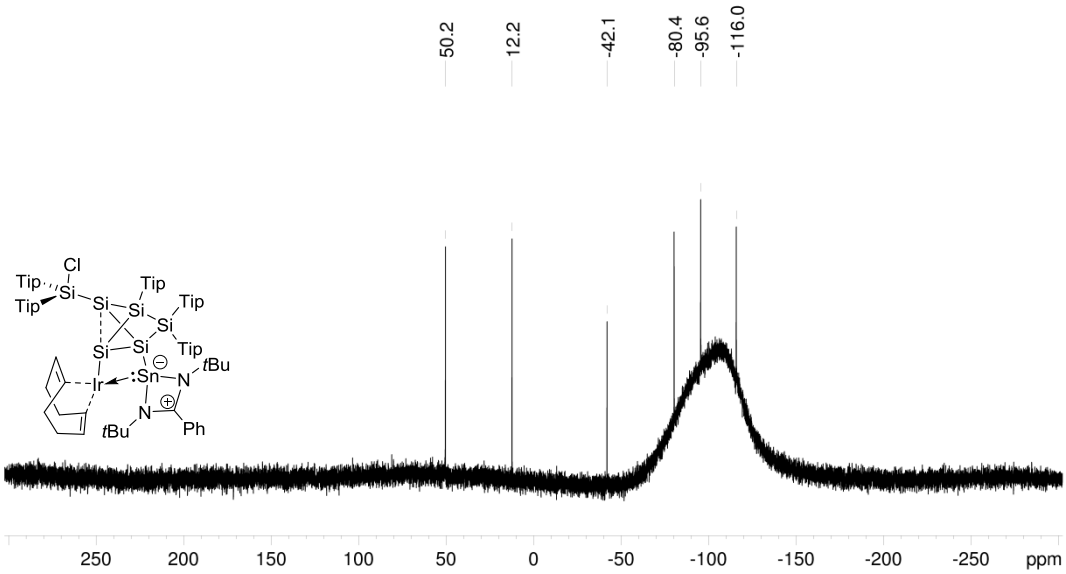

Supplementary Figure 20: ^{29}Si NMR spectrum of **2c** in C_6D_6 (79.49 MHz, 300 K).

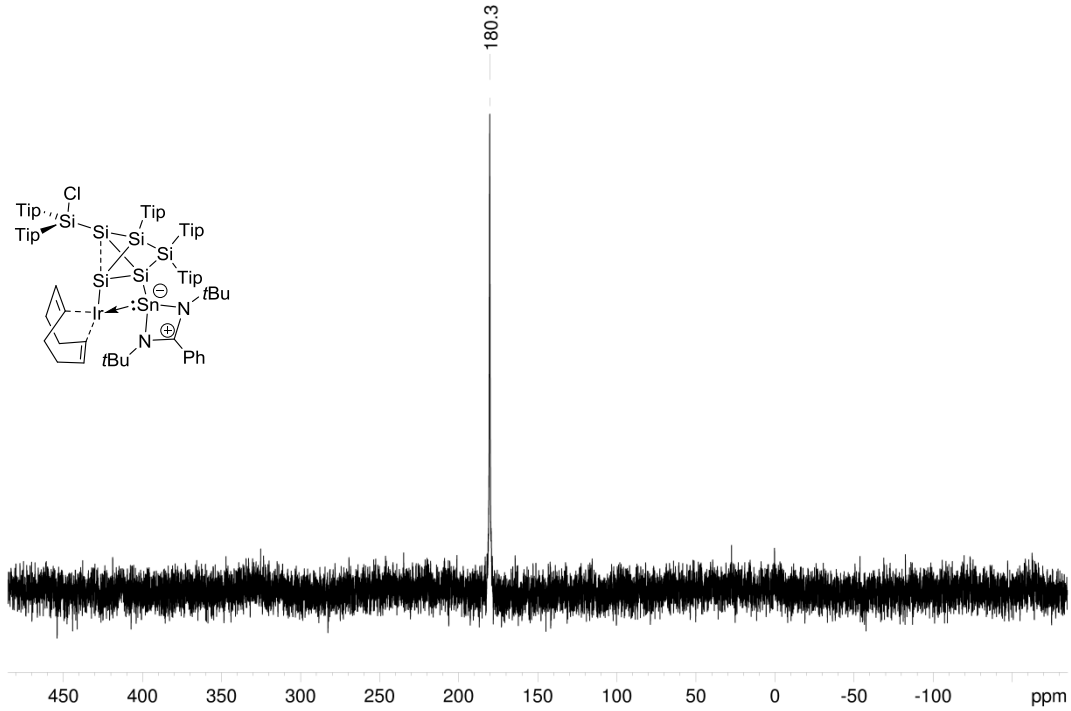

Supplementary Figure 21: ^{119}Sn NMR spectrum of **2c** in C_6D_6 (79.49 MHz, 300 K).

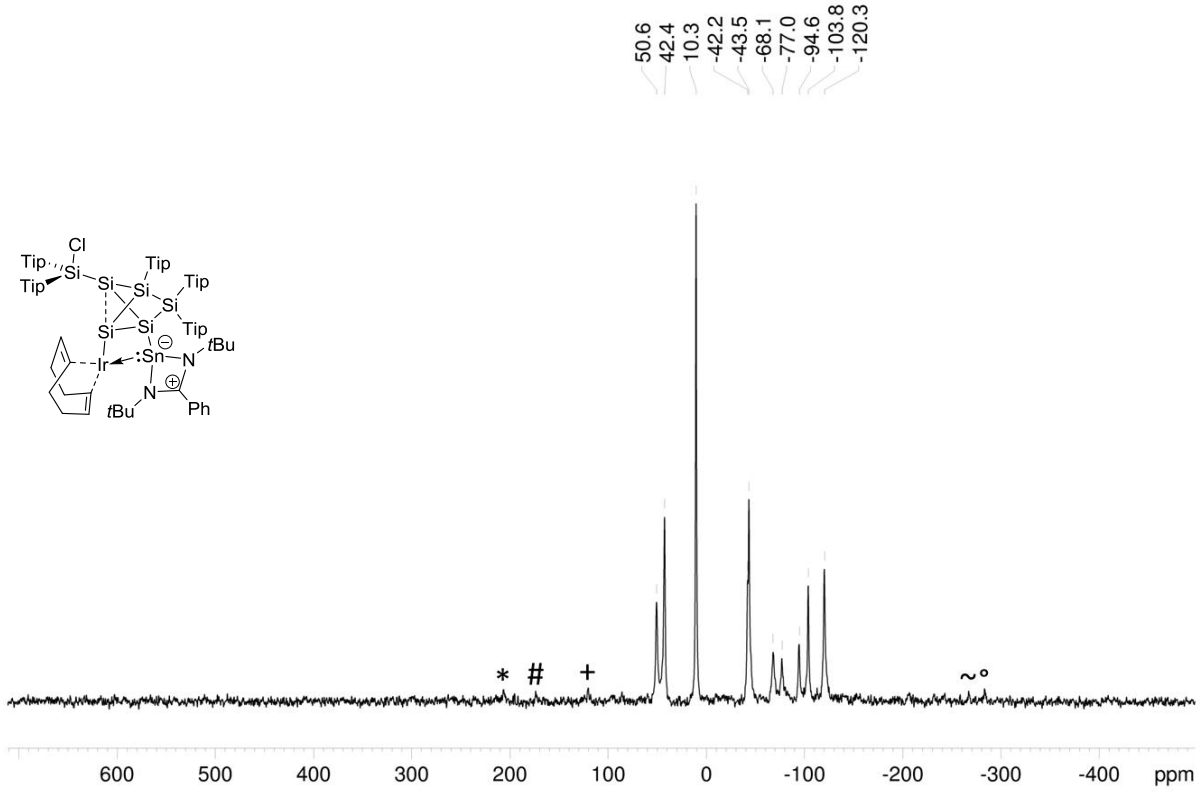

Supplementary Figure 22: CP MAS ^{29}Si NMR spectrum of **2c** (79.53 MHz, 13 KHz, 300 K), side spinning bands of: * $SiTip_2$ (42.4 ppm), # SiTip (10.3 ppm), + Si-NHSn (−68.1 ppm), ° unsubstituted Si (−120.3 ppm), ~ unsubstituted Si (−103.8 ppm).

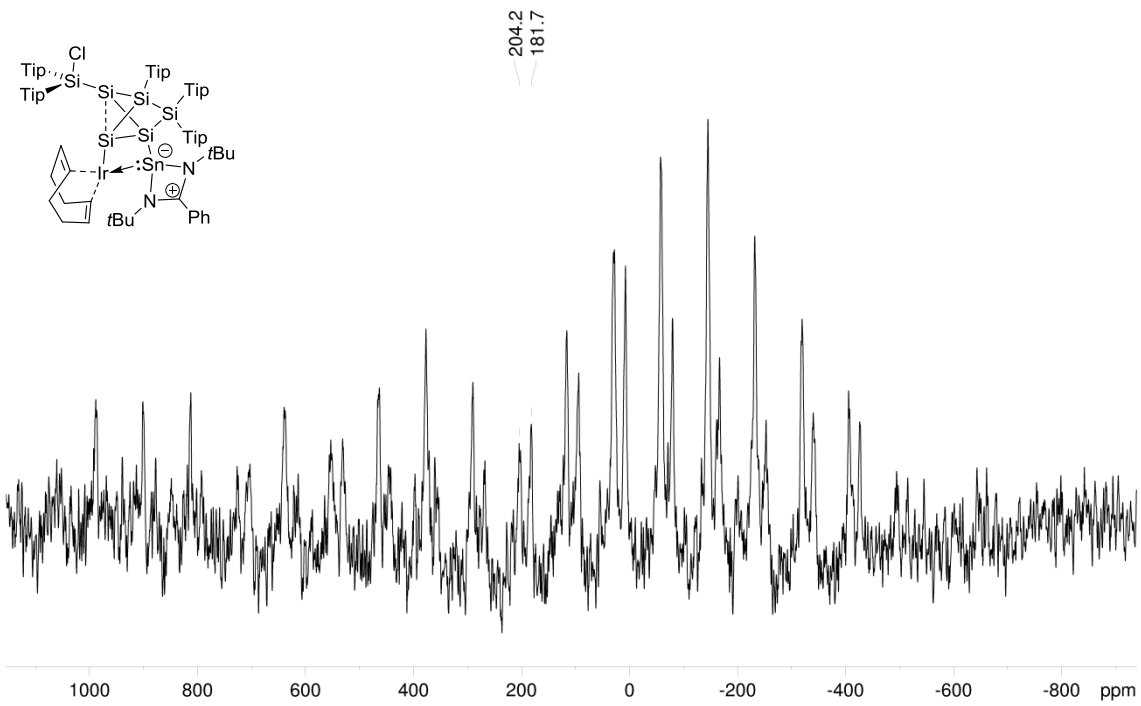

Supplementary Figure 23: CP MAS ^{119}Sn NMR spectrum of **2c** (149.27 MHz, 13 KHz, 300 K).

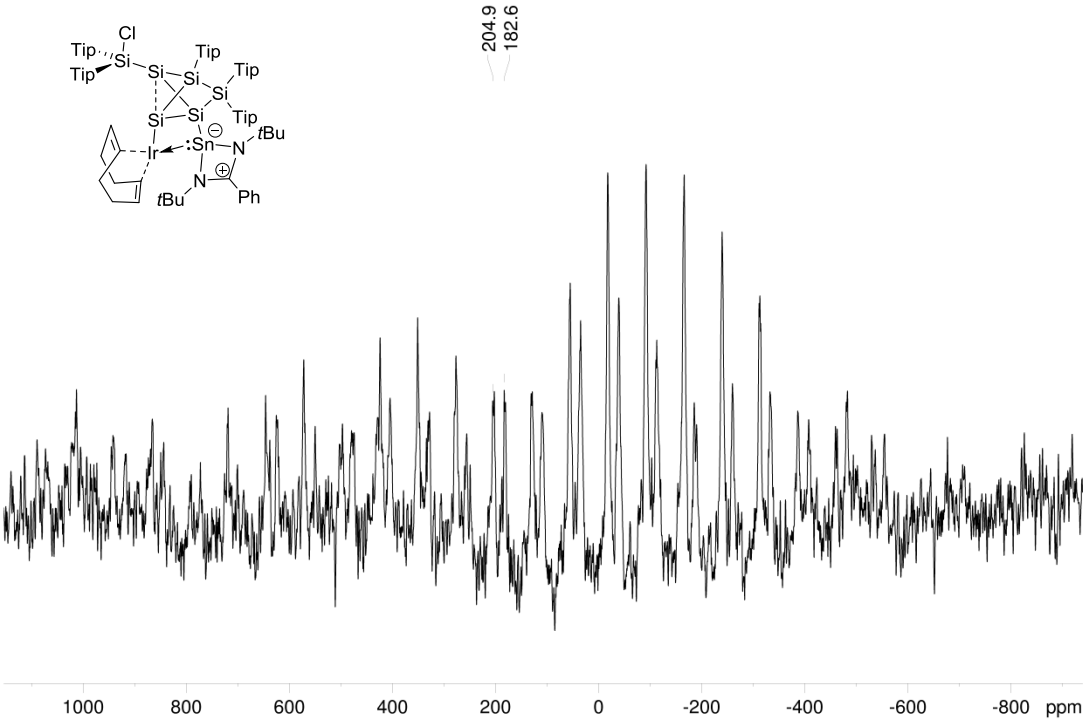

Supplementary Figure 24: CP MAS ^{119}Sn NMR spectrum of **2c** (149.27 MHz, 11 KHz, 300 K).

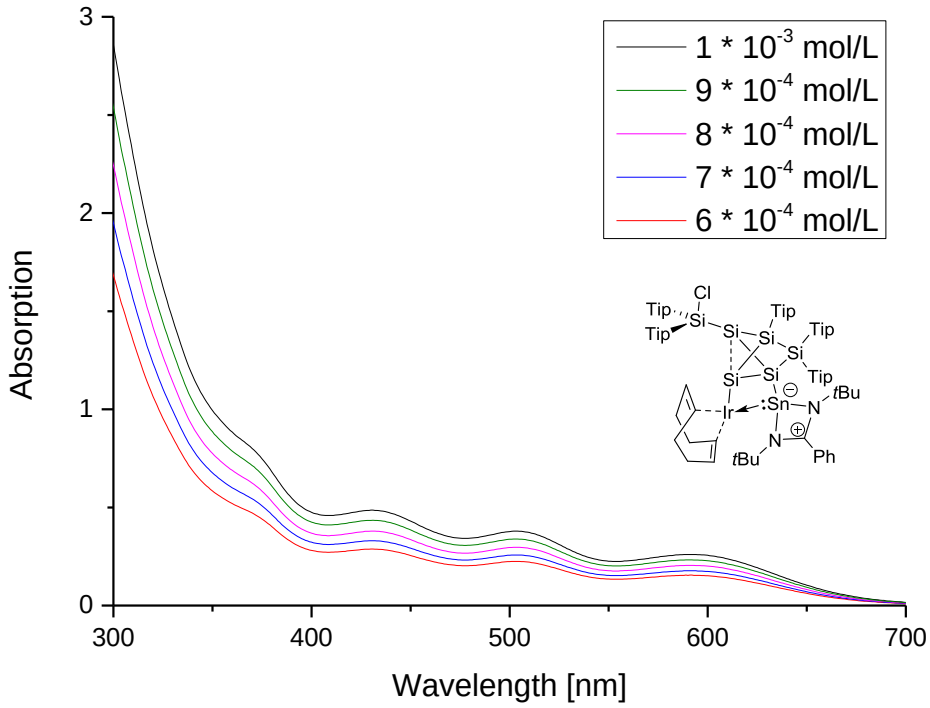

Supplementary Figure 25: UV-Vis spectrum of **2c** in hexane at different concentrations.

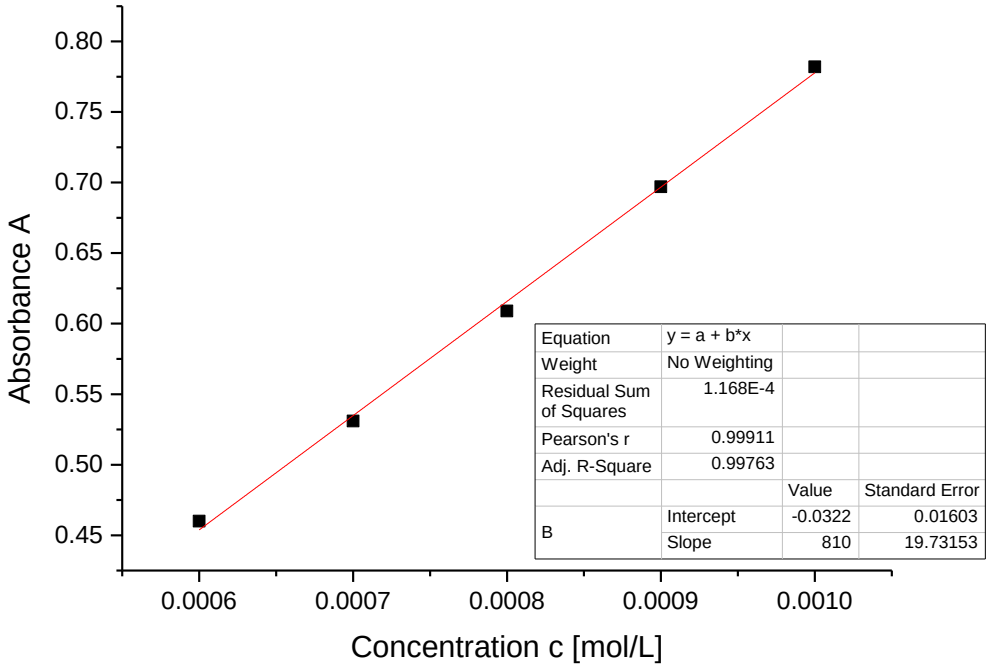

Supplementary Figure 26: Determination of ε (8100 M^{-1} cm^{-1}) by linear regression of absorptions (λ = 372 nm) of **2c** against concentration.

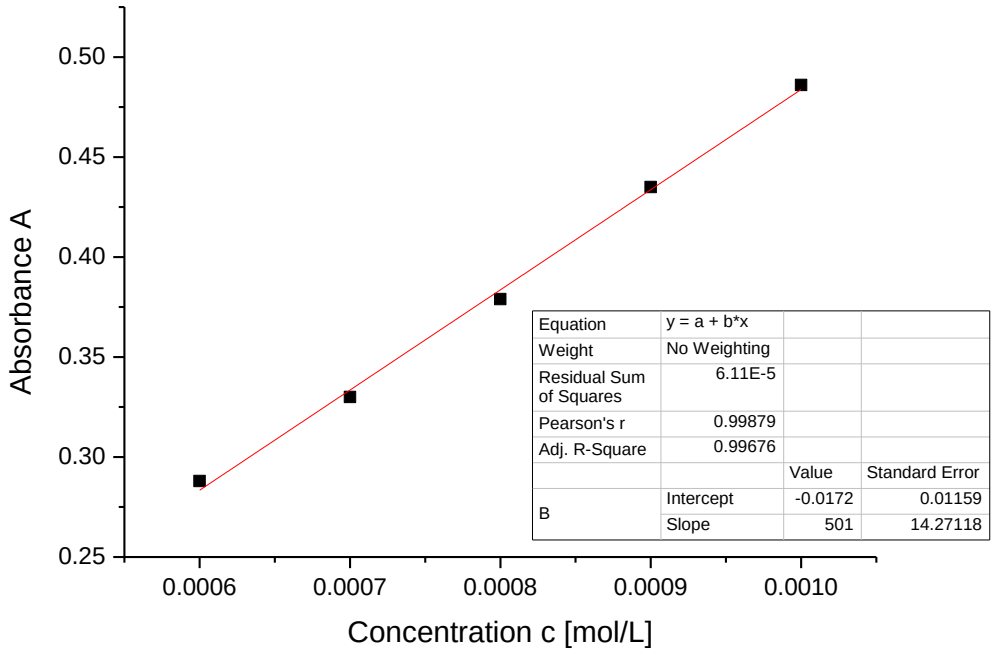

Supplementary Figure 27: Determination of ε (5010 M^{-1} cm^{-1}) by linear regression of absorptions (λ = 431 nm) of **2c** against concentration.

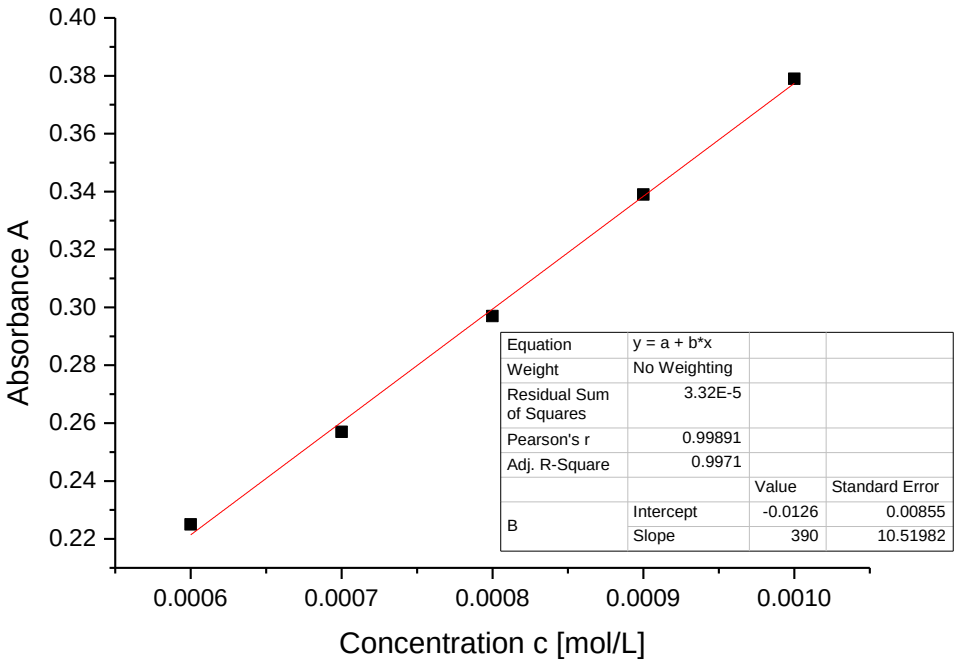

Supplementary Figure 28: Determination of ε (3390 M^{-1} cm^{-1}) by linear regression of absorptions (λ = 504 nm) of **2c** against concentration.

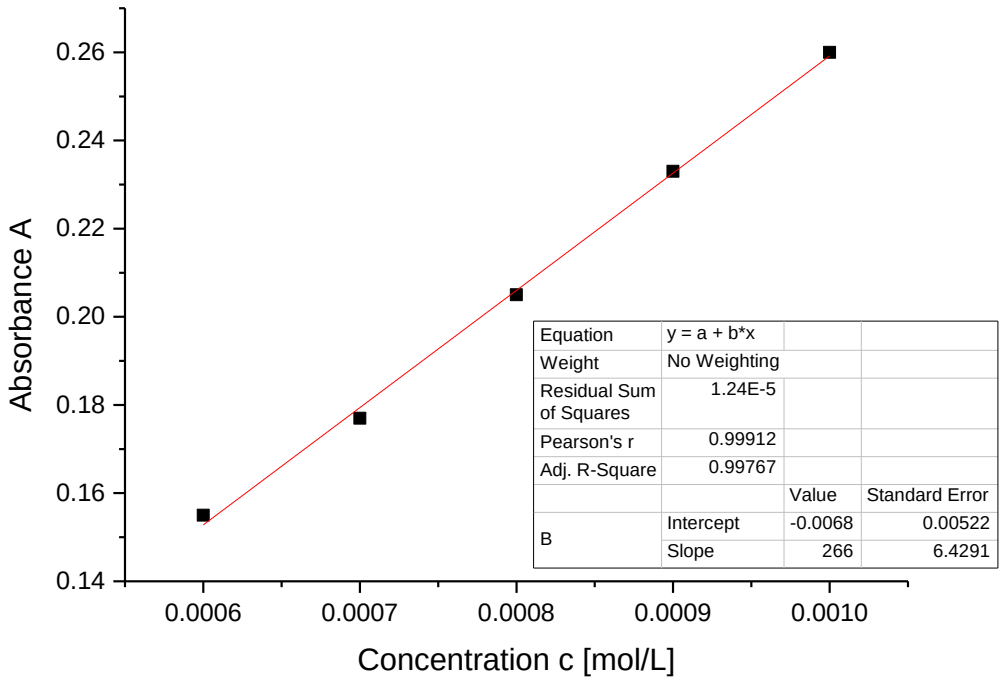

Supplementary Figure 29: Determination of ε (2660 M^{-1} cm^{-1}) by linear regression of absorptions (λ = 592 nm) of **2c** against concentration.

η^5-((2-(Chloro-λ^2-silyl)-4-(1,3-di-tert-butyl-4-phenyl-1,3,2-diazasilet-1-ium-2-id-2(3H)-yl)-1,1,2-tris(2,4,6-triisopropylphenyl)-1,2-dihydrotetrasilet-3-yl)bis(2,4,6-triisopropylphenyl)silyl) rhodium (3)

The silylene-substituted siliconoid **1a** (250 mg; 0.346 mmol) and 1 eq (67.29 mg; 0.346 mmol) of $[(CO)_2RhCl]_2$ were dissolved in 2 mL toluene and stirred for three minutes. The red-brown solution was directly stored at −26 °C for crystallization overnight. The mother liquor was removed by cannula and the crystals washed twice with 3 mL toluene each to yield red crystals of **3** (155 mg; 0.09621 mmol) in 56 % yield (mp. 178 °C, dec.).

^{1}H-NMR (400.13 MHz, C_6D_6, 300 K) δ = 7.379 (bs, 1H, Ar-H), 7.176 – 7.152 (m, 6H, Ar-H overlapping with C_6D_6), 7.125 – 7.100 (m, 3H, Ar-H), 7.062 (bs, 1H, Ar-H), 7.039 – 6.967 (m, 5H, Ar-H), 6.586 (sept, 1H, $^3J_{HH}$ = 6.30 Hz,Tip-*i*Pr-CH_2), 4.852, 4.685 (each sept, together 4H, $^3J_{HH}$ = 5.86 Hz Tip-*i*Pr-CH_2), 4.227 (sept, 1H, $^3J_{HH}$ = 6.55 Hz, Tip-*i*Pr-CH_2), 3.992 (sept, 1H, $^3J_{HH}$ = 6.55 Hz, Tip-*i*Pr-CH_2), 3.799 – 3.724 (m, 2H, Tip-*i*Pr-CH_2), 3.368 (sept, 1H, $^3J_{HH}$ = 6.40 Hz, Tip-*i*Pr-CH_2), 2.840 – 2.585 (m, 5H, Tip-*i*Pr-CH_2), 2.107 – 1.988 (m, 12H, Tip-*i*Pr-CH_3 overlapping with toluene), 1.707 – 1.643 (m, 11H, Tip-*i*Pr-CH_3), 1.540 – 1.524 (m, 7H, Tip-*i*Pr-CH_3), 1.483 – 1.444 (m, 11H, Tip-*i*Pr-CH_3), 1.241 – 1.116 (m, 35H, Tip-*i*Pr-CH_3), 1.023 (d, 3H, $^3J_{HH}$ = 6.37 Hz, Tip-*i*Pr-CH_3), 0.942 (s, 9H, $C(CH_3)_3$), 0.652 – 0.614 (m, 12H, Tip-*i*Pr-CH_3 overlapping with $C(CH_3)_3$), 0.527 (d, 3H, $^3J_{HH}$ = 6.32 Hz, Tip-*i*Pr-CH_3), 0.471 (dd, 6H, $^3J_{HH}$ = 5.89 Hz, Tip-*i*Pr-CH_3) ppm.

^{13}C-NMR (100.61 MHz, C_6D_6, 300 K) δ = 206.72 (s, 1C, CO), 206.03 (s, 1C, CO), 166.97 (s, 1C, Ar-C), 157.40 (s, 1C, Ar-C), 155.42 (s, 1C, Ar-C), 154.08, 153.79, 153.66, 153.44, 152.89 (s, each 1C, Ar-C), 150.95 (s, 1C, Ar-C), 149.33, 148.79, 148.52, 148.27 (s, each 1C, Ar-C), 144.48 (s, 1C, Ar-C), 141.15 – 141.13 (m, 2C, Ar-C), 137.81 (s, 1C, Ar-C), 136.32 – 136.29 (m, 2C, Ar-C), 135.58 (s, 1C, Ar-C), 132.10 – 132.03 (d, 1C, J = 6.06 Hz, Ar-C), 130.61 (s, 1C, Ar-C), 129.26 (s, 1C, Ar-CH), 129.22 (s, 1C, Ar-CH), 128.87 (bs, 1C, Ar-CH), 128.49 (s, 1C, Ar-CH). 128.11, 127.87 (s, each 1C, Ar-CH overlapping with C_6D_6), 125.63 (s, 1C, Ar-CH), 124.47, 123.95, 123.54 (s, each 1C, Ar-CH), 122.61 (s, 1C, Ar-CH), 122.35 (s, 1C, Ar-CH), 122.23, 122.15, 122.10 (bs, together 3C, Ar-CH), 121.50 (s, 1C, Ar-CH), 56.21 (s, 1C, $C(CH_3)_3$), 55.36 (s, 1C, $C(CH_3)_3$), 37.02 – 36.93 (d, 2C, J = 9.58 Hz, Tip-*i*Pr-CH), 36.43, 36.32, 36.28 (ns, together 3C, Tip-*i*Pr-CH), 35.90 (s, 1C, Tip-*i*Pr-CH), 34.75 (s, 1C, Tip-*i*Pr-CH), 34.56 – 34.49 (d, 2C, J = 6.70 Hz, Tip-*i*Pr-CH), 34.30 – 34.27 (m, 2C, Tip-*i*Pr-CH), 34.18 (s, 1C, Tip-*i*Pr-CH), 33.95 (s, 1C, Tip-*i*Pr-CH), 33.53 (s, 1C, Tip-*i*Pr-CH), 31.05 (s, 1C, Tip-*i*Pr-CH), 29.64, 29.60 (bs, together 2C, Tip-*i*Pr-CH_3), 29.25, 28.68 (s, each 1C, Tip-*i*Pr-CH_3), 28.04 (s, 1C, Tip-*i*Pr-CH_3), 27.49, 27.37 (s, each 1C, Tip-*i*Pr-CH_3), 26.52, 26.48 (s, together 2C, Tip-*i*Pr-CH_3), 26.18, 26.03, 25.95 (s, each 1C, Tip-*i*Pr-CH_3), 25.30 (s, 1C, Tip-*i*Pr-CH_3), 24.87, 24.81, 24.71 (s, each 1C, Tip-*i*Pr-CH_3), 24.41 (s, 1C, Tip-*i*Pr-CH_3), 24.28, 24.26, 24.17, 24.11, 24.03, 23.83, 23.75 (m, together 7C, Tip-*i*Pr-CH_3), 22.99 (s, 1C, Tip-*i*Pr-CH_3), 21.39 (s, 1C, Tip-*i*Pr-CH_3) ppm.

^{29}Si-NMR (79.49 MHz, C_6D_6, 300 K) δ = 164.5 (d, 1Si, $^2J_{Si\text{-}Rh}$ = 53.4 Hz, Si-Cl), 158.8 (d, 1Si, $^2J_{Si\text{-}Rh}$ = 41.0 Hz, $SiTip_2$), 108.7 (d, 1Si, $^2J_{Si\text{-}Rh}$ = 59.6 Hz, NHSi), 58.3 (d, 1Si, $^2J_{Si\text{-}Rh}$ = 14.3 Hz, SiTip), −58.3 (s, $SiTip_2$), −122.1 (s, unsubstituted Si), −140.2 (s, unsubstituted Si) ppm.

CP-MAS ^{29}Si-NMR (79.53 MHz, 13 KHz, 300K) δ = 165.7 (bs, Si-Cl), 157.3 (bs, $SiTip_2$), 107.7 (d, 1Si, $^2J_{Si\text{-}Rh}$ = 62.6 Hz, NHSi), 54.1 (bs, SiTip), −62.3 (s, $SiTip_2$), −120.3 (s, unsubstituted Si), −142.1 (s, unsubstituted Si) ppm.

Elemental analysis: calculated for $C_{91}H_{138}ClN_2ORhSi_7$: C: 67.84 % ; H: 8.63 % ; N: 1.74 %. Found: C: 66.73 % ; H: 7.78 % ; N: 1.63 %.

UV/VIS (hexane): λ_{max} (ε) = 461 nm (11630 M^{-1} cm^{-1}).

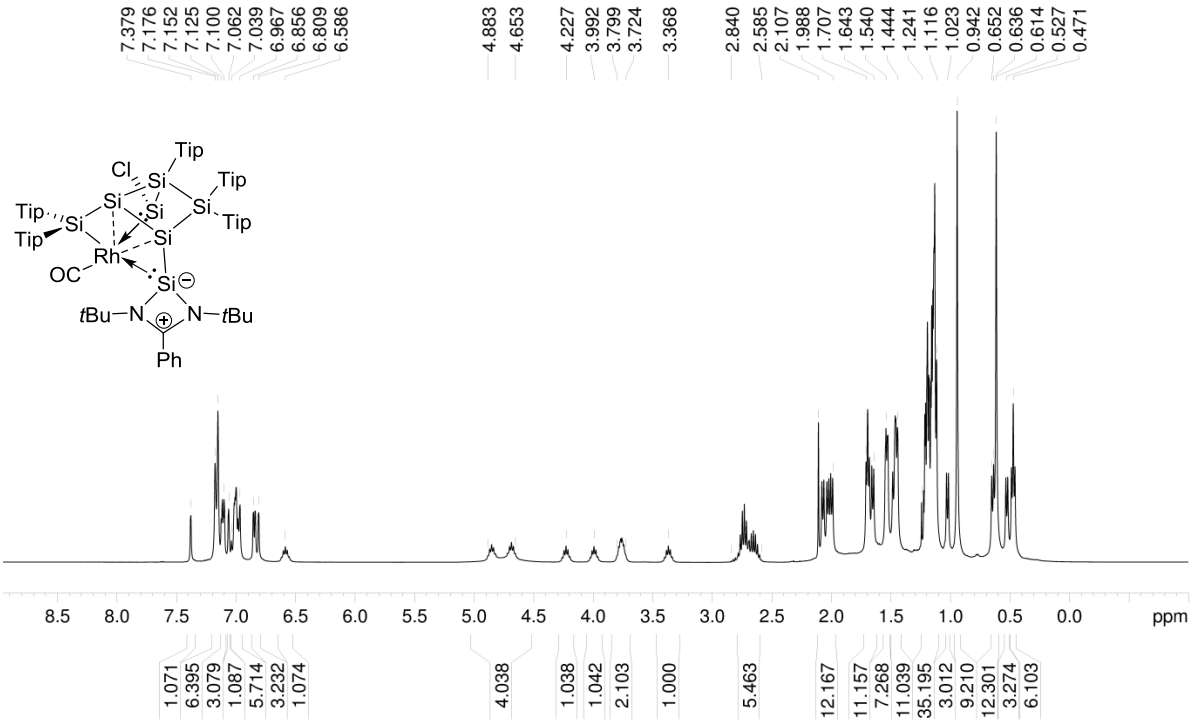

Supplementary Figure 30: ^{1}H NMR spectrum of **3** in C_6D_6 (400.13 MHz, 300 K).

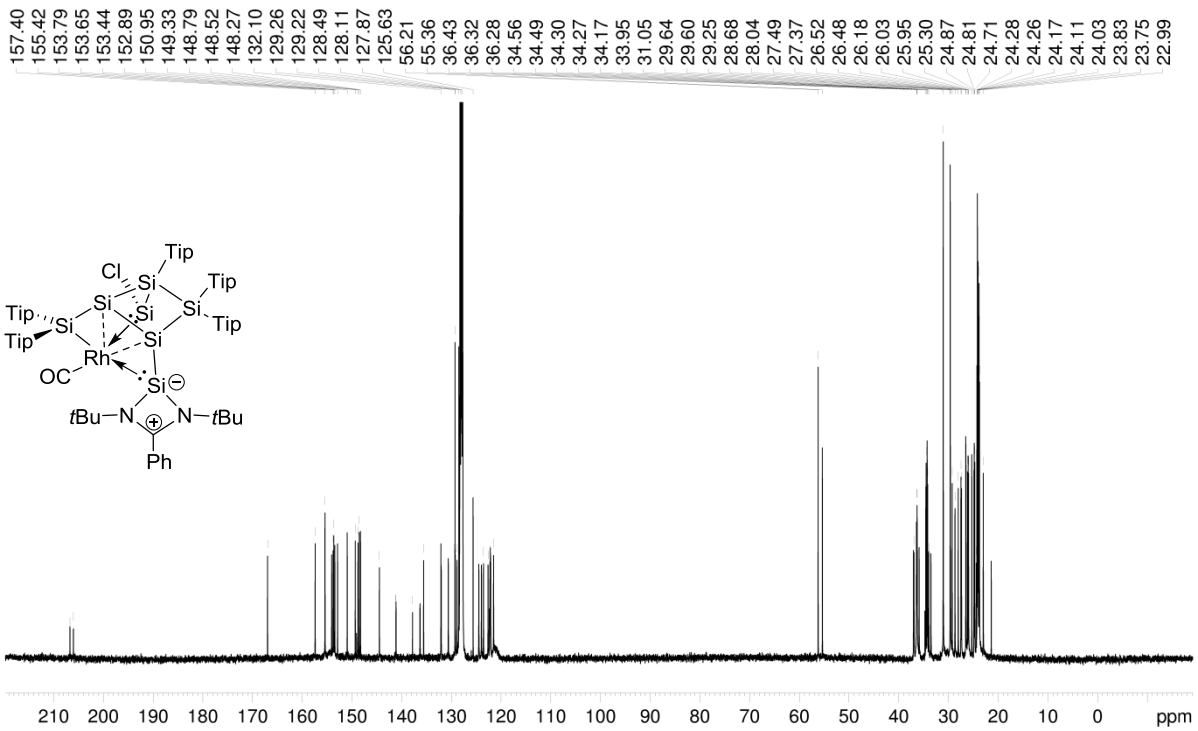

Supplementary Figure 31: ^{13}C NMR spectrum of **3** in C_6D_6 (100.61 MHz, 300 K).

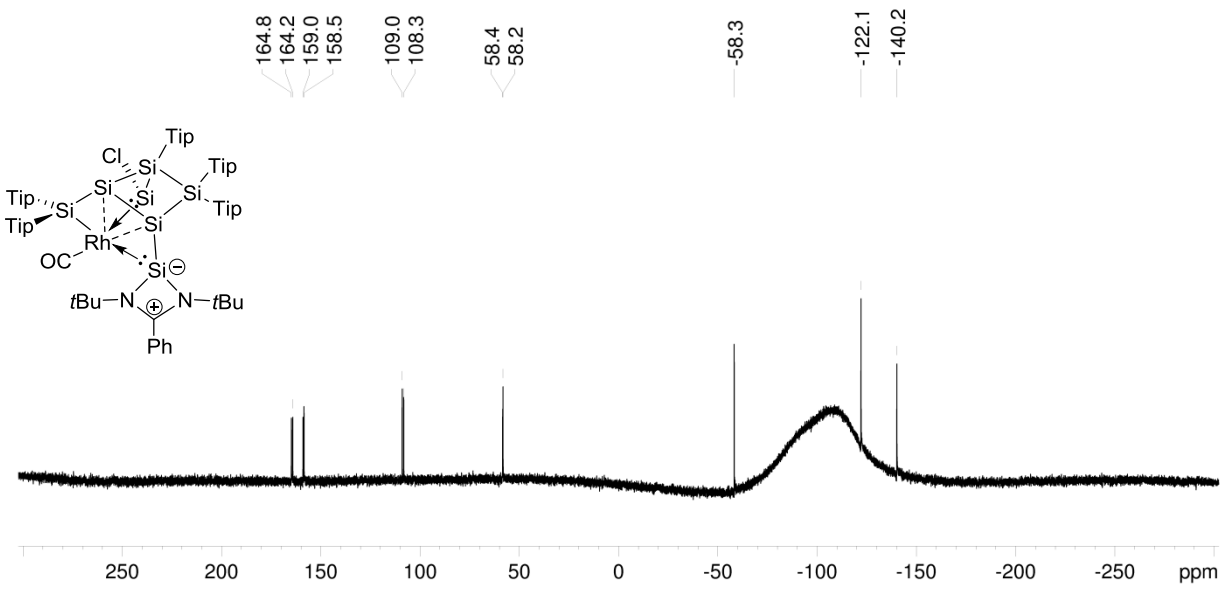

Supplementary Figure 32: ^{29}Si NMR spectrum of **3** in C_6D_6 (79.49 MHz, 300 K).

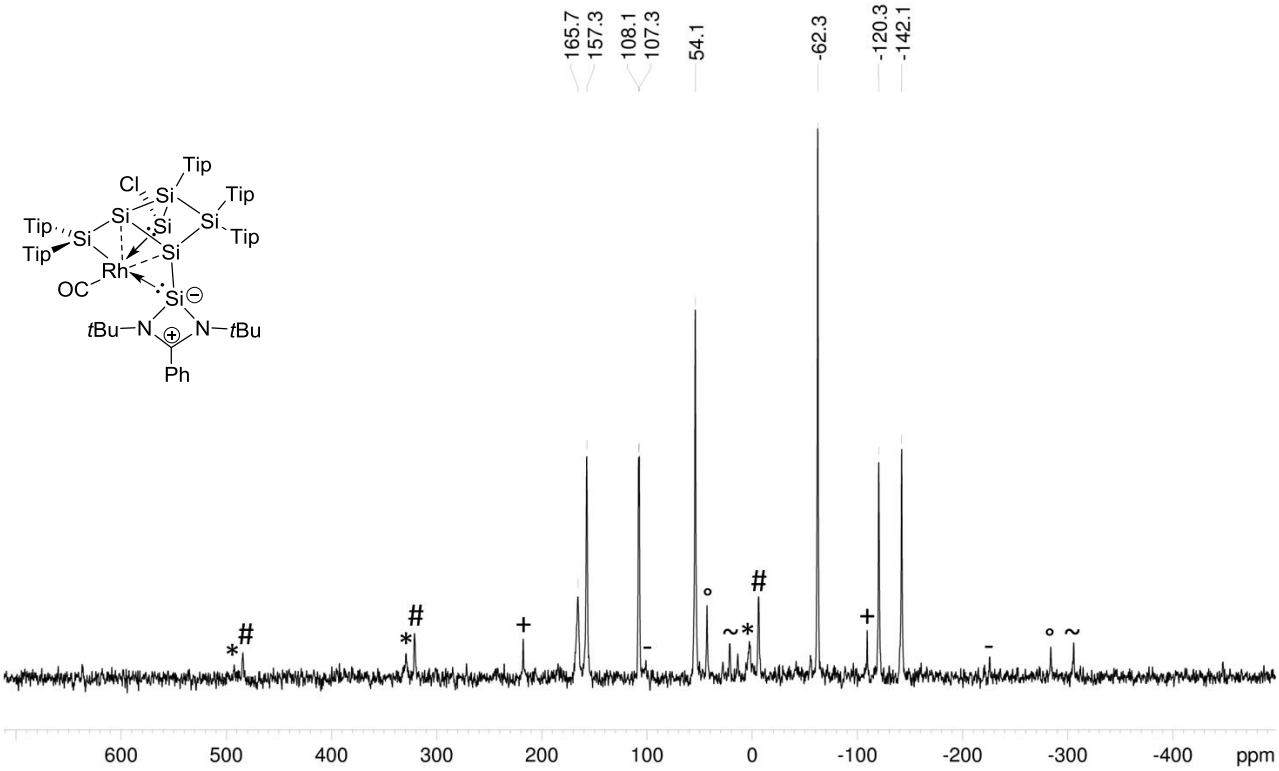

Supplementary Figure 33: CP MAS ^{29}Si NMR spectrum of **3** (79.53 MHz, 13 KHz, 300 K), side spinning bands of: * Si-Cl (165.7 ppm), # $SiTip_2$ (157.3 ppm), + SiTip (54.1 ppm), - $SiTip_2$ (−62.3 ppm), ° unsubstituted Si (−120.3 ppm), ~ unsubstituted Si (−124.1 ppm).

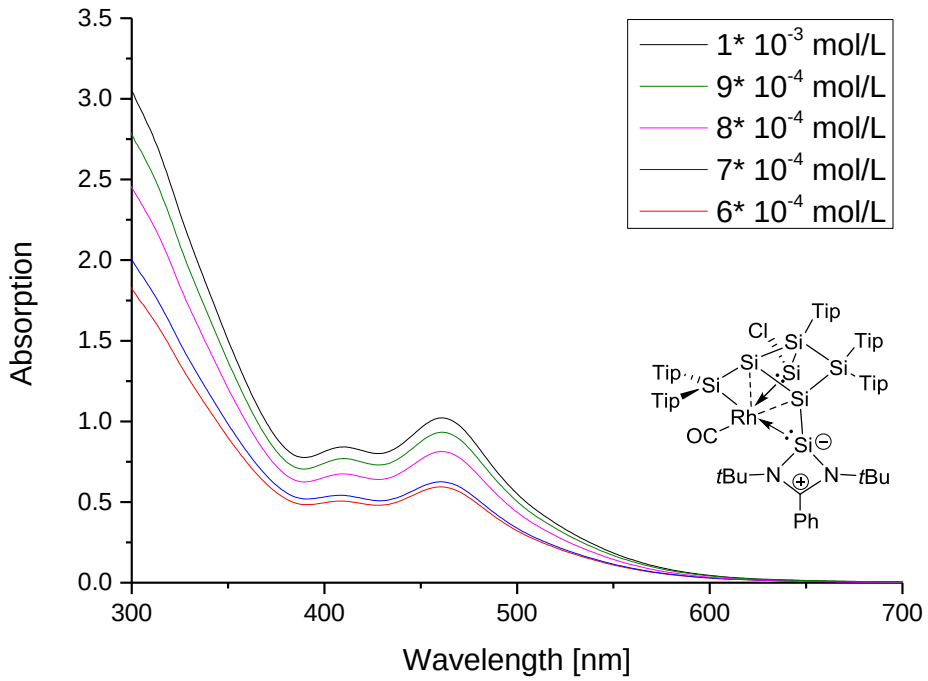

Supplementary Figure 34: UV-Vis spectrum of **3** in hexane at different concentrations.

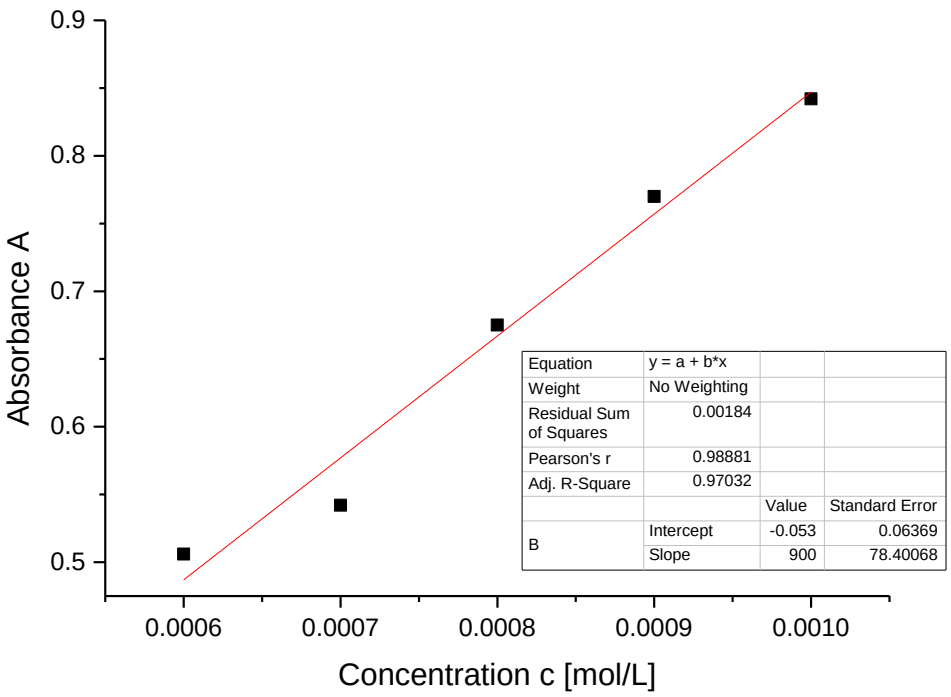

Supplementary Figure 35: Determination of ε (9000 M^{-1} cm^{-1}) by linear regression of absorptions (λ = 410 nm) of **3** against concentration.

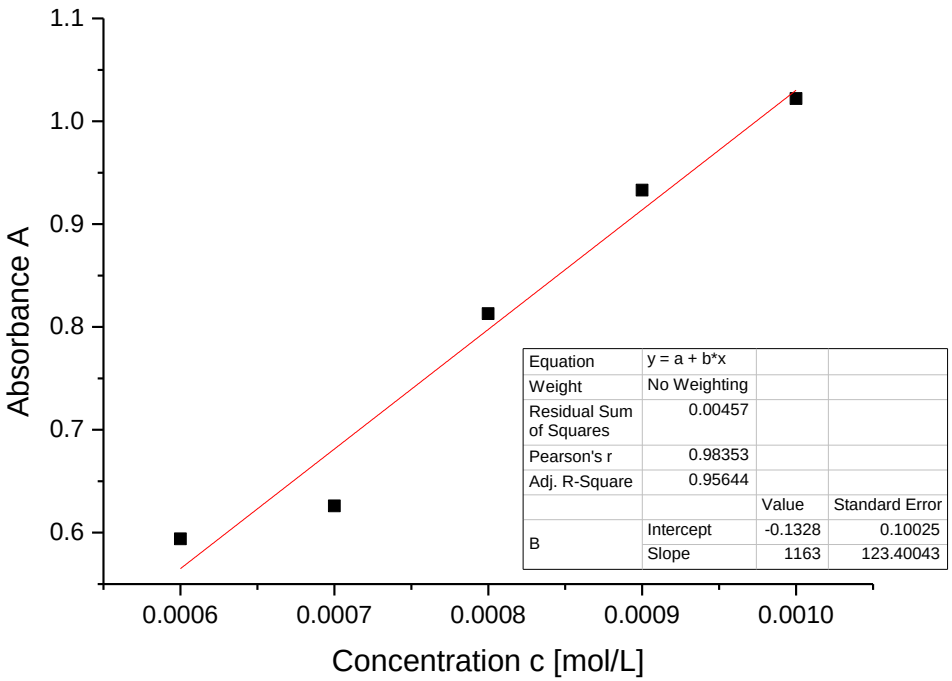

Supplementary Figure 36: Determination of ε (11630 M^{-1} cm^{-1}) by linear regression of absorptions (λ = 461 nm) of **3** against concentration.

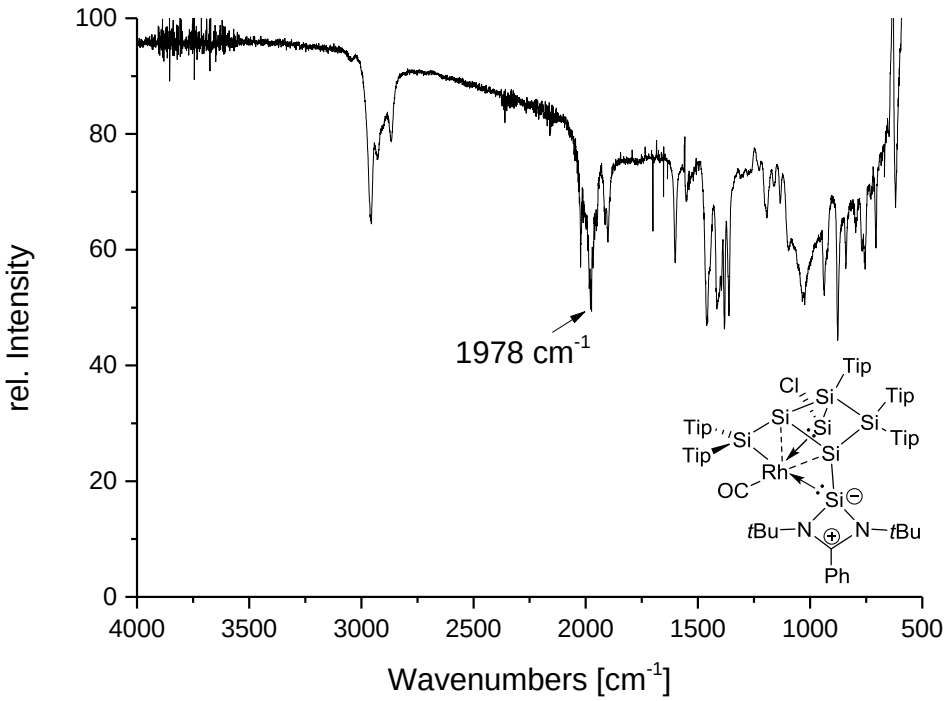

Supplementary Figure 37: Infrared spectrum of **3**.

***trans*-Dicarbonyl-(1,3-di-tert-butyl-2-chloro-4-phenyl-2,3-dihydro-1,3,2-diazasilet-1-ium-2-ide)-*ligato*-(2,2,5,5,6-pentakis(2,4,6-triisopropylphenyl)tetra cyclo[2.2.0.01,3.03,6]hexasilan-4-yl)rhodium (4)**

The silylene-substituted siliconoid **1a** (500 mg; 0.346 mmol) and 1 eq (134.6 mg; 0.346 mmol) of $[(CO)_2RhCl]_2$ were dissolved in benzene 10 mL and stirred overnight at room temperature. The solvent was removed in vacuo and the dark red-brownish residue was filtered twice from each 7 mL hexane. The solution was concentrated to 1 mL and stored at −26 °C for one day to yield red-brownish crystals of **4** (280 mg; 0.217 mmol) in 63 % yield (mp. > 192 °C, dec.).

^{1}H-NMR (400.13 MHz, C_6D_6, 300 K) δ = 7.270 (s, 2H, Ar-H), 7.092 – 7.038 (m, 5H, Ar-H), 6.959 (bs, 1H, Ar-H), 6.883 – 6.842 (m, 4H, Ar-H), 6.809 – 6.752 (m, 3H, Ar-H), 5.415 (sept, 1H, $^3J_{HH}$ = 6.80 Hz, Tip-*i*Pr-CH_2), 5.286 (sept, 1H, $^3J_{HH}$ = 6.46 Hz, Tip-*i*Pr-CH_2), 5.088 (sept, 1H, $^3J_{HH}$ = 6.46 Hz, Tip-*i*Pr-CH_2), 4.729 (sept, 1H, $^3J_{HH}$ = 6.78 Hz, Tip-*i*Pr-CH_2), 4.206 (sept, 1H, $^3J_{HH}$ = 6.42 Hz, Tip-*i*Pr-CH_2), 4.099 (sept, 1H, $^3J_{HH}$ = 6.76, Tip-*i*Pr-CH_2), 3.879 (sept, 1H, $^3J_{HH}$ = 6.42 Hz, Tip-*i*Pr-CH_2), 3.556 (sept, 1H, $^3J_{HH}$ = 6.48 Hz, Tip-*i*Pr-CH_2), 3.424 (sept, 2H, $^3J_{HH}$ = 6.79 Hz, Tip-*i*Pr-CH_2), 2.860 – 2.760 (m, 2H, Tip-*i*Pr-CH_2), 2.738 – 2.562 (m, 3H, Tip-*i*Pr-CH_2), 2.335 (d, 3H, $^3J_{HH}$ = 5.69 Hz, Tip-*i*Pr-CH_3), 2.153 (d, 3H, $^3J_{HH}$ = 6.64 Hz, Tip-*i*Pr-CH_3), 1.811 (d, 3H, $^3J_{HH}$ = 6.23 Hz, Tip-*i*Pr-CH_3), 1.655 – 1.486 (m, 28 H, Tip-*i*Pr-CH_3), 1.276 – 1.228 (m, 16 H, Tip-*i*Pr-CH_3), 1.178 – 1.139 (m, 13H, Tip-*i*Pr-CH_3), 1.076 – 1.042 (m, 19H, Tip-*i*Pr-CH_3 overlapping with $C(CH_3)_3$), 0.939 (s, 9H, $C(CH_3)_3$), 0.889 (t, hexane), 0.786 – 0. 757 (m 6H, Tip-iPr-CH3), 0.554 – 0.516 (m, 6H, Tip-*i*Pr-CH_3), 0.433 (d, 3H, $^3J_{HH}$ = 6.45 Hz, Tip-*i*Pr-CH_3), 0.355 (d, 3H, $^3J_{HH}$ = 6.45 Hz, Tip-*i*Pr-CH_3), 0.280 (d, 3H, $^3J_{HH}$ = 6.45 Hz, Tip-*i*Pr-CH_3) ppm.

^{13}C-NMR (100.61 MHz, C_6D_6, 300 K) δ = 172.72 (s, 1C, Ar-C), 156.04, 155.40, 154.11, 153.86, 153.61, 153.37, 153.06, 152.52, 152.37, 152.24 (s, each 1C, Ar-C), 149.76, 149.18, 148.43, 148.39. 148.23 (s, each 1C, Ar-C), 140.73, 139.98, 138.28, 138.16 (s, each 1C, Ar-C), 133.11, 133.09 (bs, each 1C, Ar-C), 130.46 (s, 1C, Ar-CH), 129.99 (s, 1C, Ar-CH), 128.17 (s, 1C, Ar-CH), 127.82, 127.67 (s, each 1C, overlapping with C_6D_6, Ar-CH), 122.89, 122.84, 122.63, 122.56, 122.36, 121.69, 121.51, 121.03, 120.75, 120.33 (s, each 1C, Ar-CH), 54.59 (s, 1C, $C(CH_3)_3$), 54.54 (s, 1C, $C(CH_3)_3$), 37.16 (s, 1C, Tip-*i*Pr-CH), 36.03, 35.94, 35.81, 35.65, 35.20, 34.91, 34,46, 34.41, 34.24, 34.05, 34.02, 33.90, 33.80 (s, each 1C, Tip-*i*Pr-CH), 31.61, 30.88, 30.74 (s, each 1C, Tip-*i*Pr-CH), 28.20, 28.10, 27.48, 27.11, 26.43, 25.61 (s, each 1C, Tip-*i*Pr-CH_3), 24.68, 24.57, 24.51, 24.39, 24.33, 24.15, 23.96, 23.86, 23.74, 23.70 (bs, each 1C, Tip-*i*Pr-CH_3), 23.37, 23.30, 23.01, 22.98 (bs, each 1C, Tip-*i*Pr-CH_3), 22.70, 22.55 (s, each 1C, Tip-*i*Pr-CH_3), 14.02 (s, 1C, Tip-*i*Pr-CH_3) ppm.

^{29}Si-NMR (79.49 MHz, C_6D_6, 300 K) δ = 162.6 (s, *privo*-$SiTip_2$), 48.2 (d, $^2J_{Si\text{-}Rh}$ = 84.5 Hz, NHSi), 21.8 (d, $^2J_{Si\text{-}Rh}$ = 8.5 Hz, *ligato*-SiTip), 17.6 (s, *remoto*-$SiTip_2$), −9.0 (d, $^2J_{Si\text{-}Rh}$ = 31.5 Hz, *ligato*-Si-NHSi), −256.1 (s, *nudo*-Si1), −258.3 (s, *nudo*-Si3) ppm.

CP-MAS ^{29}Si-NMR (79.53 MHz, 13KHz, 300K) δ = 161.8 (s, *privo*-$SiTip_2$), 42.7 (d, $^2J_{Si\text{-}Rh}$ = 69.7 Hz, NHSi), 14.5 (s, *ligato*-SiTip), −5.8 (*remoto*-$SiTip_2$), −23.4 (s, *ligato*-Si-NHSi), −263.8 (s, *nudo*-Si), −266.0 (s, *nudo*-Si) ppm.

Elemental analysis: calculated for $C_{92}H_{138}N_2O_2RhSi_7Cl$: C: 67.42 % ; H: 8.49 % ; N: 1.71 %. Found: C: 67.09 % ; H: 8.38 % ; N: 1.62 %.

UV/VIS (hexane): λmax (ε) = 466 nm (4090 M^{-1} cm^{-1}).

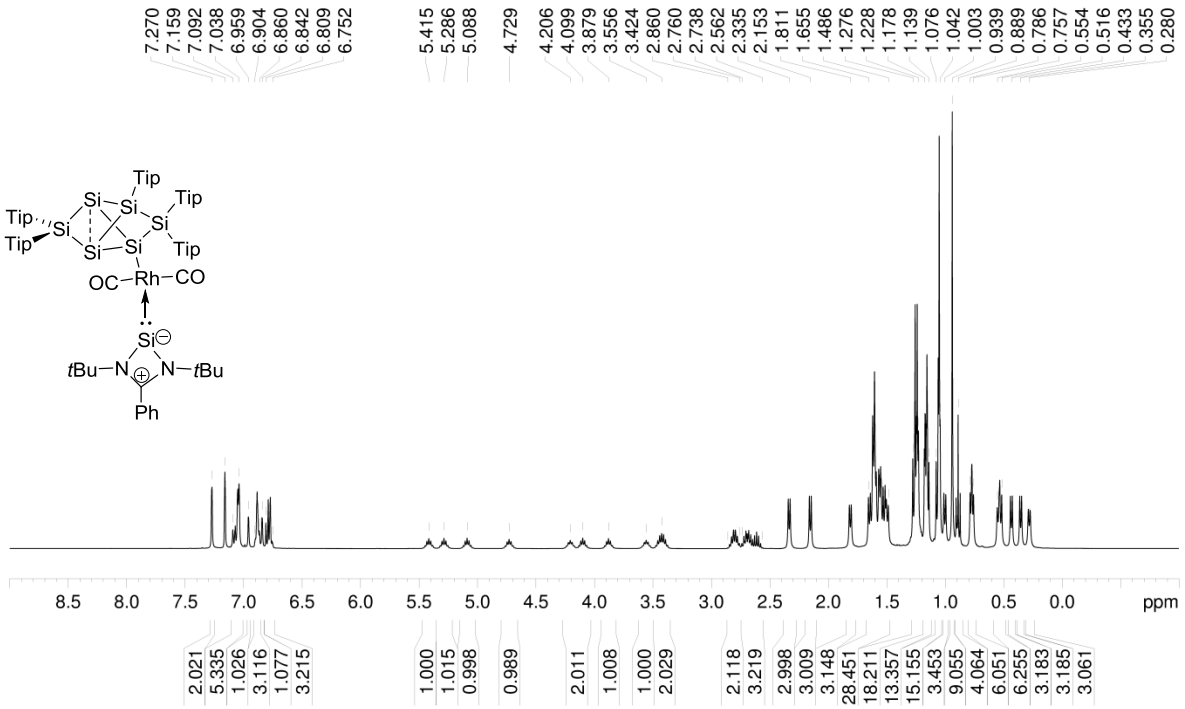

Supplementary Figure 38: ^{1}H NMR spectrum of **4** in C_6D_6 (400.13 MHz, 300 K).

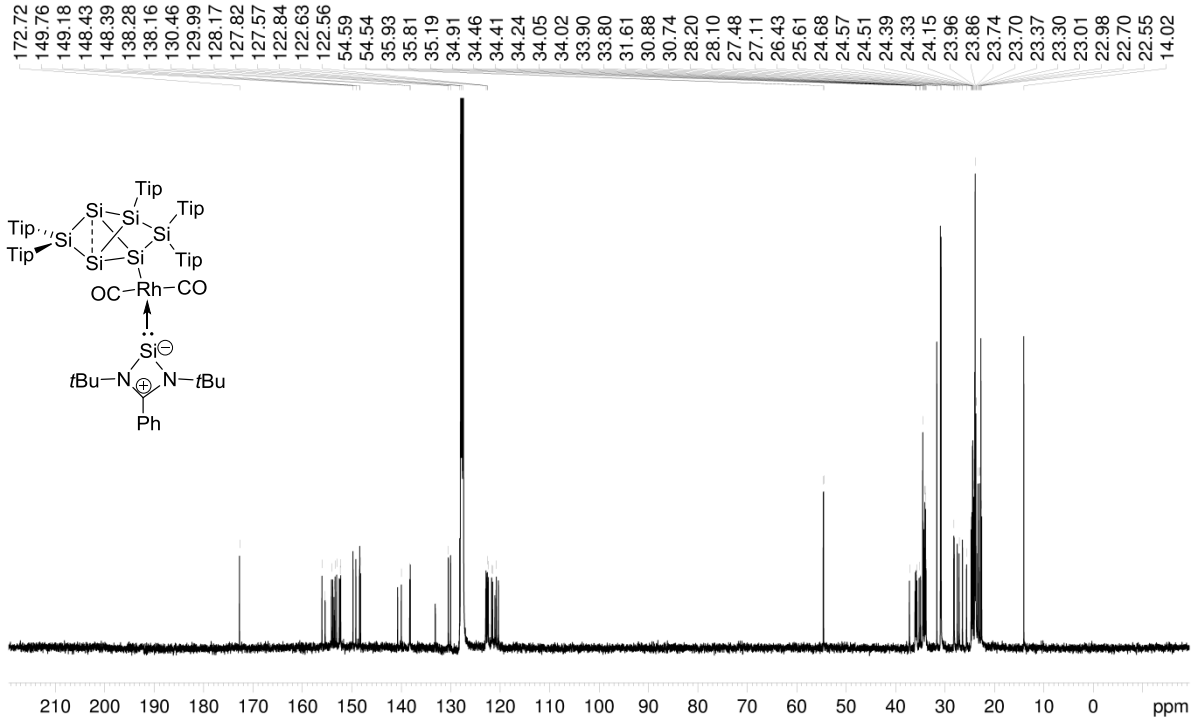

Supplementary Figure 39: ^{13}C NMR spectrum of **4** in C_6D_6 (100.61 MHz, 300 K).

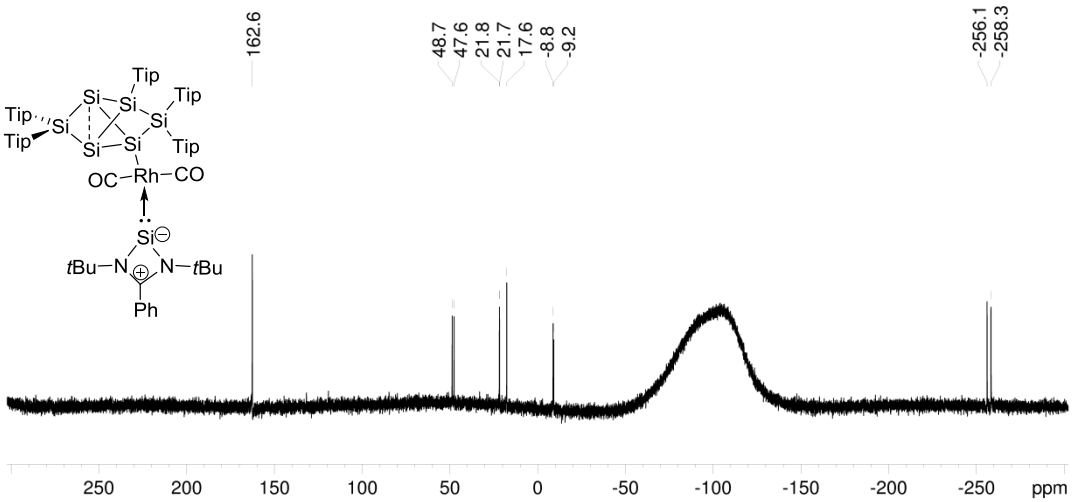

Supplementary Figure 40: ^{29}Si NMR spectrum of **4** in C_6D_6 (79.49 MHz, 300 K).

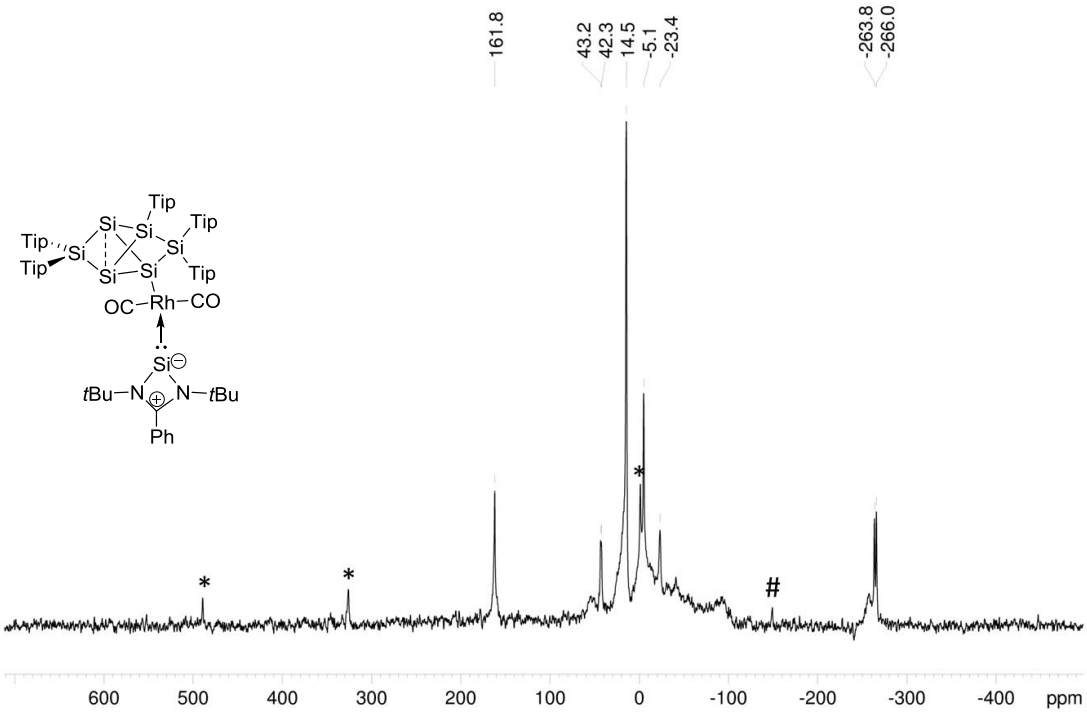

Supplementary Figure 41: CP MAS ^{29}Si NMR spectrum of **4** (79.53 MHz, 13 KHz, 300 K), side spinning bands of: * *privo*-SiTip$_2$ (161.8 ppm), # *ligato*-SiTip (14.5 ppm).

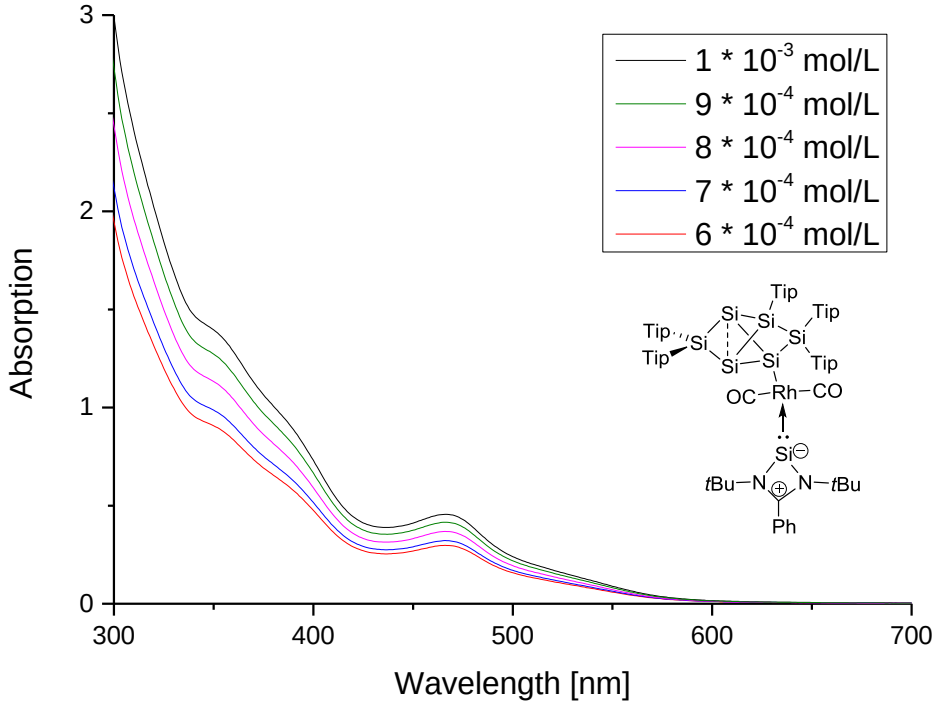

Supplementary Figure 42: UV-Vis spectrum of **4** in hexane at different concentrations.

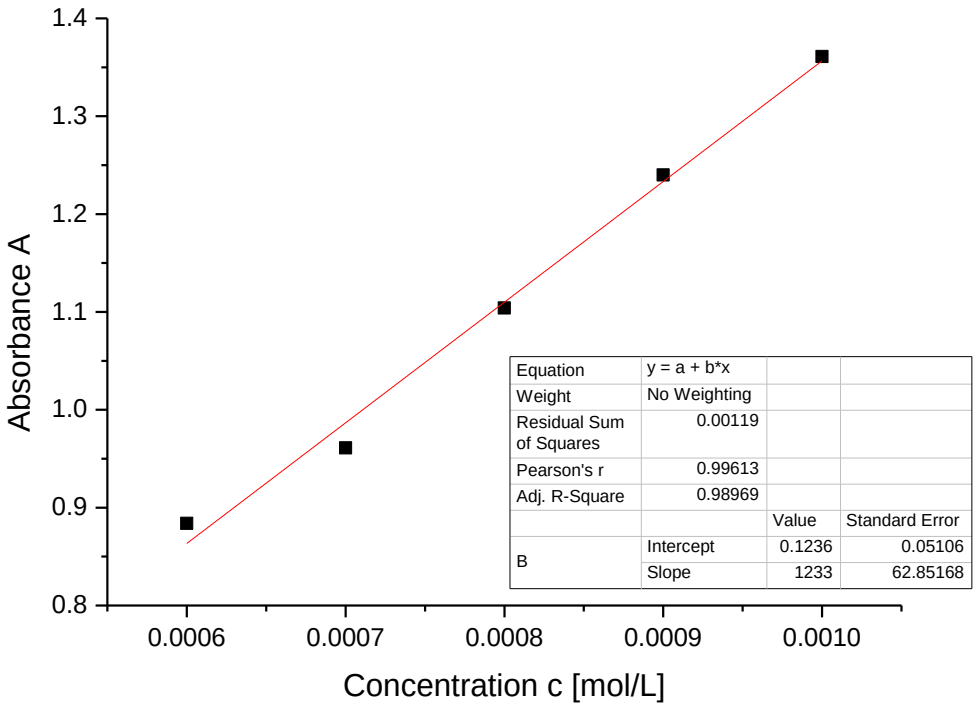

Supplementary Figure 43: Determination of ε (12330 M^{-1} cm^{-1}) by linear regression of absorptions (λ = 354 nm) of **4** against concentration.

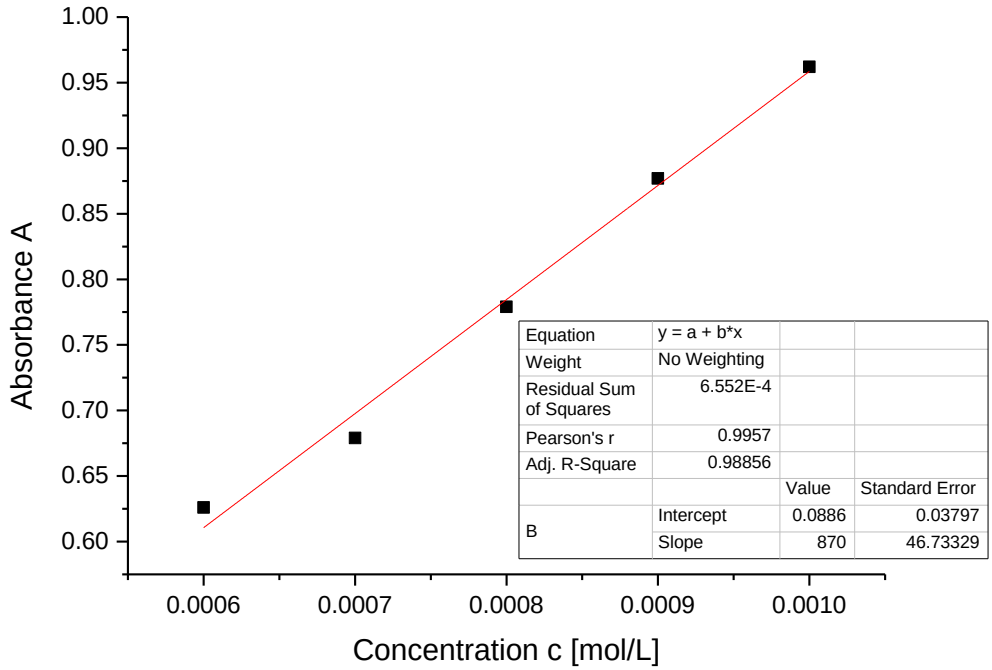

Supplementary Figure 44: Determination of ε (8700 M^{-1} cm^{-1}) by linear regression of absorptions (λ =384 nm) of **4** against concentration.

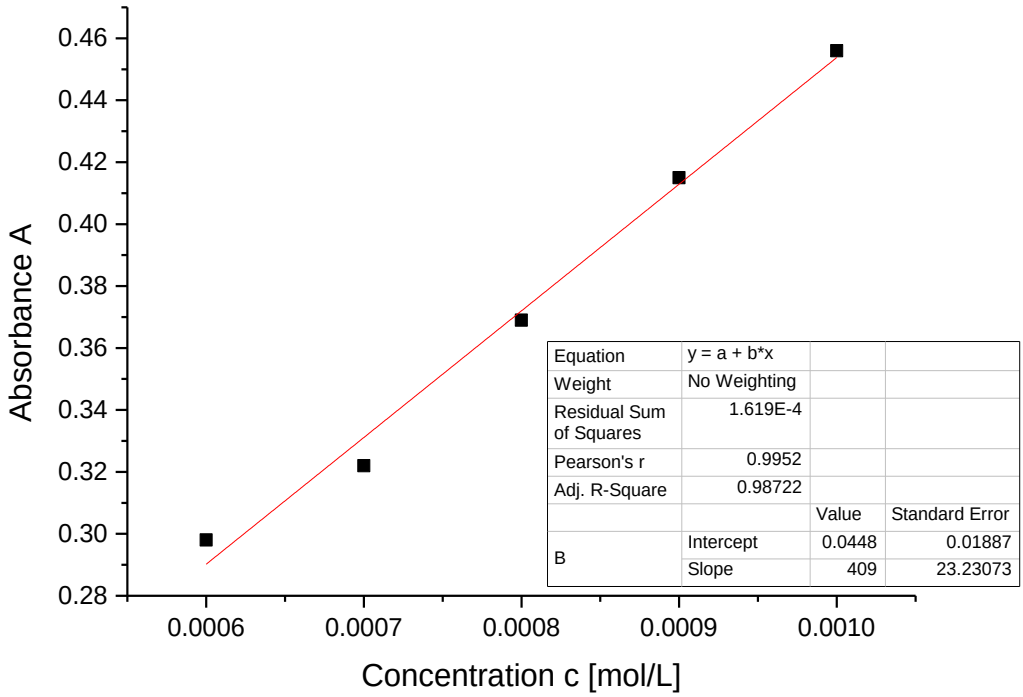

Supplementary Figure 45: Determination of ε (4090 M^{-1} cm^{-1}) by linear regression of absorptions (λ = 466 nm) of **4** against concentration.

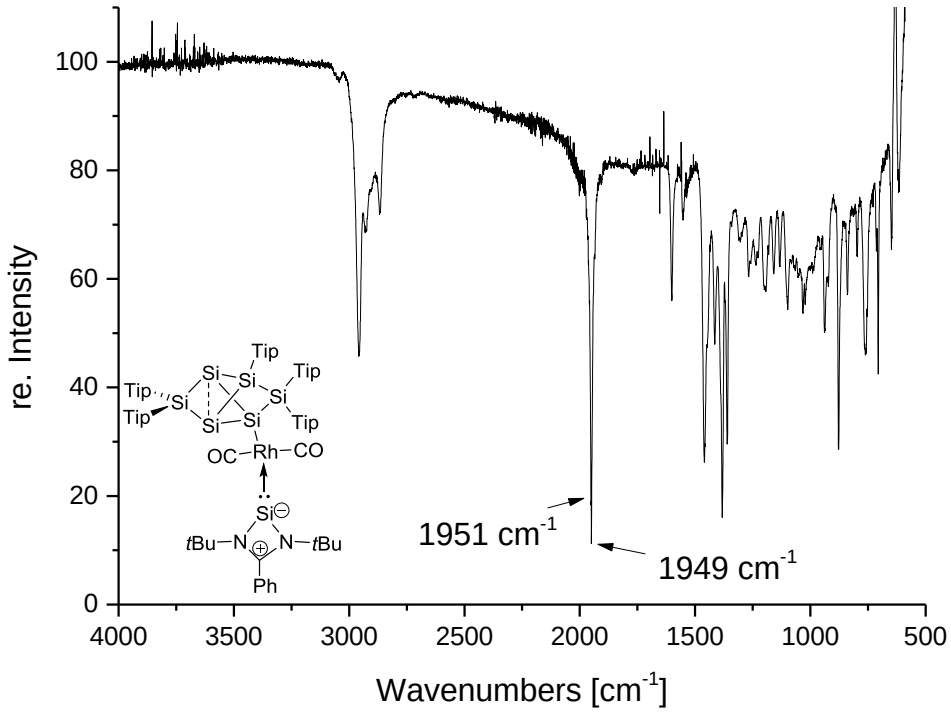

Supplementary Figure 46: Infrared spectrum of **4**.

(5-(Chlorobis(2,4,6-triisopropylphenyl)silyl)-2-(1,3-di-*tert*-butyl-4-phenyl-1,3,2λ^3-diazagermet-1-ium-2(3*H*)-yl)-3,3,4-tris(2,4,6-triisopropylphenyl)tricyclo [2.1.0.0$^{2.5}$]pentasilane-1-yl-rhodium

The reaction was prepared in NMR scale. The germylene-substituted siliconoid **1b** (70 mg; 0.046 mmol) and 1 eq (22.59 mg; 0.046 mmol) of $[(cod)RhCl]_2$ were dissolved in deuterated benzene 0.5 mL and a color change of bright orange to dark red-brown was observed. The solvent was removed in vacuo and the dark red-brownish residue was filtered from 2 mL hexane. The solution was concentrated to 1 mL and stored at −26 °C for eight weeks to yield a few red-brownish crystals of **Si_6Ge-Rh(cod)Cl** which were investigated to X-ray analysis.

3. Data and Plots of spectroscopic conversion in alkene isomerization

Allyltrimethylsilane and 1-hexene were used as neat substrates on an NMR scale using a C_6D_6 capillary as locking signal and the respective amount of the catalysts **2a-c**, **3** and **4**. The yields, turn-over-numbers and turn-over-frequencies were calculated from the ^{1}H NMR integrations and given in the supplementary tables 2-9.

Supplementary Table 1: Reaction conditions.

Catalyst	Substrate	Temperature [°C]	n (substrate) [mmol]	n (catalyst) [mmol]	m (substrate) [mg]	m (catalyst) [mg]
2a	1-hexene	25	3.967	0.002	333.87	3.5
2b	1-hexene	25	3.868	0.004	325.53	7
2c	1-hexene	25	3.77	0.004	317.56	7
3	1-hexene	25	2.483	0.006	208.95	10
4	1-hexene	25	2.441	0.006	205.38	10
2a	Allyl-$SiMe_3$	60	2.125	0.017	242.81	30
2b	Allyl-$SiMe_3$	60	2.073	0.017	236.85	30
2c	Allyl-$SiMe_3$	60	2.021	0.016	230.97	30

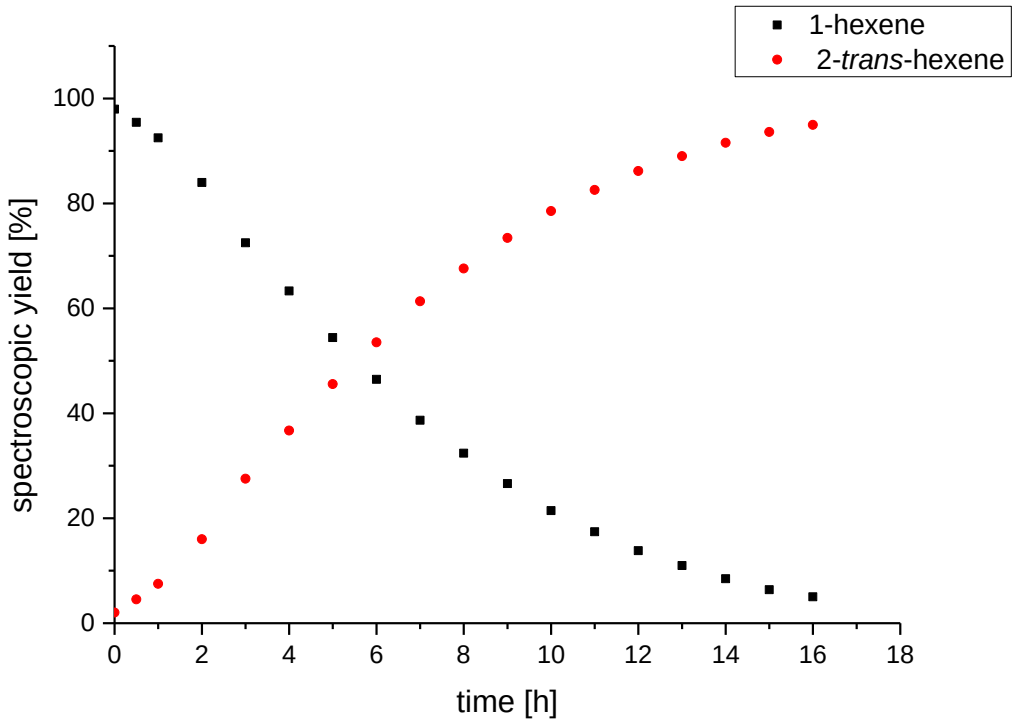

Supplementary Figure 47: Plot of the spectroscopically determined conversion to 2-*trans*-hexene with 0.05 mol% Si-Ir **2a**.

Supplementary Table 2: Catalytic activity of **2a** with 1-hexene: determined conversion by ^{1}H NMR spectroscopy, calculated TON and TOF

Time [h]	n (1-hexene) [mmol]	n (2-hexene) [mmol]	1-hexene [%]	2-hexene [%]	TON	TOF [h^{-1}]
0	3.887	0.081	98.00	2.03	40.7	-
0.5	3.786	0.181	95.44	4.55	91.2	182.5
1	3.669	0.298	92.50	7.50	15.3	150.3
2	3.332	0.635	83.99	16.01	320.8	160.4
3	2.875	1.092	72.47	27.53	551.5	183.8
4	2.511	1.456	63.30	36.70	735.2	183.8
5	2.159	1.808	54.43	45.60	912.9	182.6
6	1.844	2.123	46.48	53.50	1072.4	178.7
7	1.534	2.433	38.67	61.33	1228.8	175.5
8	1.285	2.682	32.40	67.60	1354.4	169.3
9	1.055	2.912	26.59	73.41	1470.8	163.4
10	0.851	3.116	21.45	78.55	1573.8	157.4
11	0.691	3.276	17.42	82.58	1654.5	150.4
12	0.548	3.419	13.83	86.18	1726.6	143.9
13	0.436	3.531	10.99	89.02	1783.4	137.2
14	0.336	3.631	8.46	91.54	1834.0	131.0
15	0.253	3.714	6.38	93.62	1875.7	125.1
16	0.200	3.767	5.03	94.97	1902.7	118.9

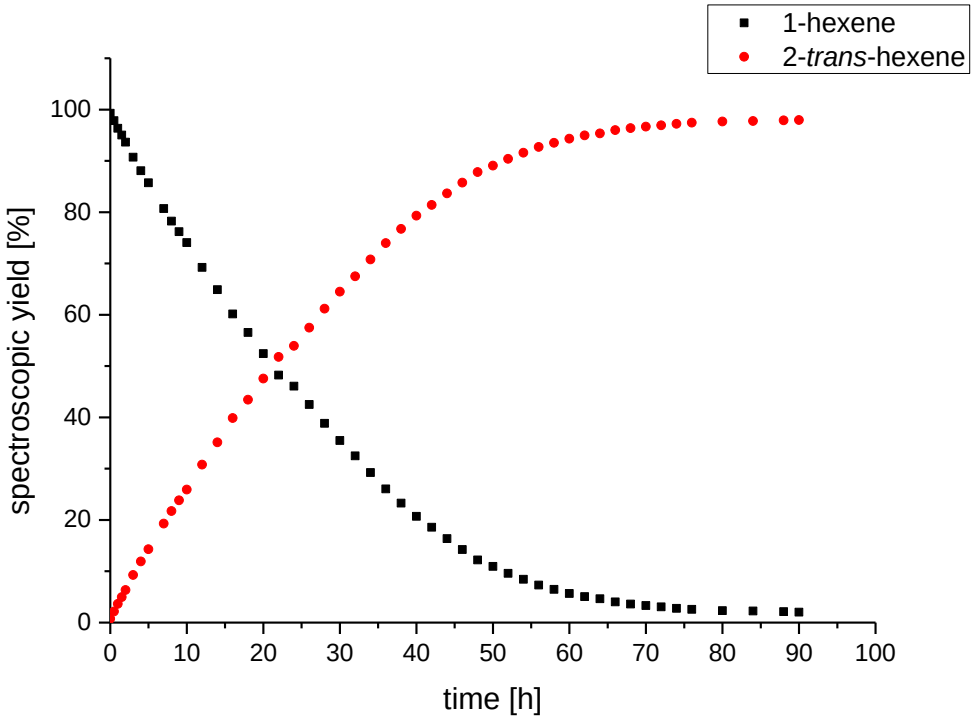

Supplementary Figure 48: Plot of the spectroscopically determined conversion to 2-*trans*-hexene with 0.1 mol% Ge-Ir **2b**.

Supplementary Table 3: Catalytic activity of **2b** with 1-hexene: determined conversion by ^{1}H NMR spectroscopy, calculated TON and TOF

Time [h]	n (1-hexene) [mmol]	n (2-hexene) [mmol]	1-hexene [%]	2-hexene [%]	TON	TOF [h^{-1}]
0	3.840	0.028	99.27	0.73	7.3	-
0.5	3.784	0.084	97.84	2.16	21.6	43.2
1	3.727	0.141	96.35	3.65	36.5	36.5
1,5	3.676	0.192	95.03	4.97	49.7	33.1
2	3.622	0.246	93.65	6.35	63.4	31.7
3	3.509	0.359	90.71	9.29	92.8	30.9
4	3.407	0.461	88.08	11.92	119.1	29.8
5	3.315	0.553	85.71	14.29	142.8	28.6
7	3.122	0.746	80.71	19.29	192.8	27.5
8	3.027	0.841	78.25	21.75	217.4	27.2
9	2.947	0.921	76.18	23.82	238.1	26.5
10	2.865	1.003	74.07	25.93	259.2	25.9
12	2.678	1.190	69.23	30.77	307.6	25.6
14	2.509	1.359	64.87	35.13	351.1	25.1
16	2.326	1.542	60.14	39.86	398.4	24.9
18	2.187	1.681	56.55	43.45	434.3	24.1
20	2.028	1.840	52.43	47.57	475.4	23.8
22	1.865	2.003	48.22	51.78	517.5	23.5
24	1.782	2.086	46.07	53.93	539.0	22.5
26	1.644	2.224	42.51	57.49	574.6	22.1
28	1.502	2.366	38.83	61.17	611.4	21.8
30	1.373	2.495	35.49	64.51	644.7	21.5
32	1.257	2.611	32.49	67.51	674.7	21.1
34	1.131	2.737	29.23	70.77	707.3	20.8
36	1.008	2.860	26.05	73.95	739.1	20.5
38	0.900	2.968	23.28	76.72	766.8	20.2
40	0.801	3.067	20.70	79.30	792.6	19.8
42	0.719	3.149	18.59	81.41	813.6	19.4
44	0.633	3.235	16.36	83.64	836.0	19.0
46	0.551	3.317	14.24	85.76	857.1	18.6
48	0.472	3.396	12.19	87.81	877.6	18.3
50	0.423	3.445	10.94	89.06	890.2	17.8
52	0.371	3.497	9.60	90.40	903.5	17.4
54	0.326	3.542	8.43	91.57	915.3	16.9
56	0.282	3.586	7.30	92.70	926.5	16.5
58	0.251	3.617	6.48	93.52	934.8	16.1
60	0.220	3.648	5.68	94.32	942.7	15.7
62	0.195	3.673	5.04	94.96	949.1	15.3
64	0.179	3.689	4.64	95.36	953.1	14.9
66	0.155	3.713	4.01	95.99	959.4	14.5
68	0.140	3.728	3.61	96.39	963.4	14.2

70	0.128	3.740	3.32	96.68	966.3	13.8
72	0.119	3.749	3.07	96.93	968.7	13.5
74	0.107	3.761	2.78	97.22	971.7	13.1
76	0.099	3.769	2.57	97.43	973.8	12.8
80	0.090	3.778	2.32	97.68	976.3	12.2
84	0.087	3.781	2.24	97.76	977.1	11.6
88	0.082	3.786	2.12	97.88	978.3	11.1
90	0.078	3.790	2.03	97.97	979.2	10.9

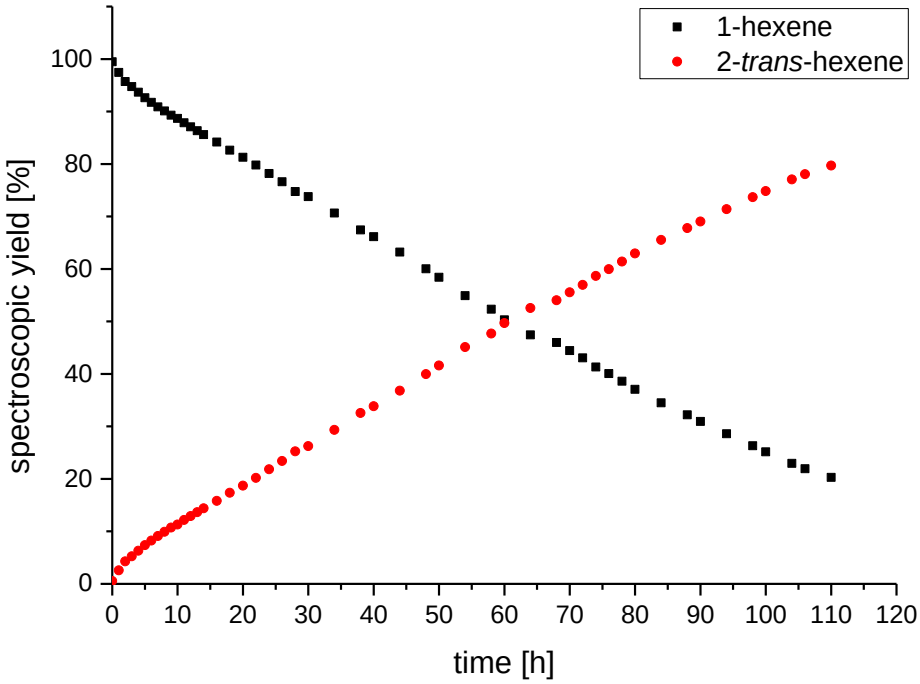

Supplementary Figure 49: Plot of the spectroscopically determined conversion to 2-*trans*-hexene with 0.1 mol% Sn-Ir **2c**.

Supplementary Table 4: Catalytic activity of **2c** with 1-hexene: determined conversion by ^{1}H NMR spectroscopy, calculated TON and TOF

Time [h]	**n (1-hexene) [mmol]**	**n (2-hexene) [mmol]**	**1-hexene [%]**	**2-hexene [%]**	**TON**	**TOF [h^{-1}]**
0	3.750	0.020	99.46	0.54	5.4	-
1	3.673	0.097	97.43	2.57	25.7	25.7
2	3.609	0.162	95.72	4.28	42.8	21.4
3	3.572	0.198	94.74	5.26	52.6	17.5
4	3.532	0.239	93.67	6.33	63.3	15.8
5	3.492	0.278	92.62	7.38	73.8	14.8
6	3.459	0.311	91.75	8.25	82.5	13.7

7	3.426	0.344	90.87	9.13	91.3	13.0
8	3.397	0.373	90.10	9.90	99.0	12.4
9	3.366	0.404	89.29	10.71	107.1	11.9
10	3.343	0.427	88.68	11.32	113.2	11.3
11	3.311	0.459	87.83	12.17	121.7	11.1
12	3.283	0.487	87.08	12.92	129.2	10.8
13	3.255	0.515	86.34	13.66	136.6	10.5
14	3.227	0.543	85.61	14.39	143.9	10.3
16	3.174	0.596	84.18	15.82	158.2	9.9
18	3.115	0.655	82.63	17.37	173.7	9.6
20	3.065	0.706	81.29	18.71	187.2	9.4
22	3.009	0.761	79.81	20.19	201.9	9.2
24	2.948	0.822	78.18	21.82	218.2	9.1
26	2.888	0.882	76.60	23.40	234.0	9.0
28	2.818	0.952	74.75	25.25	252.5	9.0
30	2.781	0.990	73.77	26.23	262.3	8.7
34	2.664	1.106	70.65	29.35	293.5	8.6
38	2.542	1.228	67.43	32.57	325.7	8.6
40	2.494	1.276	66.15	33.86	338.6	8.5
44	2.383	1.387	63.20	36.80	368.0	8.4
48	2.263	1.507	60.04	39.96	399.6	8.3
50	2.202	1.568	58.41	41.59	415.9	8.3
54	2.069	1.701	54.89	45.11	451.2	8.4
58	1.973	1.797	52.32	47.68	476.8	8.2
60	1.896	1.874	50.30	49.70	497.2	8.3
64	1.789	1.981	47.44	52.56	525.6	8.2
68	1.734	2.036	45.98	54.02	540.2	7.9
70	1.676	2.094	44.45	55.55	555.5	7.9
72	1.623	2.147	43.05	56.95	569.5	7.9
74	1.558	2.212	41.31	58.69	586.9	7.9
76	1.510	2.260	40.05	59.95	599.5	7.9
78	1.455	2.315	38.60	61.40	614.1	7.9
80	1.397	2.373	37.06	62.94	629.4	7.9
84	1.300	2.470	34.50	65.52	655.2	7.8
88	1.214	2.556	32.21	67.79	677.9	7.7
90	1.167	2.603	30.95	69.05	690.5	7.7
94	1.078	2.692	28.60	71.40	714.0	7.6
98	0.992	2.778	26.31	73.69	736.9	7.5
100	0.949	2.821	25.16	74.84	748.4	7.5
104	0.865	2.905	22.95	77.05	770.5	7.4
106	0.827	2.943	21.94	78.06	780.6	7.4
110	0.765	3.005	20.29	79.71	797.1	7.2

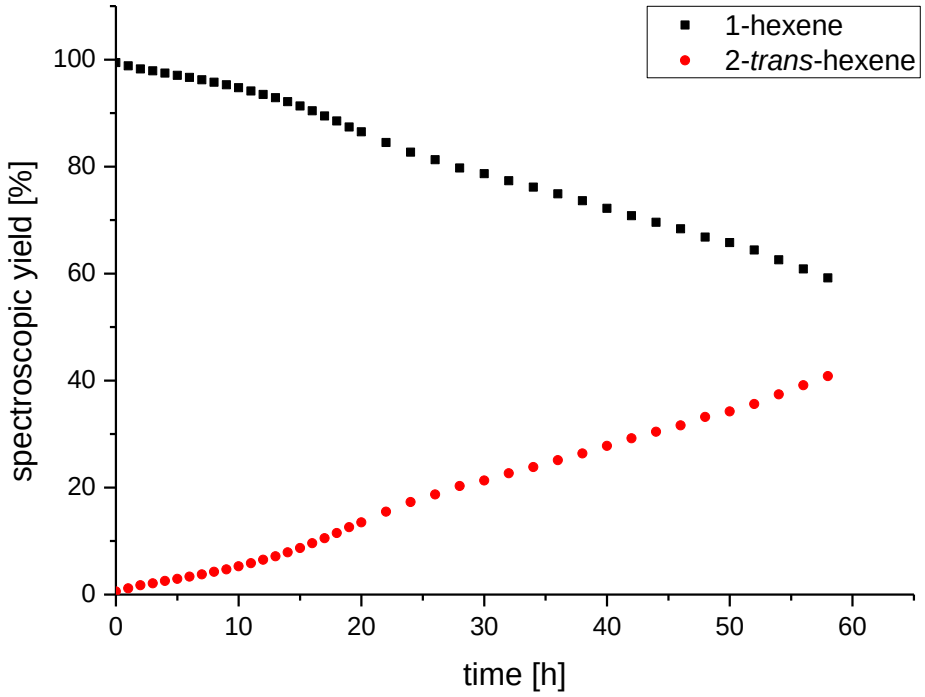

Supplementary Figure 50: Plot of the spectroscopically determined conversion to 2-*trans*-hexene with 0.25 mol% Rh **3**.

Supplementary Table 5: Catalytic activity of Rh-**3** with 1-hexene: determined conversion by ^{1}H NMR spectroscopy, calculated TON and TOF

Time [h]	n (1-hexene) [mmol]	n (2-hexene) [mmol]	1-hexene [%]	2-hexene [%]	TON	TOF [h^{-1}]
0	2.469	0.014	99.42	0.58	2.3	-
1	2.454	0.029	98.84	1.16	4.6	4.6
2	2.439	0.043	98.25	1.75	7.0	3.5
3	2.430	0.052	97.89	2.11	8.4	2.8
4	2.420	0.063	97.46	2.54	10.1	2.5
5	2.410	0.073	97.06	2.94	11.7	2.3
6	2.400	0.083	96.66	3.34	13.3	2.2
7	2.389	0.094	96.22	3.78	15.1	2.2
8	2.378	0.105	95.76	4.24	16.9	2.1
9	2.366	0.117	95.29	4.71	18.8	2.1
10	2.352	0.131	94.73	5.27	21.1	2.1
11	2.337	0.146	94.14	5.86	23.4	2.1
12	2.321	0.162	93.49	6.51	26.0	2.2
13	2.305	0.177	92.86	7.14	28.6	2.2
14	2.287	0.196	92.13	7.87	31.5	2.2
15	2.267	0.216	91.32	8.68	34.7	2.3

16	2.245	0.238	90.41	9.59	38.3	2.4
17	2.221	0.262	89.46	10.54	42.2	2.5
18	2.197	0.285	88.51	11.49	46.0	2.6
19	2.170	0.313	87.41	12.59	50.3	2.6
20	2.147	0.335	86.49	13.51	54.0	2.7
22	2.098	0.385	84.51	15.49	61.9	2.8
24	2.053	0.430	82.70	17.30	69.2	2.9
26	2.018	0.465	81.28	18.72	74.8	2.9
28	1.979	0.503	79.73	20.27	81.1	2.9
30	1.953	0.530	78.67	21.33	85.3	2.8
32	1.920	0.563	77.34	22.66	90.6	2.8
34	1.891	0.592	76.16	23.84	95.3	2.8
36	1.859	0.623	74.89	25.11	100.4	2.8
38	1.828	0.655	73.62	26.38	105.5	2.8
40	1.793	0.690	72.21	27.79	111.1	2.8
42	1.758	0.725	70.80	29.20	116.7	2.8
44	1.727	0.755	69.58	30.42	121.6	2.8
46	1.698	0.785	68.37	31.63	126.4	2.7
48	1.659	0.824	66.80	33.20	132.7	2.8
50	1.633	0.850	65.77	34.23	136.8	2.7
52	1.599	0.884	64.39	35.61	142.4	2.7
54	1.553	0.929	62.57	37.43	149.7	2.8
56	1.511	0.972	60.87	39.13	156.4	2.8
58	1.469	1.013	59.18	40.82	163.2	2.8

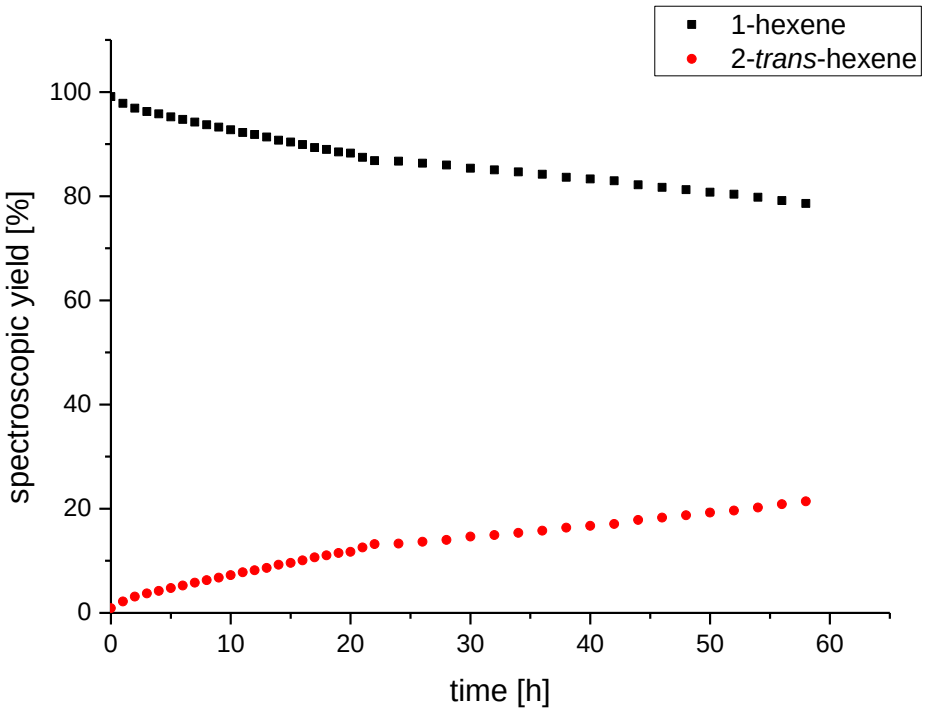

Supplementary Figure 51: Plot of the spectroscopically determined conversion to 2-*trans*-hexene with 0.25 mol% Rh **4**.

Supplementary Table 6: Catalytic activity of Rh-**4** with 1-hexene: determined conversion by ^{1}H NMR spectroscopy, calculated TON and TOF.

Time [h]	n (1-hexene) [mmol]	n (2-hexene) [mmol]	1-hexene [%]	2-hexene [%]	TON	TOF [h^{-1}]
0	2.419	0.022	99.10	0.90	3.6	-
1	2.387	0.053	97.82	2.18	8.7	8.7
2	2.364	0.076	96.88	3.12	12.5	6.2
3	2.349	0.091	96.25	3.75	15.0	5.0
4	2.338	0.103	95.79	4.21	16.9	4.2
5	2.324	0.116	95.23	4.77	19.1	3.8
6	2.312	0.128	94.74	5.26	21.0	3.5
7	2.299	0.141	94.21	5.79	23.2	3.3
8	2.287	0.153	93.72	6.28	25.1	3.1
9	2.276	0.165	93.25	6.75	27.0	3.0
10	2.263	0.177	92.74	7.26	29.0	2.9
11	2.250	0.190	92.21	7.79	31.2	2.8
12	2.241	0.199	91.84	8.16	32.7	2.7
13	2.230	0.211	91.36	8.64	34.6	2.7
14	2.215	0.226	90.75	9.25	37.0	2.6
15	2.206	0.234	90.40	9.60	38.4	2.6
16	2.194	0.246	89.91	10.09	40.4	2.5
17	2.180	0.260	89.34	10.66	42.7	2.5
18	2.171	0.269	88.97	11.03	44.1	2.5
19	2.160	0.281	88.50	11.50	46.0	2.4
20	2.154	0.286	88.27	11.73	46.9	2.3
21	2.134	0.306	87.45	12.55	50.2	2.4
22	2.119	0.322	86.81	13.19	52.8	2.4
24	2.116	0.324	86.71	13.29	53.2	2.2
26	2.107	0.333	86.34	13.66	54.7	2.1
28	2.099	0.342	85.99	14.01	56.0	2.0
30	2.083	0.357	85.36	14.64	58.6	2.0
32	2.076	0.365	85.05	14.95	59.8	1.9
34	2.066	0.375	84.64	15.36	61.4	1.8
36	2.055	0.385	84.22	15.78	63.1	1.8
38	2.041	0.399	83.64	16.36	65.5	1.7
40	2.033	0.408	83.29	16.71	66.9	1.7
42	2.024	0.416	82.94	17.06	68.3	1.6
44	2.005	0.435	82.17	17.83	71.3	1.6
46	1.994	0.446	81.70	18.30	73.2	1.6
48	1.983	0.457	81.26	18.74	75.0	1.6
50	1.971	0.470	80.75	19.25	77.0	1.5
52	1.961	0.479	80.37	19.63	78.5	1.5
54	1.947	0.493	79.78	20.22	80.9	1.5
56	1.931	0.509	79.14	20.86	83.4	1.5
58	1.918	0.522	78.60	21.40	85.6	1.5

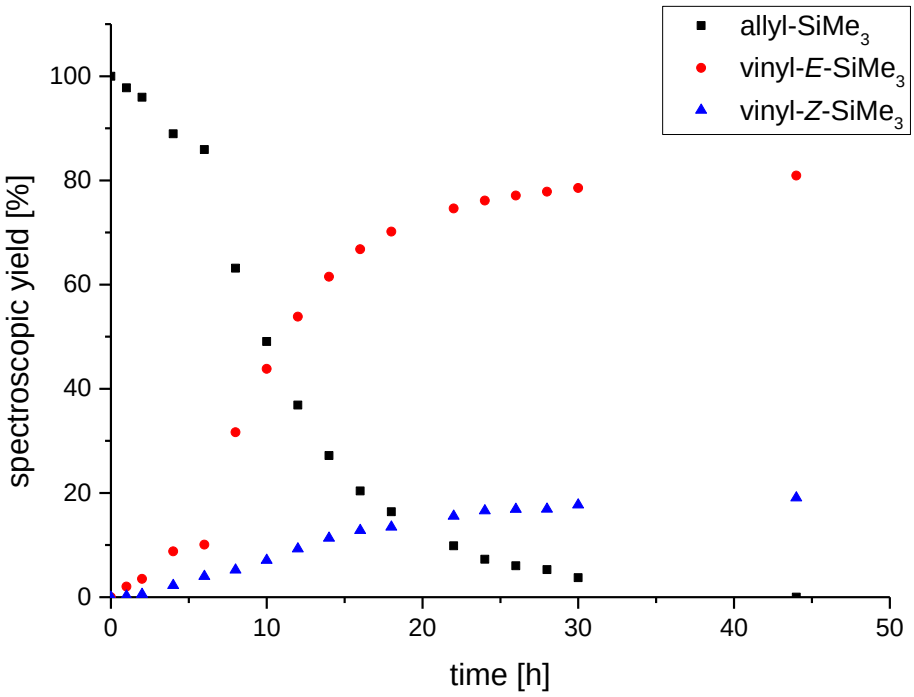

Supplementary Figure 52: Plot of the spectroscopically determined conversion to *E*/*Z*-vinyltrimethylsilane with 0.8 mol% Si-Ir **2a** at 60 °C. black = allyltrimethylsilane, red = *E*-vinyltrimethylsilane, blue = *Z*-vinyltrimethylsilane.

Supplementary Table 7: Catalytic activity of **2a** with allyltrimethylsilane: determined conversion by ^{1}H NMR spectroscopy, calculated TON and TOF

Time [h]	n (allyl-$SiMe_3$) [mmol]	n (*E*-vinyl) [mmol]	n (*Z*-vinyl) [mmol]	allyl-$SiMe_3$ [%]	*E*-vinyl [%]	*Z*-vinyl [%]	TON	TOF [h^{-1}]
0	2.125	0.00	0.000	100.00	0.00	0.00	0.0	-
1	2.078	0.04	0.004	97.77	2.02	0.21	2.8	2.8
2	2.039	0.07	0.012	95.95	3.50	0.55	5.1	2.5
4	1.890	0.19	0.048	88.94	8.79	2.27	13.8	3.5
6	1.826	0.21	0.085	85.91	10.09	4.00	17.6	2.9
8	1.342	0.67	0.111	63.13	31.66	5.20	46.1	5.8
10	1.043	0.93	0.151	49.09	43.82	7.10	63.6	6.4
12	0.784	1.14	0.197	36.88	53.84	9.28	78.9	6.6
14	0.577	1.31	0.241	27.17	61.49	11.34	91.0	6.5
16	0.433	1.42	0.273	20.39	66.79	12.82	99.5	6.2
18	0.348	1.49	0.286	16.40	70.15	13.45	104.5	5.8
22	0.209	1.59	0.330	9.85	74.60	15.55	112.7	5.1
24	0.155	1.62	0.353	7.29	76.12	16.60	115.9	4.8
26	0.128	1.64	0.359	6.03	77.09	16.88	117.5	4.5
28	0.112	1.65	0.359	5.27	77.83	16.90	118.4	4.2

30	0.080	1.67	0.377	3.75	78.53	17.72	120.3	4.0
44	0.000	1.72	0.405	0.01	80.93	19.05	125.0	2.8

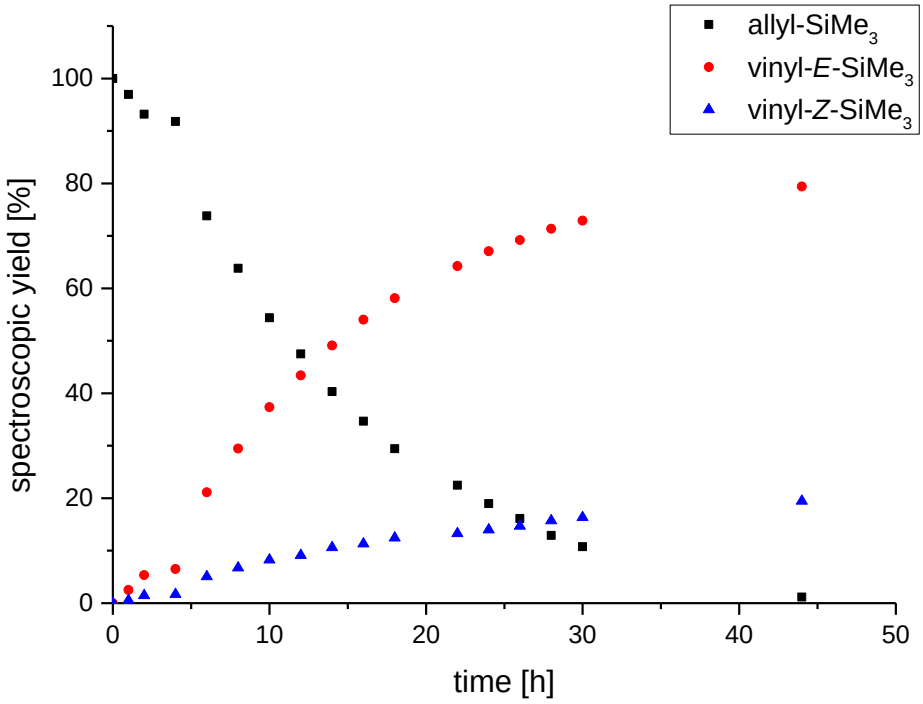

Supplementary Figure 53: Plot of the spectroscopically determined conversion to *E*/*Z*-vinyltrimethylsilane with 0.8 mol% Ge-Ir **2b** at 60 °C. black = allyltrimethylsilane, red = *E*-vinyltrimethylsilane, blue = *Z*-vinyltrimethylsilane.

Supplementary Table 8: Catalytic activity of **2b** with allyltrimethylsilane: determined conversion by ^{1}H NMR spectroscopy, calculated TON and TOF

Time [h]	n (allyl-$SiMe_3$) [mmol]	n (*E*-vinyl) [mmol]	n (*Z*-vinyl) [mmol]	allyl-$SiMe_3$ [%]	*E*-vinyl [%]	*Z*-vinyl [%]	TON	TOF [h^{-1}]
0	2.073	0.000	0.000	100.00	0.00	0.00	0.0	-
1	2.010	0.052	0.011	96.96	2.50	0.55	3.8	3.8
2	1.932	0.111	0.030	93.20	5.36	1.44	8.5	4.2
4	1.903	0.135	0.035	91.82	6.50	1.68	10.2	2.6
6	1.530	0.438	0.105	73.82	21.11	5.07	32.7	5.5
8	1.323	0.611	0.139	63.82	29.47	6.72	45.2	5.7
10	1.128	0.774	0.171	54.39	37.35	8.26	57.0	5.7
12	0.984	0.900	0.189	47.48	43.41	9.11	65.7	5.5
14	0.836	1.018	0.219	40.31	49.10	10.59	74.6	5.3
16	0.719	1.120	0.234	34.68	54.02	11.29	81.7	5.1
18	0.610	1.205	0.258	29.44	58.12	12.43	88.2	4.9
22	0.466	1.332	0.275	22.49	64.24	13.27	96.9	4.4
24	0.393	1.390	0.290	18.96	67.07	13.97	101.3	4.2

26	0.334	1.434	0.305	16.12	69.19	14.69	104.9	4.0
28	0.268	1.480	0.326	12.92	71.37	15.70	108.9	3.9
30	0.223	1.511	0.338	10.77	72.91	16.32	111.6	3.7
44	0.024	1.646	0.403	1.16	79.40	19.44	123.6	2.8

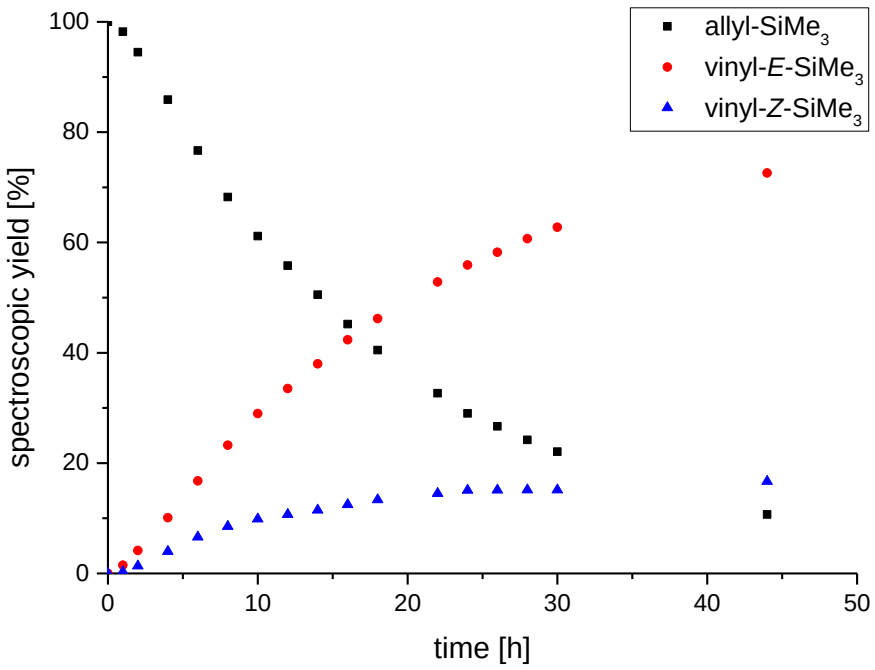

Supplementary Figure 54: Plot of the spectroscopically determined conversion to *E*/*Z*-vinyltrimethylsilane with 0.8 mol% Sn-Ir **2c** at 60 °C. black = allyltrimethylsilane, red = *E*-vinyltrimethylsilane, blue = *Z*-vinyltrimethylsilane.

Supplementary Table 9: Catalytic activity of **2c** with allyltrimethylsilane: determined conversion by ^{1}H NMR spectroscopy, calculated TON and TOF

Time [h]	n (allyl-$SiMe_3$) [mmol]	n (*E*-vinyl) [mmol]	n (*Z*-vinyl) [mmol]	allyl-$SiMe_3$ [%]	*E*-vinyl [%]	*Z*-vinyl [%]	TON	TOF [h^{-1}]
0	2.021	0.000	0.000	100.00	0.00	0.00	0.0	-
1	1.985	0.030	0.006	98.21	1.51	0.28	2.2	2.2
2	1.910	0.084	0.027	94.49	4.16	1.35	6.9	3.4
4	1.736	0.204	0.081	85.89	10.11	3.99	17.6	4.4
6	1.549	0.339	0.133	76.66	16.76	6.58	29.2	4.9
8	1.379	0.470	0.172	68.23	23.25	8.53	39.7	5.0
10	1.236	0.586	0.199	61.15	28.98	9.87	48.6	4.9
12	1.128	0.677	0.216	55.79	33.52	10.69	55.2	4.6
14	1.021	0.768	0.232	50.53	37.99	11.47	61.8	4.4
16	0.913	0.856	0.252	45.19	42.35	12.46	68.5	4.3
18	0.818	0.933	0.270	40.47	46.18	13.34	74.4	4.1
22	0.660	1.068	0.293	32.67	52.85	14.48	84.2	3.8

24	0.586	1.130	0.305	29.00	55.92	15.08	88.7	3.7
26	0.539	1.177	0.306	26.66	58.22	15.12	91.7	3.5
28	0.489	1.226	0.306	24.20	60.67	15.12	94.7	3.4
30	0.446	1.269	0.306	22.09	62.77	15.15	97.4	3.2
44	0.216	1.468	0.337	10.70	72.61	16.69	111.6	2.5

4. Details on X-ray Diffraction Studies

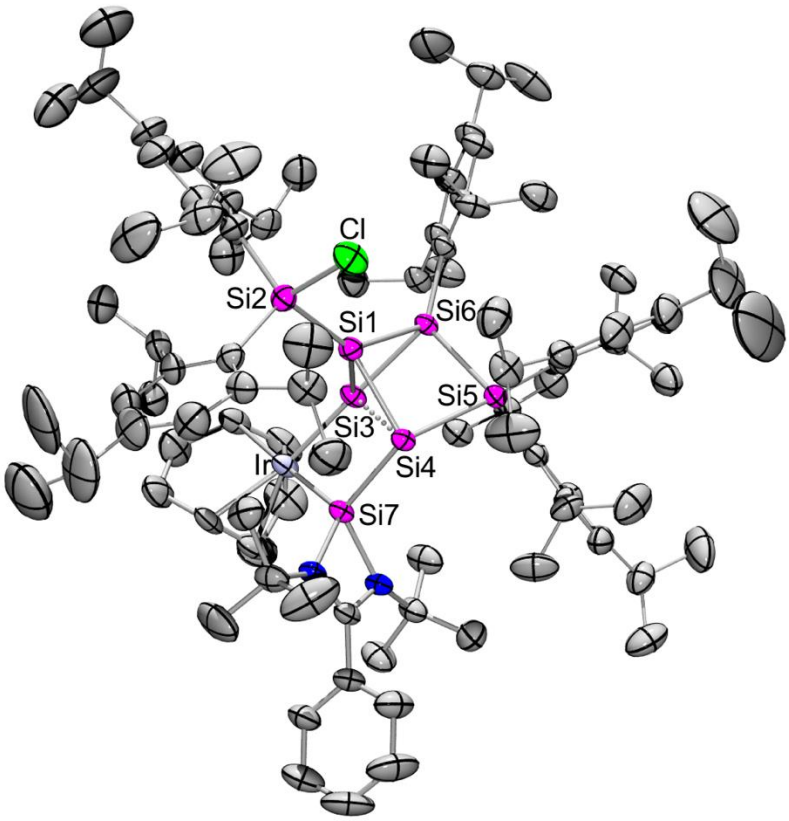

Supplementary Figure 55: Molecular structure of siliconoid **2a** in the solid state. Hydrogen atoms omitted for clarity. Thermal ellipsoids represent 50% probability.

Supplementary Table 10: Crystal data and structure refinement for **2a** (CCDC: 2000911).

Identification code	sh3975
Empirical formula	C_{98} H_{150} Cl Ir N_2 Si_7, 0.5(C_7 H_{14})
Formula weight	1823.56
Temperature	232(2) K
Wavelength	0.71073 Å
Crystal system	Triclinic
Space group	P-1

Unit cell dimensions	a = 16.5707(18) Å	α = 105.174(4)°.
	b = 16.9084(19) Å	β = 96.576(4)°.
	c = 21.231(2) Å	γ = 109.461(4)°.
Volume	5278.5(10) $Å^3$	
Z	2	
Density (calculated)	1.147 Mg/m^3	
Absorption coefficient	1.411 mm^{-1}	
F(000)	1938	
Crystal size	0.225 x 0.223 x 0.203 mm^3	
Theta range for data collection	1.337 to 27.228°.	
Index ranges	-21<=h<=21, -21<=k<=21, -27<=l<=25	
Reflections collected	86047	
Independent reflections	23228 [R(int) = 0.0613]	
Completeness to theta = 25.242°	99.8 %	
Absorption correction	Semi-empirical from equivalents	
Max. and min. transmission	0.7455 and 0.6468	
Refinement method	Full-matrix least-squares on F^2	
Data / restraints / parameters	23228 / 118 / 1081	
Goodness-of-fit on F^2	1.009	
Final R indices [I>2sigma(I)]	R1 = 0.0491, wR2 = 0.1193	
R indices (all data)	R1 = 0.0797, wR2 = 0.1340	
Extinction coefficient	n/a	
Largest diff. peak and hole	2.194 and -0.953 e.$Å^{-3}$	

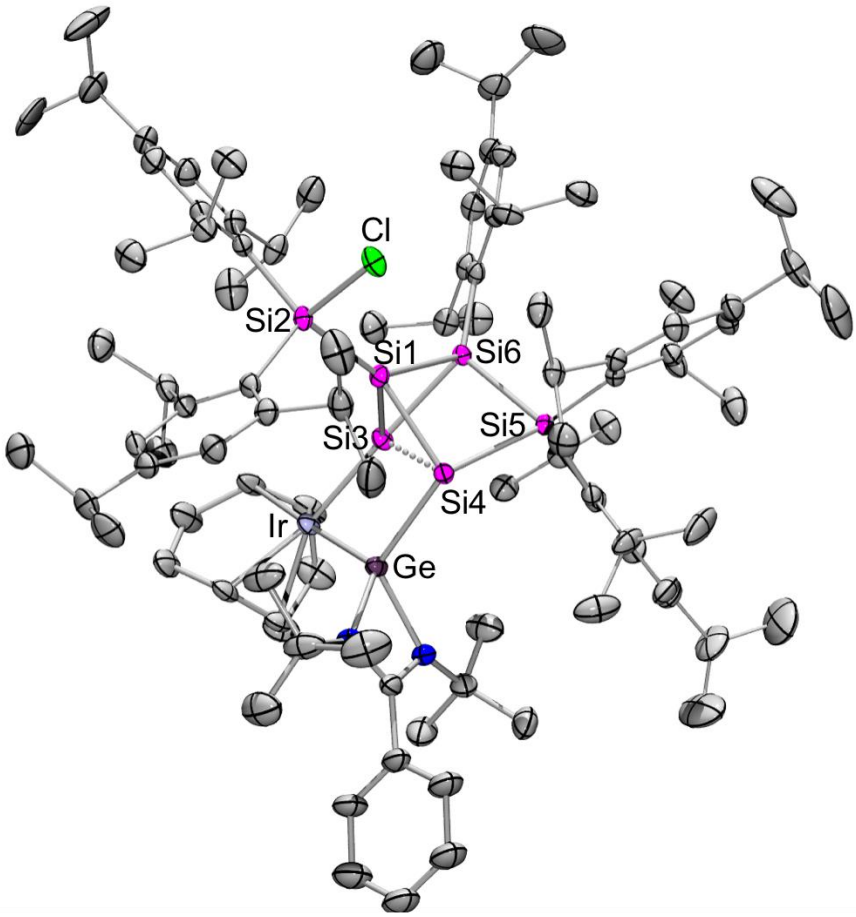

Supplementary Figure 56: Molecular structure of siliconoid **2b** in the solid state. Hydrogen atoms omitted for clarity. Thermal ellipsoids represent 50% probability.

Supplementary Table 11: Crystal data and structure refinement for **2b** (CCDC: 2000912).

Identification code	sh3966	
Empirical formula	C_{98} H_{150} Cl Ge Ir N_2 Si_6, 0.5(C_6 H_{14})	
Formula weight	1868.06	
Temperature	152(2) K	
Wavelength	0.71073 Å	
Crystal system	Monoclinic	
Space group	$P2_1/n$	
Unit cell dimensions	a = 15.7711(4) Å	α = 90°.
	b = 31.3736(8) Å	β = 106.081(2)°.
	c = 21.3327(6) Å	γ = 90°.
Volume	10142.3(5) $Å^3$	
Z	4	
Density (calculated)	1.223 Mg/m^3	
Absorption coefficient	1.748 mm^{-1}	
F(000)	3948	

Crystal size	0.501 x 0.302 x 0.284 mm^3
Theta range for data collection	1.187 to 26.801°.
Index ranges	-19<=h<=19, -39<=k<=39, -27<=l<=27
Reflections collected	237683
Independent reflections	21643 [R(int) = 0.0473]
Completeness to theta = 25.242°	100.0 %
Absorption correction	Semi-empirical from equivalents
Max. and min. transmission	0.7454 and 0.6349
Refinement method	Full-matrix least-squares on F^2
Data / restraints / parameters	21643 / 267 / 1147
Goodness-of-fit on F^2	1.144
Final R indices [I>2sigma(I)]	R1 = 0.0332, wR2 = 0.0676
R indices (all data)	R1 = 0.0437, wR2 = 0.0710
Extinction coefficient	n/a
Largest diff. peak and hole	1.172 and -0.942 e.$Å^{-3}$

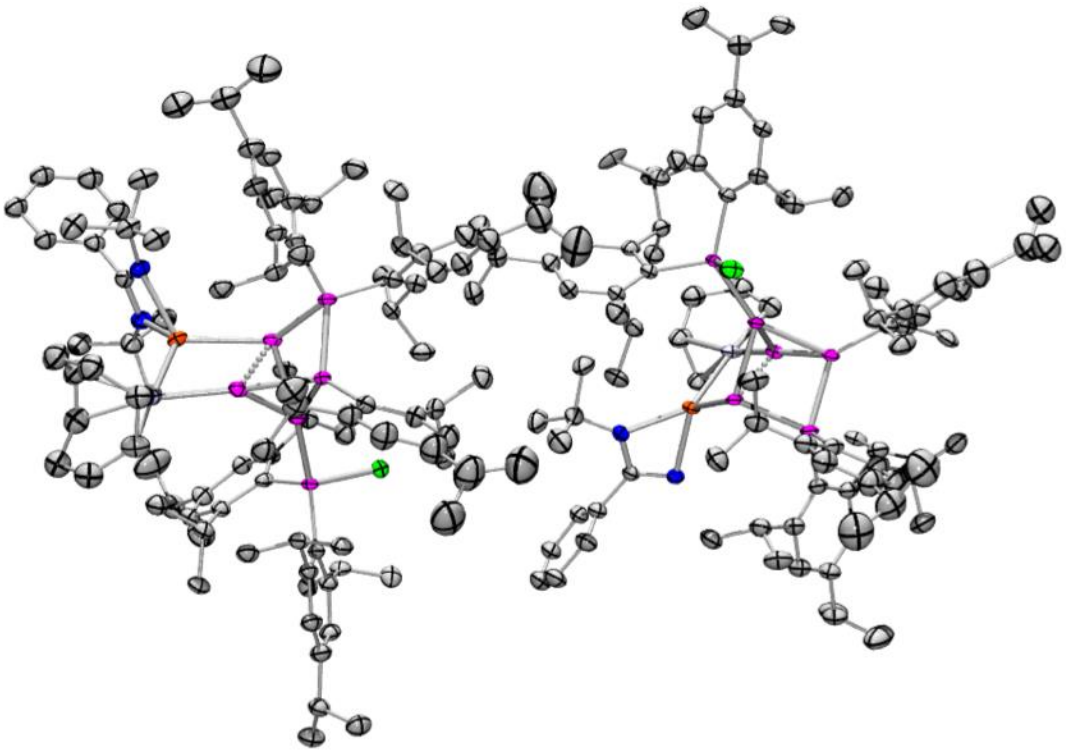

Supplementary Figure 57: Molecular structure of siliconoid **2c** in the solid state with two molecules in the asymmetric unit. Hydrogen atoms omitted for clarity. Thermal ellipsoids represent 50% probability.

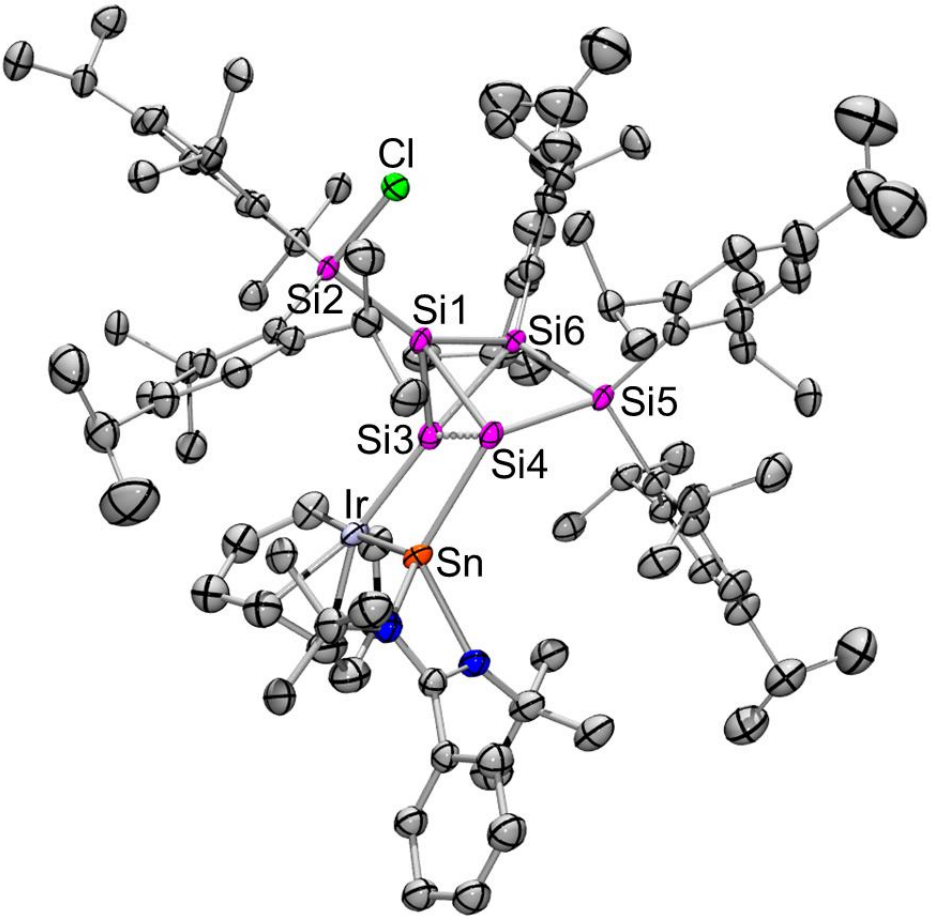

Supplementary Figure 58: Molecular structure of siliconoid **2c** in the solid state. Hydrogen atoms and second molecule omitted for clarity. Thermal ellipsoids represent 50% probability.

Supplementary Table 12: Crystal data and structure refinement for **2c** (CCDC: 2000913).

Identification code	sh4029	
Empirical formula	C_{98} H_{150} Cl Ir N_2 Si_6 Sn, 0.5(C_6 H_{14})	
Formula weight	1914.16	
Temperature	100(2) K	
Wavelength	0.71073 Å	
Crystal system	Triclinic	
Space group	P-1	
Unit cell dimensions	a = 15.7798(19) Å	α = 104.327(6)°.
	b = 26.095(3) Å	β = 106.150(6)°.
	c = 27.363(4) Å	γ = 90.156(6)°.
Volume	10455(2) $Å^3$	
Z	4	
Density (calculated)	1.216 Mg/m^3	
Absorption coefficient	1.647 mm^{-1}	
F(000)	4020	

Crystal size	0.432 x 0.317 x 0.197 mm^3
Theta range for data collection	1.277 to 27.832°.
Index ranges	-20<=h<=20, -33<=k<=33, -35<=l<=35
Reflections collected	151379
Independent reflections	47657 [R(int) = 0.0833]
Completeness to theta = 25.242°	98.9 %
Absorption correction	Semi-empirical from equivalents
Max. and min. transmission	0.7455 and 0.5496
Refinement method	Full-matrix least-squares on F^2
Data / restraints / parameters	47657 / 4639 / 2128
Goodness-of-fit on F^2	2.470
Final R indices [I>2sigma(I)]	R1 = 0.1685, wR2 = 0.3641
R indices (all data)	R1 = 0.1945, wR2 = 0.3704
Extinction coefficient	n/a
Largest diff. peak and hole	5.451 and -5.133 e.$Å^{-3}$

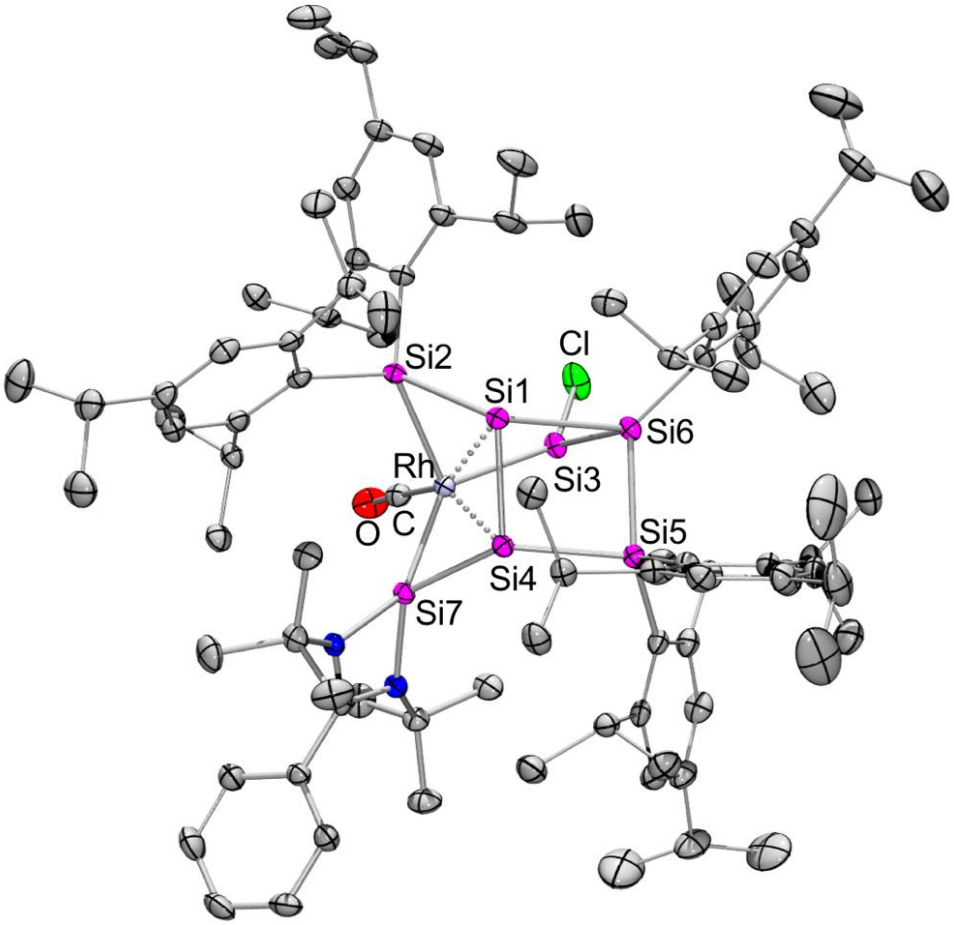

Supplementary Figure 59: Molecular structure of siliconoid **3** in the solid state. Hydrogen atoms omitted for clarity. Thermal ellipsoids represent 50% probability.

Supplementary Table 13: Crystal data and structure refinement for **3** (CCDC: 2000914).

Identification code	sh3984	
Empirical formula	C_{91} H_{138} Cl N_2 O Rh Si_7, 2(C_7 H_8)	
Formula weight	1795.28	
Temperature	142(2) K	
Wavelength	0.71073 Å	
Crystal system	Triclinic	
Space group	P-1	
Unit cell dimensions	a = 14.9387(8) Å	α = 102.165(3)°.
	b = 17.6518(9) Å	β = 92.721(3)°.
	c = 21.0713(11) Å	γ = 108.260(3)°.
Volume	5119.4(5) $Å^3$	
Z	2	
Density (calculated)	1.165 Mg/m^3	
Absorption coefficient	0.321 mm^{-1}	
F(000)	1932	
Crystal size	0.244 x 0.193 x 0.058 mm^3	
Theta range for data collection	1.251 to 27.694°.	
Index ranges	-19<=h<=19, -23<=k<=22, -27<=l<=21	
Reflections collected	86147	
Independent reflections	23261 [R(int) = 0.0620]	
Completeness to theta = 25.242°	98.4 %	
Absorption correction	Semi-empirical from equivalents	
Max. and min. transmission	0.7456 and 0.6703	
Refinement method	Full-matrix least-squares on F^2	
Data / restraints / parameters	23261 / 134 / 1120	
Goodness-of-fit on F^2	1.018	
Final R indices [I>2sigma(I)]	R1 = 0.0487, wR2 = 0.1050	
R indices (all data)	R1 = 0.0847, wR2 = 0.1200	
Extinction coefficient	n/a	
Largest diff. peak and hole	0.786 and -0.692 e.$Å^{-3}$	

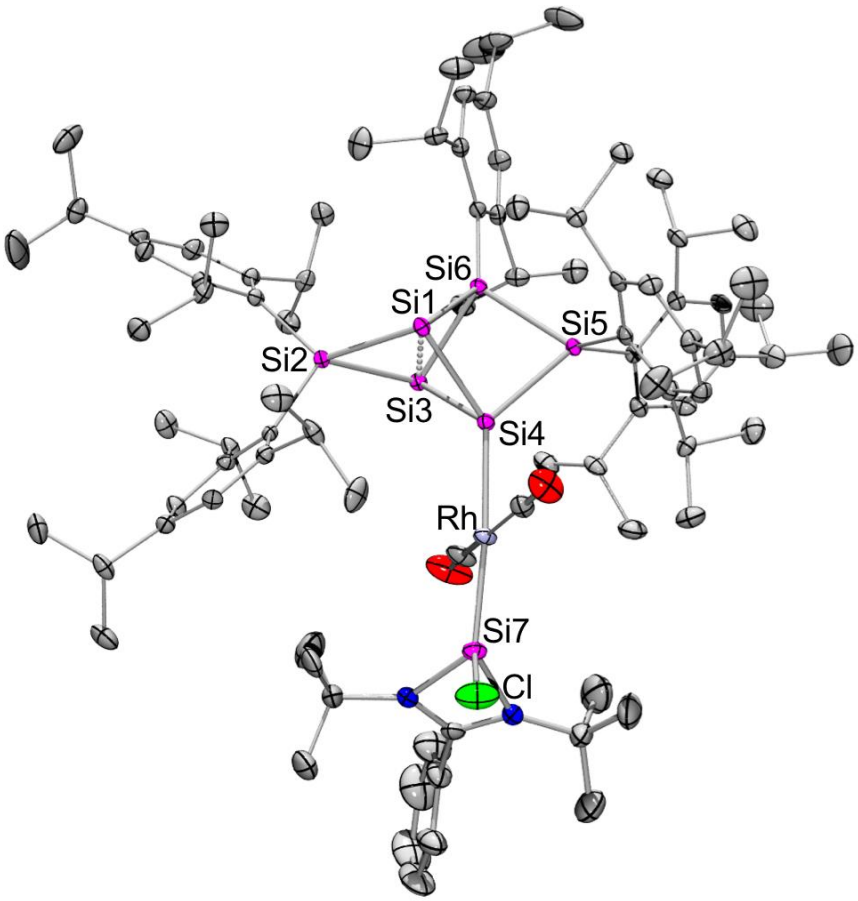

Supplementary Figure 60: Molecular structure of siliconoid **4** in the solid state. Hydrogen atoms omitted for clarity. Thermal ellipsoids represent 50% probability.

Supplementary Table 14: Crystal data and structure refinement for **4** (CCDC: 2000915).

Identification code	sh3959	
Empirical formula	C_{92} H_{138} Cl N_2 O_2 Rh Si_7	
Formula weight	1639.03	
Temperature	142(2) K	
Wavelength	0.71073 Å	
Crystal system	Orthorhombic	
Space group	$Pna2_1$	
Unit cell dimensions	a = 37.608(4) Å	α = 90°.
	b = 13.6961(14) Å	β = 90°.
	c = 18.1426(19) Å	γ = 90°.
Volume	9345.0(17) $Å^3$	
Z	4	
Density (calculated)	1.165 Mg/m^3	
Absorption coefficient	0.346 mm^{-1}	
F(000)	3520	

Crystal size	0.375 x 0.222 x 0.054 mm^3
Theta range for data collection	1.560 to 27.934°.
Index ranges	-49<=h<=49, -18<=k<=10, -23<=l<=23
Reflections collected	85115
Independent reflections	22265 [R(int) = 0.0551]
Completeness to theta = 25.242°	100.0 %
Absorption correction	Semi-empirical from equivalents
Max. and min. transmission	0.7456 and 0.6838
Refinement method	Full-matrix least-squares on F^2
Data / restraints / parameters	22265 / 70 / 1034
Goodness-of-fit on F^2	1.008
Final R indices [I>2sigma(I)]	R1 = 0.0408, wR2 = 0.0760
R indices (all data)	R1 = 0.0566, wR2 = 0.0807
Absolute structure parameter	-0.014(8)
Extinction coefficient	n/a
Largest diff. peak and hole	0.645 and -0.493 e.$Å^{-3}$

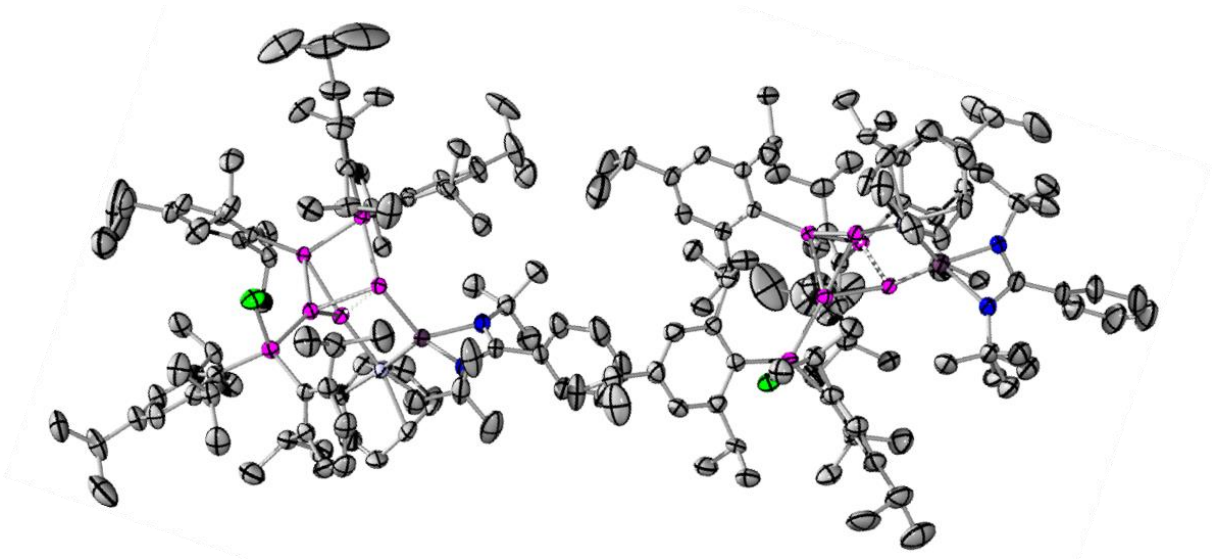

Supplementary Figure 61: Molecular structure of siliconoid **4** in the solid state with two molecules in the asymmetric unit. Hydrogen atoms omitted for clarity. Thermal ellipsoids represent 50% probability.

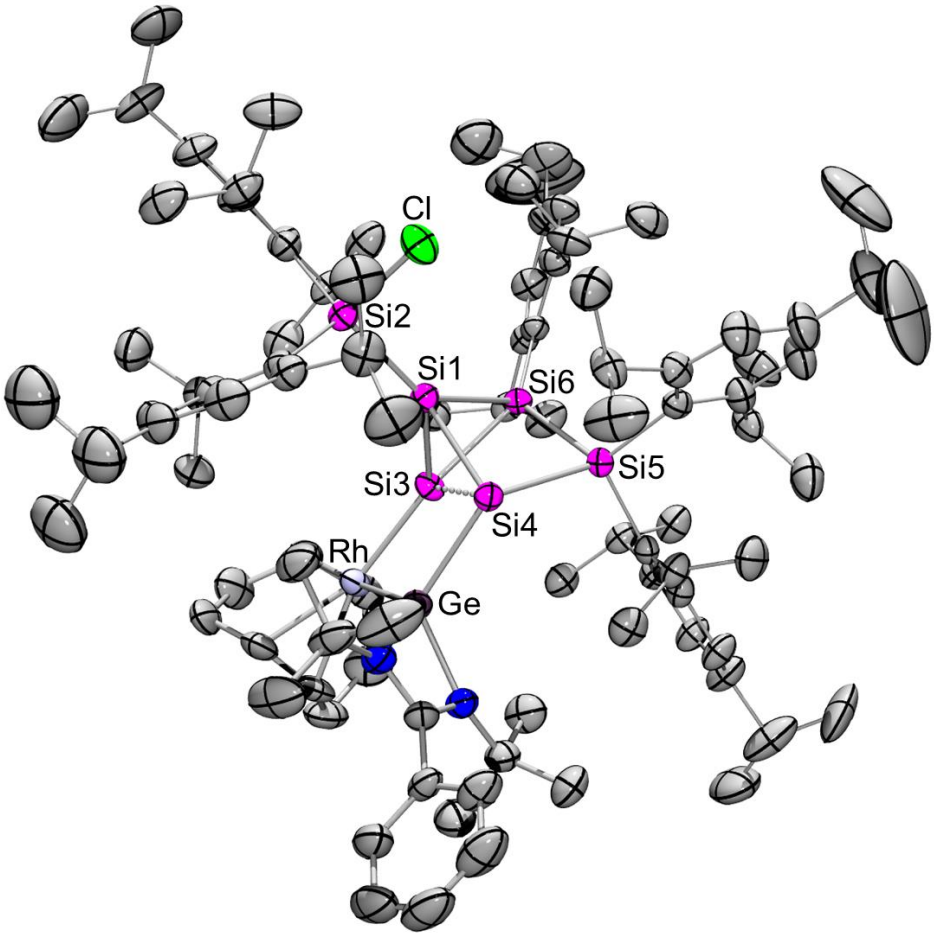

Supplementary Figure 62: Molecular structure of siliconoid **4** in the solid state. Hydrogen atoms and second molecule omitted for clarity. Thermal ellipsoids represent 50% probability.

Supplementary Table 15: Crystal data and structure refinement for **Si_6Ge-[Rh(cod)Cl]** (CCDC: 2000916).

Identification code	sh3988	
Empirical formula	C_{98} H_{150} Cl Ge N_2 Rh Si_6, C_6 H_{14}	
Formula weight	1821.85	
Temperature	202(2) K	
Wavelength	0.71073 Å	
Crystal system	Monoclinic	
Space group	$P2_1/n$	
Unit cell dimensions	a = 29.9006(13) Å	α = 90°.
	b = 22.5250(8) Å	β = 103.500(2)°.
	c = 32.5302(12) Å	γ = 90°.
Volume	21304.1(14) $Å^3$	
Z	8	
Density (calculated)	1.136 Mg/m^3	
Absorption coefficient	0.572 mm^{-1}	

F(000)	7840
Crystal size	0.363 x 0.222 x 0.200 mm^3
Theta range for data collection	1.144 to 27.160°.
Index ranges	-38<=h<=38, -28<=k<=20, -41<=l<=41
Reflections collected	189652
Independent reflections	47061 [R(int) = 0.0881]
Completeness to theta = 25.242°	100.0 %
Absorption correction	Semi-empirical from equivalents
Max. and min. transmission	0.7455 and 0.6530
Refinement method	Full-matrix least-squares on F^2
Data / restraints / parameters	47061 / 457 / 2245
Goodness-of-fit on F^2	1.024
Final R indices [I>2sigma(I)]	R1 = 0.0639, wR2 = 0.1421
R indices (all data)	R1 = 0.1527, wR2 = 0.1768
Extinction coefficient	n/a
Largest diff. peak and hole	1.273 and -0.624 e.$Å^{-3}$

5. References

[1] N. E. Poitiers, L. Giarrana, K. I. Leszczyńska, V. Huch, M. Zimmer, D. Scheschkewitz, *Angew. Chem. Int. Ed.* 2020, **59**, 8532-8536.